

## INFORMATION TO USERS

This was produced from a copy of a document sent to us for microfilming. While the most advanced technological means to photograph and reproduce this document have been used, the quality is heavily dependent upon the quality of the material submitted.

The following explanation of techniques is provided to help you understand markings or notations which may appear on this reproduction.

1. The sign or "target" for pages apparently lacking from the document photographed is "Missing Page(s)". If it was possible to obtain the missing page(s) or section, they are spliced into the film along with adjacent pages. This may have necessitated cutting through an image and duplicating adjacent pages to assure you of complete continuity.
2. When an image on the film is obliterated with a round black mark it is an indication that the film inspector noticed either blurred copy because of movement during exposure, or duplicate copy. Unless we meant to delete copyrighted materials that should not have been filmed, you will find a good image of the page in the adjacent frame.
3. When a map, drawing or chart, etc., is part of the material being photographed the photographer has followed a definite method in "sectioning" the material. It is customary to begin filming at the upper left hand corner of a large sheet and to continue from left to right in equal sections with small overlaps. If necessary, sectioning is continued again—beginning below the first row and continuing on until complete.
4. For any illustrations that cannot be reproduced satisfactorily by xerography, photographic prints can be purchased at additional cost and tipped into your xerographic copy. Requests can be made to our Dissertations Customer Services Department.
5. Some pages in any document may have indistinct print. In all cases we have filmed the best available copy.

University  
Microfilms  
International

300 N. ZEEB ROAD, ANN ARBOR, MI 48106  
18 BEDFORD ROW, LONDON WC1R 4EJ, ENGLAND

7913175

WILK, EUGENE WARREN  
STRUCTURAL CHANGES IN THE FERTILIZED ARBACIA  
EGG DURING THE FIRST MITOTIC CYCLE.

CITY UNIVERSITY OF NEW YORK, PH.D., 1979

University  
Microfilms  
International

300 N. ZEEB ROAD, ANN ARBOR, MI 48106

© 1979

EUGENE WARREN WILK

ALL RIGHTS RESERVED

PLEASE NOTE:

In all cases this material has been filmed in the best possible way from the available copy. Problems encountered with this document have been identified here with a check mark .

1. Glossy photographs
2. Colored illustrations \_\_\_\_\_
3. Photographs with dark background
4. Illustrations are poor copy \_\_\_\_\_
5. Print shows through as there is text on both sides of page \_\_\_\_\_
6. Indistinct, broken or small print on several pages \_\_\_\_\_ throughout  
\_\_\_\_\_
7. Tightly bound copy with print lost in spine \_\_\_\_\_
8. Computer printout pages with indistinct print \_\_\_\_\_
9. Page(s) \_\_\_\_\_ lacking when material received, and not available  
from school or author \_\_\_\_\_
10. Page(s) \_\_\_\_\_ seem to be missing in numbering only as text  
follows \_\_\_\_\_
11. Poor carbon copy \_\_\_\_\_
12. Not original copy, several pages with blurred type \_\_\_\_\_
13. Appendix pages are poor copy \_\_\_\_\_
14. Original copy with light type \_\_\_\_\_
15. Curling and wrinkled pages \_\_\_\_\_
16. Other \_\_\_\_\_

STRUCTURAL CHANGES IN THE FERTILIZED ARBACIA  
EGG DURING THE FIRST MITOTIC CYCLE

by

Eugene W. Wilk

A dissertation submitted to the Graduate Faculty  
in Biology in partial fulfillment of the require-  
ments for the degree of Doctor of Philosophy, The  
City University of New York.

1979

Eugene Wilk

This manuscript has been read and accepted for the Executive Committee in Biology in satisfaction of the dissertation requirement for the degree of Doctor of Philosophy.

December 15, 1978

Date

William D. Cohen

Chairman of Examining Committee  
Professor Wm. Cohen

January 22, 1979

Date

Louis G. Moriber

Executive Officer  
Professor Louis G. Moriber

Kathleen M. Lyser  
Prof. K. Lyser

Hunter College

Institution

Robert J. Grant  
Prof. R. Grant

Hunter College

Institution

Thomas T. Jensen  
Prof. T. Jensen

Lehman College

Institution

Ray H. Gavin  
Prof. R. Gavin

Brooklyn College

Institution

Eugenia Wang  
Prof. E. Wang

Rockefeller University

Institution

Robert A. Bloodgood  
Prof. R. Bloodgood

Albert Einstein College of Medicine

Institution

The City University of New York

## Abstract

STRUCTURAL CHANGES IN THE FERTILIZED ARBACIA  
EGG DURING THE FIRST MITOTIC CYCLE

by

Eugene W. Wilk

Adviser: Professor William D. Cohen

Changes in cell structure during the first mitotic cycle of the sea urchin Arbacia punctulata were observed by light and electron microscopy. The mature unfertilized egg, streak stage, prophase, metaphase, and anaphase were studied.

Cytoplasm of the mature egg contains yolk granules, pigment vacuoles, lipid droplets, cortical granules, mitochondria, and a heterogeneous smooth vesicular ER. No microtubules are present.

During streak stage, a streak zone devoid of yolk, pigment, and lipid droplets encircles the nucleus. It is shaped like a curved, elongated donut with the nucleus in the hole. Its major components are rough saccular ER and annulate lamellae. What appears to be C-microtubules can be seen among the latter, suggesting a relationship to microtubules. Although it excludes most organelles, the streak does not exclude heavy bodies which are found in or near the zone. This organelle consists of a granular dense mass bounded incompletely by annulate lamellae. It, too, seems to be associated with microtubules. Since the streak zone apparently determines the plane and axis of the future mitotic apparatus, and since both annulate lamellae and heavy bodies (which are localized in this zone) dis-

appear just before the growth of prophase microtubules, it is proposed that these organelles probably store or process microtubule protein.

At prophase the exclusion zone becomes thicker and shorter, no longer containing annulate lamellae or heavy bodies. Most of the saccular ER has become smooth. Near the nucleus smooth tubular ER predominates. Since  $\text{Ca}^{++}$ -dependent ATPase activity peaks at this time, tubular ER may function to remove  $\text{Ca}^{++}$  in a manner analogous to that of muscle sarcoplasmic reticulum. Mitochondria surrounding the nucleus may also serve as  $\text{Ca}^{++}$  pumps as well as suppliers of ATP. A decrease in  $\text{Ca}^{++}$  probably permits the assembly of mitotic apparatus microtubules from subunits released from their storage sites.

As microtubules become oriented and grow toward the nucleus, some apparently push portions of the nuclear envelope inward toward the chromosomes while others run along the nuclear surface. The microtubule-containing "fingers" of cytoplasm are thought to be an intermediate stage in mitotic apparatus assembly. Their microtubules are probably interpolar ones although there is a possibility that they may become attached to chromosomes. Such microtubules often terminate as C-microtubules and the "fingers" extend only as far as their microtubules do. Evidence of nuclear envelope breakdown and release of nuclear pores into the cytoplasm is also observed.

At metaphase the mitotic apparatus is complete, consisting of two asters separated by the spindle, the chromosomes aligned at the metaphase plate. In the chromosome-to-pole region, only 10% of the microtubules are C-microtubules while at the plate, over 50% are C-microtubules. This is in situ confirmation

of work done previously on isolated spindles. Smooth saccular ER radiates from the aster and surrounds the spindle periphery. Smooth tubular ER is found in the center of the spindle, especially near the chromosomes.

At anaphase the chromosomes separate and move toward the poles, defining an interzone area between them. Over 50% of interzone microtubules are C-microtubules, again confirming earlier work on isolated spindles. Anaphase ER is much reduced, especially in the interzone. It is distributed in the same way as metaphase ER except that there is more mixing of the smooth saccular ER with the smooth tubular ER.

Isolated spindles fixed in the presence of tannic acid demonstrate that C-microtubules have less than 13 protofilaments, possibly explaining their failure to form a cylinder. Polarization microscopy on Lytechinus variegatus zygotes shows a great decline in interzonal birefringence, some of which may be due to interzonal C-microtubules in vivo.

## ACKNOWLEDGEMENTS

I would like to thank my sponsor, Dr. W. D. Cohen, whose patience, understanding, guidance, and advice made this thesis possible. But, perhaps more importantly, I thank him for his warmth and friendship during some difficult times in my life. He is a real MENSCH.

I would like to thank Dr. K. M. Lyser and Dr. R. J. Grant, the other members of my advisory committee at Hunter Collège, who were always available when I needed them. I especially appreciate the helpful suggestions made by Dr. Lyser during the writing of this thesis

I would also like to thank Dr. L. Rebhun. During a short telephone conversation with him, I learned how to isolate mitotic apparatuses in polymerizing medium.

In addition, I would like to thank my beautiful wife and devoted parents (of blessed memory) for their support, patience, and understanding during the long years required to finish this work.

Finally, I would like to thank my family and friends who encouraged me and had patience when I had little time to spend with them.

## TABLE OF CONTENTS

Title page	
Copyright page	i
Approval page	ii
Abstract	iii
Acknowledgements	vi
Table of Contents	vii
List of Tables	x
List of Figures	xi
Text	1 - 144
I. Introduction	1
A. The mitotic apparatus of animal cells	1
B. Current hypotheses of mitosis	4
C. Background	6
1. Light microscopy	6
a. Polarizing microscopy <u>in vivo</u>	6
b. Light microscopy <u>in vivo</u> and <u>in situ</u>	7
c. Immunofluorescence <u>in situ</u>	12
d. The isolated mitotic apparatus	15
2. Electron microscopy	18
3. Biochemical events	21
D. The sea urchin zygote as a system for studying cell division	23
E. Major research objectives	24
II. Materials and Methods	28
A. Collection of eggs and sperm	28
B. <u>In situ</u> studies	30
C. Mitotic apparatus isolation	37
1. Hexylene glycol	37
2. Modified polymerizing medium	40

D. Counts of microtubules	41
E. Polarization microscopy	42
III. Results	43
A. Fine structure of the mature, unfertilized <u>Arbacia</u> egg	43
1. Endoplasmic reticulum	43
2. Yolk	43
3. Pigment vacuoles	46
4. Lipid droplets	46
5. Mitochondria	49
6. Golgi apparatus	49
7. Cortex	50
8. Annulate lamellae	50
9. Microtubules	51
10. Nucleus	51
B. Fine structure of the streak stage	51
1. Endoplasmic reticulum	57
2. Annulate lamellae	58
3. Golgi apparatus	63
4. Mitochondria	63
5. Heavy bodies	64
6. Microtubules	67
7. Nucleus	67
C. Fine structure of prophase	70
1. Endoplasmic reticulum	70
2. Annulate lamellae	70
3. Golgi apparatus	77
4. Mitochondria	77
5. Heavy bodies	77
6. Microtubules	80

7. Nucleus	80
D. Fine structure of the metaphase cell	86
1. Endoplasmic reticulum	89
2. Annulate lamellae and heavy bodies	89
3. Golgi apparatus	89
4. Mitochondria	94
5. Mitotic apparatus	94
E. Fine structure of the anaphase cell	98
1. Endoplasmic reticulum	98
2. Annulate lamellae and heavy bodies	101
3. Golgi apparatus	101
4. Mitochondria	101
5. Microtubules	101
F. Fine structure of isolated spindles	112
1. The substructure of C-MTs	112
2. Spindles isolated in modified MT polymerization medium	113
3. Microtubule clear zones	117
G. Sea urchin spindle birefringence	117
IV. Discussion	118
A. Structural changes <u>in situ</u> versus biochemical events during the first mitotic cycle	118
1. Microtubules and endoplasmic reticulum	118
2. C-Microtubules	124
3. Streak stage endoplasmic reticulum	127
4. Annulate lamellae and nuclear pores	130
5. Heavy bodies and a unifying hypothesis for tubulin-containing-structures	132
6. The nucleus	137
B. Summary and conclusions	142
Bibliography	145

## LIST OF TABLES

1. MBL formulae for synthetic sea waters	29
2. All cells examined by electron microscopy at each mitotic stage	31
3. Various fixation methods tried	31
4. Tabulation of metaphase spindle microtubules	97
5. Tabulation of anaphase spindle microtubules	111
6. Curvilinear measurements of C-MT cross sections	114
7. Biochemical events and structural changes during sea urchin zygote mitosis	120

## LIST OF FIGURES

1. Diagram of the typical animal zygote mitotic apparatus representing metaphase and anaphase as seen by light microscopy	3
2. Classical light microscopy views of sectioned <u>Arbacia punctulata</u> zygotes during various stages of the mitotic cycle	11
3. Use of thick sections	34
4. Interzone of early anaphase cell	34
5. Cytoplasm of the mature unfertilized egg	45
6. High magnification of nuclear area of egg	45
7. Annulate lamellae of unfertilized egg	48
8. Heterogeneous form of yolk granules in the egg	48
9. Cortical region of egg	48
10. Nuclear region of unfertilized egg	48
11. Serial sections through the streak stage cell	53
12. Diagram of the relationship between the nucleus and the surrounding streak based on a clay model reconstruction of the serial sections of Fig. 11	53
13. Thick section of streak stage cells viewed by darkfield illumination	53
14. Thick section comparing an unfertilized mature egg to a streak stage cell	53
15. Low magnification view of portion of a streak stage cell	56
16. Streak zone of cell shown in Fig. 14	60
17. Higher magnification of another part of the same streak zone	60
18. Annulate lamellae from cell of Fig. 14	62
19. Heavy bodies from the same cell	62
20. Heavy body located in a side channel outside the streak zone	66

21. Perinuclear area of streak stage cell	66
22. Series of sections through the streak stage nucleus	69
23. Serial sections through the streak nucleus showing invagination of nuclear envelope by formation of an invaginating stalk which balloons out at its end	69
24. Serial sections of invagination by "ballooning" of the streak stage nuclear envelope directly into the nucleus	69
25. Thick section of the late prophase cell	72
26. The prophase exclusion zone full of vesicular and smooth ER	72
27. Cortical area of prophase cell	74
28. Golgi apparatus at periphery of prophase exclusion zone	74
29. Area just outside this exclusion zone penetrated by MTs	74
30. Area of prophase exclusion zone with evaginations from the nucleus clearly visible	76
31. Cross-section nearly tangential to the prophase nucleus with nuclear envelope intact on left but not on right where tubular ER seems to mix with nucleoplasm	76
32. Serial sections through prophase perinuclear region	79
33. Serial sections through a group of perinuclear pores from the same cell	79
34. Serial sections through an area of the prophase nucleus showing how a single MT can be associated with a nuclear invagination	82
35. Serial sections of prophase nucleus showing relationship of MTs with the nuclear invaginations	82
36. Section through the prophase nucleus	85
37. Thick sections of metaphase cells	88
38. Longitudinal section through the metaphase spindle of Fig. 37A	88
39. Cross-section through the metaphase chromosome-to-pole region near the chromosomes	91
40. Cross-section through the metaphase plate of the cell shown in Fig. 37B	91

41. Longitudinal section through the metaphase aster of the cell shown in Fig. 37A	93
42. Higher magnification of the centriole in Fig. 41	93
43. Continuity of metaphase mitotic apparatus ER with that of the general cytoplasm	96
44. Golgi apparatus aligned with the chromosomes of the metaphase plate	96
45. The cortex of the metaphase cell	96
46. Possible C-MTs in longitudinal section at the metaphase plate	100
47. Thick section of early anaphase cell	103
48. Thick section of mid-anaphase cell	103
49. Longitudinal section through the mitotic apparatus of the mid-anaphase cell of Fig. 48.	105
50. Continuation of anaphase mitotic apparatus ER into that of the general cytoplasm	107
51. Cross section through the chromosome-to-pole region of a mid-anaphase cell	107
52. Cross section through the middle of the interzone of the same mid-anaphase cell as Fig. 51	109
53. Cross section through the interzone of the early anaphase of Fig. 47.	109
54. MT subunits	116
55. Cross section of the chromosome-to-pole region of an anaphase spindle isolated in the modified polymerization medium	116
56. Cross section through the metaphase plate of a spindle isolated in modified polymerization medium	116
57. Spindle birefringence during the first mitotic cycle of the <u>Lytechinus variegatus</u> zygote	116
58. Spindle birefringence during the third mitotic cycle of the <u>Lytechinus variegatus</u> zygote	116

## I. INTRODUCTION

It is 120 years since Virchow (1858) wrote "omnis cellula e cellula," calling attention to the fact that all cells arise from previously existing cells. Ever since, elucidation of the mechanisms underlying cell division has been a major goal in cell biology. Nevertheless, the formation, control, and function of the mitotic apparatus (MA), the complex of organelles responsible for chromosome movement, are still poorly understood.

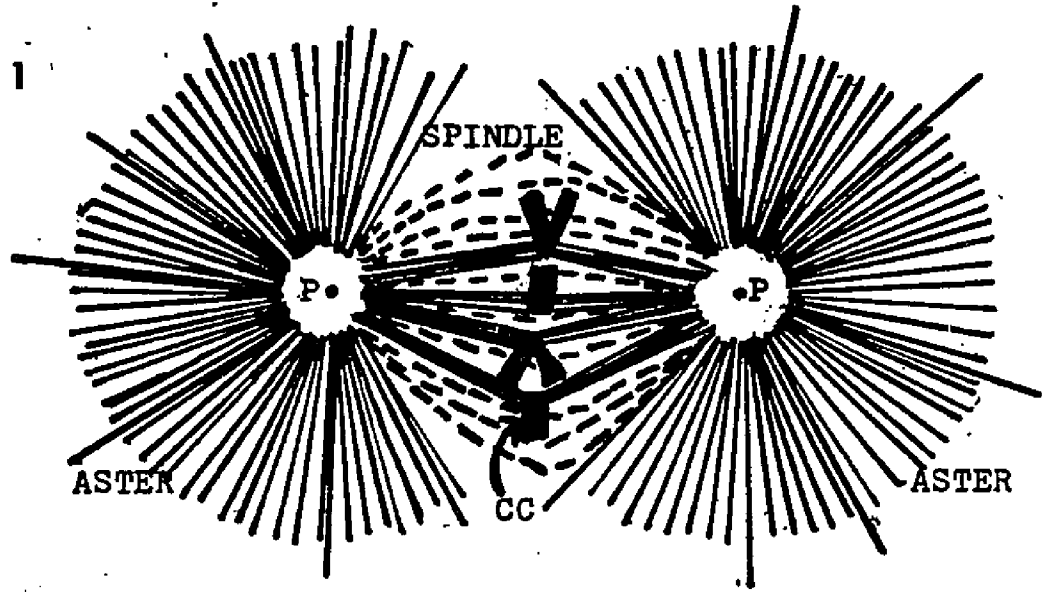
The fundamental nature of mitosis is reflected in its enormous literature, which has been reviewed many times previously (Wilson, 1928; Schrader, 1953; Mazia, 1961; Levine, 1963; Nicklas, 1971; Bajer and Molé-Bajer, 1972; Inoué and Stephens, 1975). Thus, only a summary of the most important aspects will be presented here.

### A. The Mitotic Apparatus of Animal Cells

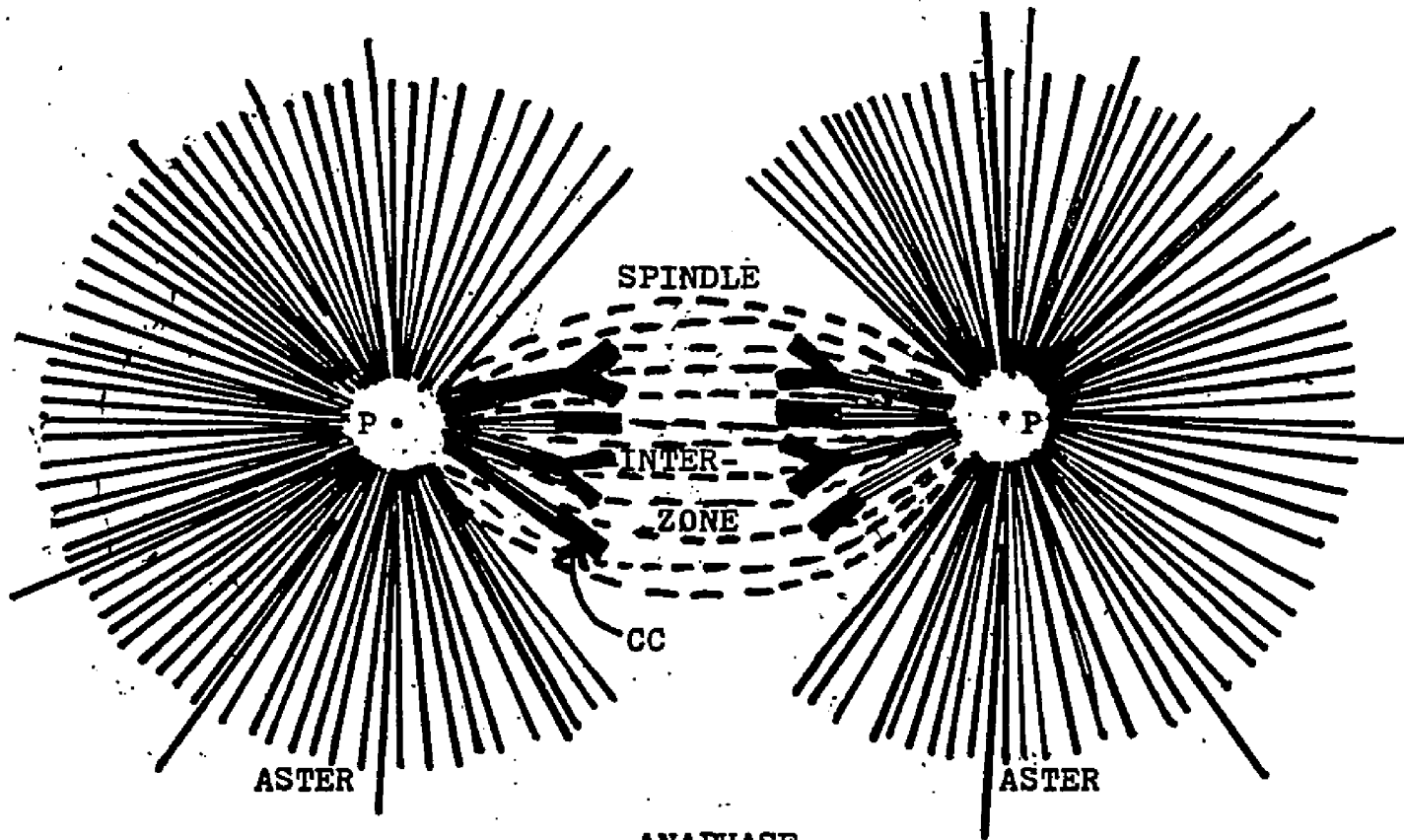
Classical cytology (see reviews above) shows that at the time of cell division there is a dramatic reorganization of cell structure. The new assemblage of organelles which effects mitosis is called the mitotic apparatus (MA). Generally it consists of chromosomes ("chromatic figure") and a fibrous component ("achromatic figure"). The latter has two components: the spindle located centrally and roughly shaped like an American football, and the asters, one at each end of the spindle, their fibers radiating from a central point (Fig. 1). The central point is referred to as the pole and is in the centrosome region.

Although all spindle fibers run roughly parallel to the spindle axis, two types of fibers can be distinguished: interpolar or continuous (also "non-chromosomal") fibers

FIGURE 1. Diagram of the typical animal zygote mitotic apparatus representing metaphase and anaphase as seen by light microscopy. At metaphase the chromosomes (CC) are aligned on the metaphase plate of the spindle which separates the two asters. During anaphase, the chromosomes have separated and move to the poles (P) which contain centrioles (represented by prominent dot at the center of each aster). Also at anaphase, the spindle elongates and the asters grow larger. Chromosomes are attached to the spindle by the chromosomal fibers (solid lines) while interpolar or continuous fibers (dashed lines) seem to extend from one pole to the other through the interzone, the area between the two sets of aligned chromosomes as they migrate to the poles.



METAPHASE



ANAPHASE

extending from one pole toward the other, and chromosomal fibers extending from chromosomes to poles (Fig. 1)

Chromosomes are confined to the spindle, aligning at its mid-plane to form the metaphase plate. During anaphase they separate into two groups, each group migrating to a pole and reaching it at telophase. Chromosomal fibers appear to be attached to chromosomes at specific sites, the kinetochores.

Electron microscopy reveals the presence of microtubules (MTs) in the MA where, like the fibers of light microscopy, they radiate from the poles and in the spindle are aligned parallel to its axis. They have also been observed attached to kinetochores and are deemed primarily responsible for the fibrous appearance of the MA. MTs resemble hollow rods and are between 20 and 25 nm in diameter. The walls are usually composed of 13 protofilaments which bond laterally. Each protofilament consists of a chain of tubulin monomers, a globular protein (Ledbetter and Porter, 1963; Grimstone and Klug, 1966; Tilney et al., 1973). MT structure, function, and biochemistry have been reviewed many times recently (Hepler and Palevitz, 1974; Soifer, 1975; Snyder and McIntosh, 1976; Stephens and Edds, 1976) and will not be reviewed here.

Electron microscopy also reveals many other features common to mitotic apparatuses of animal cells. These include centrioles at the astral poles, smooth ER, ribosome-like particles, and a "fuzzy" material around MTs, all having been recently reviewed (Forer, 1969; Sanger, 1977).

#### B. Current Hypotheses of Mitosis

There are four major current hypotheses of mitosis which seek to explain the mechanism(s) of anaphase chromosome movement and/or anaphase spindle elongation. Three of the

four depend principally on MTs or their cross-bridges while the fourth invokes an actomyosin-like contraction.

The "dynamic equilibrium hypothesis" was proposed by Inoué and Sato (1967) who suggested that a dynamic equilibrium exists between assembled MTs and a pool of tubulin subunits. Centrioles, kinetochores, and the cell plate of plant cells, acting as orienting centers and with other factors might shift this equilibrium as needed toward assembly or disassembly. Such changes might, in some way, move chromosomes to the poles.

A "sliding MT mechanism" analogous to the sliding of muscle microfilaments was proposed by McIntosh, Hepler, and Van Wie (1969). Assuming that MTs are polarized and citing the presence of cross-bridges, they suggested that the latter function as do the myosin cross-bridges of muscle, i.e. as an ATPase making and breaking contact cyclically, and generating the force for sliding of MTs of opposite polarity. Since chromosomes are attached to MTs, as the latter slide, the former move.

A third MT-dependent model was suggested by Bajer (1973) and is often referred to as the "zipper" model. In this hypothesis, non-parallel MTs interact laterally like two pieces of material being zipped together. The interaction between radiating chromosomal fibers and neighboring non-chromosomal fibers is deemed capable of pulling attached chromosomes to the poles.

The finding of actin in the chromosome-to-pole region of the spindle by heavy meromyosin binding (Forer and Behnke, 1972; Forer, 1974) and by immunofluorescence (Cande et al., 1975;1977) resulted in much speculation that actomyosin-like interactions

are responsible for at least chromosome-to-pole movements. It has been calculated that a single thick filament and its attendant thin filaments extending from the pole to the chromosomes could easily produce 1,000 times the force needed to pull a chromosome to the pole (Forer, 1969).

Common to all these hypotheses is the attempt to explain the generation of force required to move chromosomes. There are also other problems of a fundamental nature: How does the cell control the time, place, and rate of MT or actin microfilament assembly? By what structural route is assembly and disassembly achieved? While none of these questions have been adequately answered, their exploration is vital to understanding mitosis.

### C. BACKGROUND

Because the large volume of literature on mitosis precludes extensive review here, the literature discussed has been selected as most directly relevant to the experimental work performed. It is therefore limited primarily to work on zygotes of sea urchins and other marine species.

#### 1. Light Microscopy

Light microscopy has been used to study the sea urchin mitotic apparatus in living cells (in vivo), in sections of fixed and stained cells (in situ), and after isolation.

##### a. Polarizing microscopy in vivo

Because sea urchin eggs are large and often contain much pigment, they have been generally excluded from polarization studies. Nevertheless, work done on various living marine eggs, especially by Inoué (1964; Inoué and Sato, 1967) have demonstrated that the mitotic spindle is birefringent and that much of the birefringence is related to the state of MT assembly/dis-

assembly. Since several different treatments (cold, colchicine, pressure) affect this birefringence in a way suggesting an equilibrium reaction, the dynamic equilibrium hypothesis was proposed as the best model to fit the data (Inoué and Sato, 1967).

More recent work (Kiehart and Inoué, 1976) has shown that 1.0 mM  $\text{CaCl}_2$  micro-injected into marine embryo spindles causes reversible loss of birefringence. This demonstrates that spindle MTs in vivo are  $\text{Ca}^{++}$ -labile like those in vitro (Weisenberg, 1972a). That the loss of spindle birefringence is reversible by cell action suggests that  $\text{Ca}^{++}$  concentration near the spindle is carefully regulated, further supported by the fact that when even higher doses are micro-injected away from the spindle, no such loss is observed. In a similar vein, antibodies to egg myosin micro-injected into blastomeres prevent cytokinesis but not mitosis (Kiehart et al., 1977) raising doubts about actomyosin hypotheses of chromosome movement. Moreover, cytochalasin B, an inhibitor of actin-like microfilament-dependent processes in many systems, does not inhibit mitosis (Carter, 1967).

#### b. Light microscopy in vivo and in situ

Most structural data from light microscopy of sea urchin eggs comes from viewing either fixed, sectioned, and stained material or living cells from species with less pigment. The major studies of morphological change as a result of fertilization were reported by Wilson (1895; 1928; Wilson and Mathews, 1895) and Harvey (1956), and did much to aid our understanding of the temporal sequence of mitosis at the light microscope level.

Sea urchin eggs mature in the ovary and have already completed their meiotic divisions when the animals spawn. Several hours after shedding the second polar body they can be fertilized.

As seen by light microscopy, the mature Arbacia egg has an eccentric, spherical nucleus, approximately 11.5  $\mu\text{m}$  in diameter. In addition to the nucleus and other usual organelles like mitochondria, the cytoplasm contains yolk granules, pigment vacuoles, and lipid droplets all distributed randomly, forming a homogeneous cytoplasm. The pigment vacuoles contain "echinochrome" which imparts to the egg its reddish color and makes microscopy of the whole egg very difficult. The egg also has cortical granules which break open upon fertilization, releasing their contents outside the cell membrane. A vitelline membrane overlies the cell membrane and lifts off the surface after fertilization. Surrounding the egg is a jelly layer some 20  $\mu\text{m}$  thick, demonstrated by the observations that packed eggs do not touch each other and that sperm often get stuck in it forming a "halo" around the egg.

It is difficult to determine the polarity of the egg because, as just mentioned, the cytoplasm is uniform throughout. The polar bodies are formed at the animal pole but cannot be used as a marker because they do not remain until maturity. The micropyle is located in the egg jelly at the animal pole but cannot be seen except by the addition of India ink to swell the jelly. Not until the 8-cell stage, when an uneven division results in the formation of micromeres at the vegetal pole, can polarity be easily determined. Besides being smaller than the other cells, micromeres also lack pigment. They are thus excellent markers for the vegetal pole but only in stages subsequent to those under investigation here.

Upon fertilization, many changes occur at the cell surface. When the sperm touches the egg, a small fertilization cone rises above the spermatozoon. Although this appears

earliest, it is easier to see the next step, the lifting of the vitelline membrane by about 5  $\mu\text{m}$  to form a fertilization membrane around the cell. This is the most visible sign that fertilization has occurred. During this time, the cortical granules release their contents into the perivitelline space between the egg surface and the fertilization membrane. Some of this material contributes to the hyaline layer around the egg. This layer thickens to 2 to 3  $\mu\text{m}$  and helps bind the blastomeres together. It can be prevented from forming or dissolved by Ca-free sea water to make lysis easier. Finally, pigment vacuoles, which had been uniformly distributed in the unfertilized egg, migrate to the cortex where they form a heavily pigmented layer.

In addition to these surface reactions, many internal changes are taking place. After the sperm head enters the egg, it does an about-face so that its basal body faces the egg nucleus. From the basal body, rays appear forming a sperm aster (Fig. 2:2) which grows as the sperm nucleus meets and fuses with the egg nucleus. At this point the aster spreads throughout the cell resulting in the monaster stage (Fig. 2:3).

As the rays of the monaster disappear, the "streak stage" (Fig. 2:4) begins. Its name comes from the clear streak, free of pigment and most granules, which seems to form around the nucleus at this stage. Crenation of the cell surface is first observed at this time.

The streak stage is important because it occurs just before assembly of the mitotic apparatus and provides the first sign of the subsequent spindle axis. At the light microscope level, however, nothing seems to happen, as if the cell were arrested. In fact, a corresponding stage in the unpigmented

FIGURE 2. Classical light microscopy views of sectioned Arbacia punctulata zygotes during various stages of the mitotic cycle. Reproduced from THE AMERICAN ARBACIA AND OTHER SEA URCHINS by Ethel Browne Harvey (published by Princeton University Press, 1956): Plate V "Normal development (sections)". Reprinted by permission of Princeton University Press.

The cells were fixed in Bouin's fixative and stained with Heidenhain's hematoxylin. LM x 450.

1. Unfertilized egg
2. Sperm and sperm aster
3. Pronuclear fusion
4. Streak stage; Note the enlarged nucleus
5. Prophase
6. Metaphase
7. Anaphase
8. Telophase
9. Second cleavage
10. Second cleavage
11. Four-cell stage
12. Early blastula; Note the lack of asters

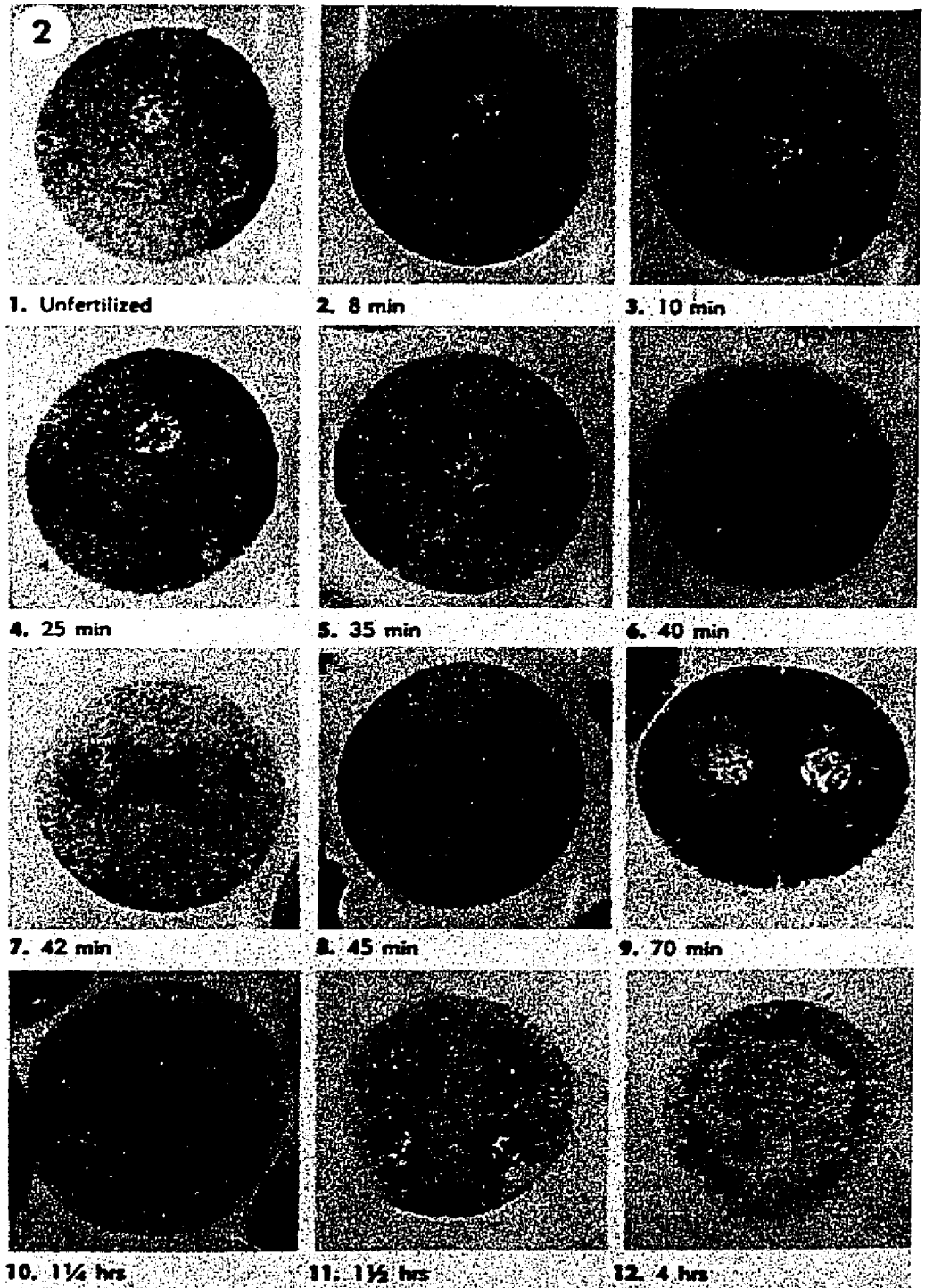


Plate V. Normal development (sections)

egg of Lytechinus variegatus is called the "pause" (Wilson, 1895; Wilson and Mathews, 1895) for this very reason. Such eggs do not have a recognizable streak presumably because there is no pigment to differentiate between the non-pigmented streak zone and the pigmented cytoplasm around it. Unfortunately, the apparent quiescence of the streak stage has limited its study although it accounts for 30% of the mitotic cycle and obviously contributes to the formation of the mitotic apparatus. Even the 3-dimensional shape of the streak zone has not been adequately determined.

The Arbacia nucleus enlarges to approximately 16  $\mu\text{m}$  in diameter and becomes elliptical as chromosomes appear. The nuclear envelope disappears and a spindle with an aster at each pole is formed (Fig. 2:5). The chromosomes remain scattered until metaphase when they are aligned in a metaphase plate. The mitotic apparatus is complete at metaphase, consisting of two asters with a spindle separating them (Fig. 2:6).

At anaphase the chromosomes separate into two sets, one set of aligned chromosomes going to one pole and the other set going to the opposite pole (Fig. 2:7). At telophase the chromosomes have reached the poles in the asters and become vesicular (Fig. 2:8). The vesicles fuse forming new nuclei as the cleavage furrow divides the cell in two (Fig. 2:9). The time from fertilization to first cleavage is 50 min at 23<sup>o</sup>C. As is the case for most biological processes, lower temperature prolongs the cell cycle so that at 20<sup>o</sup>C, for example, cleavage occurs at about 1 hr after fertilization.

#### c. Immunofluorescence in situ

In the past few years advances in immunofluorescence techniques in situ have made it possible to locate proteins

deemed important in mitosis including tubulin, actin, myosin, calcium-dependent regulator, and microtubule-associated proteins (MAPs). The technique usually involves treatment of various mammalian cells in culture with acetone or glycerol to make them permeable to antibody or other specific probes like heavy-meromyosin.

Fuller, Brinkley, and Boughter (1975) using bovine brain tubulin antibodies that had been made fluorescent, found a faint fluorescence around the nucleus and condensing chromosomes at prophase of rat kangaroo (Potorous tridactylis) cells. During prometaphase a central spot of fluorescence surrounded by chromosomes becomes more spindle-shaped with chromosomes throughout. The entire mitotic apparatus, including the interzone, is fluorescent during metaphase and anaphase but the fluorescence decreases at telophase. Since the cytoplasmic background fluorescence increases at this point, monomer release from depolymerizing MTs is suggested.

Sanger (1975) used fluorescently-labelled heavy-meromyosin to locate actin in rat kangaroo (Pt-K2) cells and found fluorescence in nucleoli, kinetochores, centriolar region, and chromosomal spindle fibers. Since actin was not present in continuous spindle fibers or in astral fibers, he suggested an actin-myosin interaction as the mechanism for chromosome-to-pole movement. Indeed, Fujiwara and Pollard (1975) found myosin both in the spindle and polar area but not in the interzone of HeLa cells using fluorescent antimyosin.

Cande, Lazarides, and McIntosh (1975; 1977) used indirect immunofluorescence on lysed rat kangaroo (Pt-K1) cells and reported actin in amorphous form at the poles and a fibrous form running from chromosome to pole. They pointed out that

fluorescence at the poles is first viewed in late prophase while that of the spindle does not appear until prometaphase and continues through anaphase. Since colcemid prevented fibrous actin fluorescence but not polar amorphous actin fluorescence, a role for tubulin in the control of actin polymerization is suggested. As mentioned before, it was the presence of actin demonstrated by these methods that led to hypotheses of chromosome movement based on actin interactions.

In what may be a major breakthrough, Welsh and Dedman (1977) reported the presence of calcium-dependent regulator by immunofluorescence in the several mammalian cultures examined. Its fluorescence pattern is similar to that of actin and it can substitute for troponin-C in the regulation of skeletal muscle actomyosin ATPase. Recently, it was shown to be responsible for in vitro control of  $Ca^{++}$  sensitivity in MT polymerization/depolymerization reactions, suggesting a major role for this protein in mitosis (Marcum et al., 1978).

Immunofluorescence has also been used to study MT-associated proteins. Lockwood (1977) made an antibody to one of these, tubulin-assembly protein, which seems necessary for both MT initiation and elongation. Its fluorescence pattern in rat kangaroo (Pt-K1) cells mimics that of antitubulin, i.e., it stains the cytoplasmic MT network until mitosis when the network disappears. It is also found in the mitotic spindle and its staining is both cold and colcemid sensitive. A similar finding for a high molecular weight MT-associated protein in mouse neuroblastoma (N115) and rat fibroblast (3T3) cells was recently reported (Sherline and Schiavone, 1977). Here, too, the cytoplasmic MT network from nucleus to periphery is fluorescent, as are the neurites of the neuroblastoma cells. The

cross-bridges on MTs cited by proponents of the sliding MT hypothesis of mitosis (McIntosh et al., 1969) might also be considered a type of MT-associated protein.

Although the specific role(s) each of these proteins play in assembly, function, or control of the mitotic apparatus remains unknown, immunofluorescence continues to yield much information on the biochemistry of mitosis as well as its temporal sequence.

#### d. The isolated mitotic apparatus

In 1952, using sea urchin eggs, Mazia and Dan were first to isolate mitotic apparatuses from cells fixed in cold ethanol. By 1961, Mazia (et al.) had isolated them from living cells using a disulfide reagent. The following year, Kane (1962a) showed that under controlled pH conditions non-electrolytes, like propylene glycol, could substitute for disulfide reagents, as could alcohols and several other agents that inhibit protein solubilization (Kane, 1965). Such mitotic apparatuses are birefringent, stabilized by divalent cations, and pH sensitive (Goldman and Rebhun, 1969). Ultrastructurally, isolates retain their MTs and display vesicles and ribosome-like particles (Kane, 1962b; Rebhun and Sander, 1967; Goldman and Rebhun, 1969). The hope has been that at some time, such isolates would be capable of functioning, i.e., to move chromosomes in a normal manner, so they can be used as a model system.

Goode and Roth (1969) reported chromosome movement in isolated ameba mitotic apparatuses when  $Mg^{++}$  and ATP are added but this results from mitotic apparatus elongation. Similarly, Cohen (1968) reported swelling and shrinking of isolated A. punctulata and S. droebachiensis mitotic apparatuses, as well as chromo-

some separation by mitotic apparatus elongation based upon pH and polyelectrolyte effects. In no case, however, were observed movements the same as in vivo ones. The reason for this inability to function may well be loss of material, since Forer and Goldman (1972) found a 40% to 80% decrease in apparatus dry matter after isolation when compared to the amount thought present in vivo from interference microscopy. Just what material is lost during isolation is unknown, but its investigation might shed light on the mechanism of mitotic apparatus function.

A new approach to functional isolated mitotic apparatuses was spurred by the introduction of  $\text{Ca}^{++}$ -regulating media which support MT assembly in vitro (Weisenberg, 1972). Cande et al. (1974) reported normal chromosome movement in mitotic apparatuses from rat kangaroo (Pt-K1) cells lysed in such a medium to which Carbowax was added. After some difficulty in reproducing their results, they have now begun to explore this system. Rebhun et al. (1974) used a similar medium without Carbowax on surf clam zygote mitotic apparatuses and thought some chromosome movement may have occurred in cells lysed during anaphase but were not definite about it. In any event, even with the new polymerizing media, regular and reproducible mitotic chromosome separation and movement has only recently been attained in lysed cells and its study only just begun.

Nevertheless, much of what is known about the mitotic apparatus has come from work on the mitotic apparatus isolated from sea urchin zygotes. Mazia et al. (1961) demonstrated the presence of a  $\text{Mg}^{++}$ -stimulated ATPase, as well as a  $\text{Ca}^{++}$ -stimulated one (1972). Both of these are probably important in mitotic apparatus assembly or function. Rebhun and Sander (1967)

correlated birefringence measurements with numbers of MTs; Cohen and Rebhun (1970) measured the amount of tubulin required for mitotic apparatus assembly; Zimmerman (1960; 1963) found interzonal RNA as well as increased solubility of the interzone in various solvents; Rebhun et al. (1974) demonstrated that kinetochores act as initiation sites for MT assembly; Bibring et al. (1976) showed MT protein from isolated sea urchin mitotic apparatuses differ from that of cilia and flagella of the same species; Salmon and Jenkins (1977) found mitotic apparatuses isolated in one of the new polymerizing media were  $\text{Ca}^{++}$ -labile and may contain dynein, the ATPase found attached to the outer doublets of cilia and flagella; Stephens (1972) demonstrated the importance of temperature prior to nuclear breakdown by "temperature jumps" using isolation to measure the size, form, and birefringence of mitotic apparatuses.

One interesting ultrastructural discovery was the finding by Cohen and Gottlieb (1971) of C-microtubules (C-MTs) in the metaphase plate and interzone of isolated A. punctulata mitotic apparatuses (Kane method). They are deemed to be MTs that have not closed, appearing C-shaped rather than O-shaped in cross-section. C-MTs have been observed in several other systems in situ and, most recently, in vitro (see discussion), where they are believed to be an intermediate form in MT assembly or disassembly. Their role in mitosis remains unknown.

The biochemistry of the isolated mitotic apparatus has been reviewed (Forer, 1969) as have the methods and advantages of the newer isolation techniques (Zimmerman, Zimmerman, and Forer, 1977; Turner and McIntosh, 1977).

## 2. Electron Microscopy

Electron microscopy was used on sea urchin eggs as early as 1943 (Harvey and Anderson), but not until the introduction of glutaraldehyde as a fixative (Sabatini et al., 1962; 1963; 1964) was good fixation of cytoplasmic MTs possible, although they are a major structural element of the mitotic apparatus. Thus, work done without glutaraldehyde (Harris, 1965; 1967; Verhey and Moyers, 1967; Sanchez and Porra, 1972) is of poor quality. Also, for some unknown reason, fixation with mixtures of glutaraldehyde and other fixatives, usually paraformaldehyde Bal et al., 1968; Longo and Anderson, 1968; Sachs and Anderson, 1970) or acrolein (Anderson, 1970; Longo, 1972; Tilney and Marsland, 1969) did not give satisfactory results. Another problem has been fixation at low temperature (Longo, 1972; Sanchez and Porra, 1972; Verhey and Moyers, 1967) since the mitotic apparatus in vivo is cold-labile (Inoué, 1964). The best fixative to date is that of Tilney and Gibbins (1969) who used it to study mesenchyme formation in later embryos of A. punctulata. Although other fixatives were tested (Table 3, p. 31), this was the only one which preserved ultrastructural details and was therefore the one used in this investigation.

Electron microscopy has shown that, in addition to the granules and organelles visible by light microscopy, sea urchin eggs and zygotes contain annulate lamellae, heavy bodies, and MTs (Harris, 1965; 1967; Anderson, 1970). The disappearance of the former organelles just before mitotic apparatus assembly suggests that even annulate lamellae and heavy bodies have a role in cell division, as explored more fully below. That MTs have such a role is obvious since as

mentioned above (Section A) they are a major, universal structural element of the mitotic apparatus and appear to be responsible for the fibers seen by light microscopy in situ and for at least a major part of the birefringence seen in vivo (Rebhun and Sander, 1967; Forer, 1969).

Electron microscopy has also been used to support the sliding MT theory (McIntosh et al., 1969) with the observation of MT cross-bridges projecting from MTs. Also, it has produced evidence that spindle elongation in diatoms is effected by MT sliding (Pickett-Heaps et al., 1975; Tippit et al., 1975). Other hypotheses of chromosome movement also depend on MTs (Inoué and Sato, 1967; Bajer, 1973) as mentioned previously.

Annulate lamellae may participate in mitosis by way of their recent implication in MT synthesis. In 1975 DeBrabander and Borgers demonstrated that formation of annulate lamellae is induced by the presence of drugs which destroy MTs (colchicine, vinblastine, vincristine, podophyllotoxin, and rotenone). The cultured cells used do not normally produce annulate lamellae, and only the disappearance of MTs was correlated with their appearance since dosages that did not destroy MTs had no effect. Earlier, Dales et al. (1973) reported that ferritin-labelled tubulin antibody accumulated in the annuli of nuclear pores and annulate lamellae but discounted it because controls showed similar, although weaker, binding.

Annulate lamellae normally proliferate in the A. punctulata primary oocyte after yolk formation late in oogenesis (Bal et al., 1968; Verhey and Moyer, 1967). At the time of the streak stage, they are a major part of the streak (Longo, 1972). Since annulate lamellae break down when the nuclear envelope does, they cannot be seen in the mitotic apparatus

(Harris, 1969; Longo, 1972), but have been implicated in the sperm aster (Longo and Anderson, 1968) and cleavage furrowing (Tilney and Marsland, 1968; Schroeder, 1969). Annulate lamellae have been studied extensively (see Kessel, 1968 and Wishnitzer, 1973 for reviews) but their nature and role remain unknown.

"Heavy bodies" were first reported by Afzelius (1957) in European sea urchin species and then confirmed by Harris (1967) for the Pacific sea urchin Strongylocentrotus purpuratus which have as many as 1500 per mature egg. Ultrastructurally, they appear as densely packed, ribosome-like granules bounded on several sides but not completely enclosed by annulate lamellae (Harris, 1967). Since it is likely that they contain RNA (Afzelius, 1956; Harris, 1969), Harris suggested that they may be a site of maternal, masked mRNA attached to ribosomes. Their name was derived from the fact that centrifugation of ripe unfertilized eggs brought them to the centrifugal pole (Afzelius, 1956), although this is not true for S. purpuratus and A. punctulata where they are brought to the light half (Harris, 1969).

In normal, uncentrifuged eggs of A. punctulata heavy bodies have been reported in primary oocytes during oogenesis (Anderson, 1968) but no reports on later stages exist so that their fate, especially during mitosis, is unknown. Harris's studies on S. purpuratus (1967; 1969) showed that unlike Arbacia, they are produced in association with the ootid nucleus and scatter widely through the cytoplasm. Even after fertilization, 5 to 10 were seen touching the female pronucleus but not after pronuclear fusion. She reported (1969) that at streak stage, those in the streak align parallel to it but do

not play a formative role. Like annulate lamellae, heavy bodies disappear when the nuclear envelope does. According to Harris (1969) those in the asters contribute their annulate lamellae to the membranous portion of the mitotic apparatus while the granules disappear into the great background mass of cytoplasmic ribosomes which she thought these granules to be. The actual role of heavy bodies, especially in A. punctulata where they have not been reported previously in the fertilized egg, remains unknown.

### 3. Biochemical Events

The unfertilized egg is relatively inactive; there is little synthetic activity and metabolism is minimal. Upon fertilization, the egg becomes active synthetically and numerous biochemical changes ensue. Many of these have been studied in S. purpuratus and have been reviewed recently (Epel et al., 1969; Epel, 1975; 1977).

Changes in ion concentrations apparently initiate the events. Within three seconds of fertilization, an influx of  $\text{Na}^+$  ions results in a membrane depolarization analogous to an action potential which propagates around the cell and may be related to an early block to polyspermy. A few seconds later, the concentration of free cytoplasmic  $\text{Ca}^{++}$  ions increases and this is associated with the cortical reaction which is triggered by  $\text{Ca}^{++}$ . Simultaneously,  $\text{Na}^+$  is pumped into the cell as  $\text{H}^+$  is pumped out, raising the pH from 6.6 to 7.2. NAD kinase is activated, converting NAD to NADP with the latter more important in synthetic activity. One proposal for mitotic apparatus assembly involves NADP levels (Rebhun et al., 1975). The main pathway for sugar metabolism is the pentose shunt

(Epel et al., 1969) which also increases NADP levels and creates ribose sugars for synthetic processes. Oxygen consumption increases five-fold while glucose-6-phosphate dehydrogenase is released into the cytoplasm. These changes all occur within the first minute and are thus termed the early changes. The  $\text{Ca}^{++}$  level returns to its original value within three minutes while the pH change remains for ten minutes before slowly returning to normal.

The late changes occur within the first ten minutes. Protein synthesis begins to rise and increases five-fold as does lipid synthesis.  $\text{K}^+$  permeability increases and transport mechanisms for amino acids, phosphate, and nucleotides are activated, although DNA synthesis does not begin until after pronuclear fusion (Epel, 1969). These late events seem to depend upon the loss of acid (pH rise) that occurs during the first ten minutes after fertilization (Epel, 1977).

As mentioned previously, control of  $\text{Ca}^{++}$  concentration is necessary for MT polymerization in vitro (Weisenberg, 1972) and such control can be seen in vivo by microinjection (Kiehart and Inoué, 1976). It is thus important to study local free  $\text{Ca}^{++}$  concentrations at various times during cell division, although this is technically impossible at present. Nevertheless, some interesting indirect data has been collected.

Using radioactive  $^{45}\text{Ca}$  in sea water, Clothier and Timourian (1972) found three peaks of  $\text{Ca}^{++}$  uptake from and subsequent release back into the sea water during sea urchin zygote mitosis. These peaks occur during prophase, metaphase, and cytokinesis, so increased  $\text{Ca}^{++}$  uptake may be important to control of mitotic apparatus assembly as well as membrane furrowing. Also, as mentioned previously, a Ca-stimulated ATPase

has been found in isolated mitotic apparatuses (Mazia et al., 1972; Petzelt, 1972). Its activity peaks just before nuclear breakdown, in metaphase, and whenever monasters or cytasters are formed (Petzelt and Von Ledebur-Villèger, 1973). It seems analogous to that of muscle sarcoplasmic reticulum where it is involved in  $\text{Ca}^{++}$  regulation. A similar role during mitosis is probable, especially since a "relaxing factor" has been reported in sea urchin zygotes (Kinoshita and Yazaki, 1967). It is interesting that cell division stops in sea urchin zygotes when the ATP level is reduced experimentally to 50% of normal (Epel, 1969). Although much more ATP remains than is needed to move chromosomes to the poles, there is no movement. This suggests that the higher levels of ATP are required for  $\text{Ca}^{++}$  pumping and that such pumping is required for mitosis. Although no role has been established for the  $\text{Mg}^{++}$ -stimulated ATPase found in isolated mitotic apparatuses (Mazia et al., 1961), it may be involved in force generation (by analogy with dynein and myosin ATPase).

#### D. THE SEA URCHIN ZYGOTE AS A SYSTEM FOR STUDYING CELL DIVISION

Sea urchins have been used routinely as a source of dividing cells for well over 100 years. The animals are easy to collect in large numbers and in recent years, ripe ones can be obtained at most times of the year. For example, A. punctulata from the waters off New Jersey are ripe in the summer while those from Florida are ripe even in the winter. They can also be kept in marine aquaria with little care.

There are many advantages in using sea urchin gametes. They are easy to obtain by electrical stimulation or KCl injection which cause the animal to spawn. As many as 4,000,000 eggs can be obtained from one ripe female (A. punctulata)

and external fertilization occurs immediately upon insemination in artificial sea water yielding nearly 100% activation. Aeration or gentle magnetic stirring assure reasonable synchrony even beyond the first division, permitting experimentation with millions of eggs at nearly the same mitotic stage. In addition, the eggs can be activated by artificial parthenogenesis. Sea urchin eggs are large; that of A. punctulata, which is smaller than those of many other species, is 75  $\mu\text{m}$  in diameter and its mitotic apparatus is 50  $\mu\text{m}$  in length, observable even at low magnification. It should also be noted that zygotes in general are probably specialized for cell division and may exaggerate certain aspects of cell division relative to other types of dividing cells. This should facilitate the study of the mitotic process in much the same way as the study of striated muscle has helped the study of cell motility.

A. punctulata is one of the best studied species, especially at the Marine Biological Laboratory at Woods Hole, Massachusetts, its northern-most habitat, where it is ripe in the summer. Although it has presented some problems in fixation, the eggs of this species are easier to fix for electron microscopy than many others. The physiology and cytology of A. punctulata has been compiled and reviewed in a now classic book on sea urchins (Harvey, 1956), one which can be used as the starting point for many investigations. For all these reasons, A. punctulata was chosen for this study.

#### E. Major Research Objectives

As has been indicated in the discussion above, biochemical information about cell division has now advanced beyond ultrastructural. Moreover, partly because of the difficulty

in fixing sea urchin eggs for electron microscopy, the bulk of work has been done on isolated mitotic apparatuses. As already mentioned, however, up to 80% of the material is lost during isolation and some of what remains is a product of the isolation itself (Forer and Goldman, 1972). Thus, artifact is a major possibility. One would like to observe the mitotic apparatus in situ to find out what is present or missing compared with isolates. Lost material may well be responsible for the inability of the isolated mitotic apparatus to function.

Only one study has ever been done on the ultrastructure of mitotic stages in A. punctulata (Longo, 1972) but it suffers from fixation at 4°C, a temperature unsuitable for studying cold-labile MTs, a major component of the mitotic apparatus and the one that may be responsible for its function. Of special interest here is the finding by Cohen and Gottlieb (1971) of C-MTs, especially in the interzone of isolated mitotic apparatuses. It is possible, however, that they are an artifact of isolation. If they are not, then their existence in the interzone might be an important clue to mitotic apparatus function. To date, there is no knowledge as to how MTs assemble or disassemble in vivo.

The substructure of mitotic C-MTs has not previously been established. Are they merely MTs that have not closed, or are they incomplete, having less than the usual 13 protofilaments (Tilney et al., 1973)? If the latter is true, then would isolation under tubulin polymerizing conditions convert them to normal MTs? In fact, if they are still present in such a medium, it is strong evidence that they are not artifacts of the hexylene glycol isolation technique. Finally, since birefringence is a reflection of the amount of assembled

MTs, do C-MTs affect it? This would demonstrate an effect in vivo of a structure observed in situ.

Besides MTs, the other major component of the mitotic apparatus is ER. The recent advances in biochemistry discussed above have shown that  $Ca^{++}$  regulation is important both in vitro and in vivo. Since  $Ca^{++}$  is known to trigger muscle contraction and to be controlled by the sarcoplasmic reticulum (Podolsky, 1968; Ebashi et al., 1969), as an analogous system ER associated with the mitotic apparatus may be an important regulator of MT assembly and mitotic apparatus control. By affecting local  $Ca^{++}$  levels, perhaps in conjunction with the  $Ca^{++}$ -stimulated ATPase (as suggested by Bryan, 1975) it might even be responsible for mitotic apparatus function if the dynamic equilibrium hypothesis is correct. It is therefore of importance to investigate changes in ER as a function of mitotic stage and in relation to MT distribution. This has not been done adequately in previous work.

Interpretation of earlier structural data has been limited to a great degree because of the methods employed. For example, Longo (1972) removed aliquots of fertilized eggs periodically for examination by both electron and light microscopy. It was assumed that the stage observed in most cells in the light microscope was the same observed in the specific sections sampled in the electron microscope. While it is true that good synchrony can be achieved, it is by no means perfect and is variable from one batch of eggs to another, thereby introducing an element of doubt.

Another problem common to all previous ultrastructural work on sea urchin mitotic apparatuses in situ is the lack of cell orientation. Random sectioning through pellets of zygotes

makes it difficult or impossible to know section location or orientation with respect to the cell and the mitotic apparatus axis. Moreover, any spindle cross-sections observed cannot be staged without serial sectioning.

To overcome the problems cited above, the present study has employed thick Epon sections of cells fixed at various times. This is necessary because osmium tetroxide, required to get good fixation, renders whole eggs opaque. Thick sections make the accurate selection of cells of known stage and orientation possible. These were then re-embedded and pre-selected cells serially thin sectioned (either cross or longitudinally) for electron microscopy, permitting 3-dimensional analysis.

The major experimental objective of this work was to examine changes in cell fine structure at critical stages of the first mitotic cycle in A. punctulata. The initial focus was on MTs and ER, in particular, attempting to establish the reality (or artificial nature) and substructure of C-MTs. In the course of this investigation, ultrastructural evidence has been observed suggesting the involvement of annulate lamellae and heavy bodies with mitosis. Additional major objectives of this work were to correlate, where possible, in situ structural events with known biochemical ones, and to compare in situ spindle structure with that of the isolated spindle.

## II. MATERIALS AND METHODS

### A. Collection of Eggs and Sperm

Mature Arbacia punctulata were obtained from the Florida Marine Biological Specimen Co., Inc., Panama City, Florida and from the Shark River Marine Laboratory, Wall, New Jersey. They were kept at 20°C in large aquaria filled with Instant Ocean synthetic sea salts (Aquarium Systems Inc.) dissolved in distilled water.

Sea urchins were sexed by placing them aboral side up in a finger bowl filled to about 1 cm with Instant Ocean sea water. Electrical stimulation at 10 to 15 volts through non-toxic lead electrodes placed across the gonopores induced shedding (after Harvey, 1956). The reddish eggs are easy to distinguish from the whitish sperm of the males.

Females selected for egg collection were thoroughly washed with Marine Biological Laboratory formula (MBL Formulae and Methods V, 1956) synthetic sea water (Table 1) to remove any sperm adhering to the animals. MBL formula sea water was the only one used in contact with eggs and was made up fresh by dilution of 3X stock solution. Eggs were collected by electrical stimulation of ripe sea urchins placed aboral side down on a beaker full of MBL formula sea water. This causes immediate shedding of eggs in long red threads or in thick clumps that sink to the bottom of the beaker where they form a thick carpet. The "egg water" was removed and the eggs washed 3 to 5 times in fresh MBL sea water to remove inhibition.

Sperm were collected by either removing the testes or by electrical stimulation across the gonopores. In the latter case, the sea urchin remained aboral side up in a finger bowl and the sperm collected by Pasteur pipette.

TABLE 1

## MBL FORMULAE FOR SYNTHETIC SEA WATERS

WITH CALCIUM (g/l)			MOORE'S CALCIUM-FREE (g/l)	
<u>SALT</u>	<u>1X</u>	<u>3X Stock</u>	<u>1X</u>	<u>5X Stock</u>
NaCl	24.72	74.16	25.48	127.40
KCl	0.67	2.01	0.72	3.60
CaCl <sub>2</sub> ·2H <sub>2</sub> O	1.36	4.08	—	—
MgCl <sub>2</sub> ·6H <sub>2</sub> O	4.66	13.98	6.94	34.70
MgSO <sub>4</sub> ·7H <sub>2</sub> O	6.29	18.87	4.11	20.55
NaHCO <sub>3</sub>	0.18	added later; see below	—	—

In practice, MBL sea water with calcium was made up as a 3X stock and diluted as needed. 0.18 g/l NaHCO<sub>3</sub> was added only after dilution to prevent precipitation. The calcium-free sea water was made up as a 5X stock and diluted as needed. Stocks were refrigerated until used.

Fertilization was effected by pouring 100 ml of a sperm suspension into 100 ml of an egg suspension and pouring back and forth. The sperm suspension was made by adding 1 drop of sperm to 100 ml MBL sea water, mixing thoroughly, pouring off all but 40 ml, and refilling to 100 ml with MBL sea water. If "dry" sperm from excised testes was used, all but 10 to 20 ml was poured off and the remainder filled to 100 ml. The egg suspension consisted of all the eggs from one female, usually about 3 to 5 ml when packed, suspended in 100 ml of MBL sea water stirred magnetically. After washing in MBL sea water to remove excess sperm, some zygotes were removed as a control to make sure that the fertilization rate was at least 95% and development normal. All experiments were done in a water bath at 20°C with constant, gentle, magnetic stirring of the cells to maintain synchrony.

#### B. In Situ Studies

The zygotes were allowed to develop until the desired mitotic stage (Table 2) and then fixed in 6% glutaraldehyde in MBL sea water (after Tilney and Gibbins, 1969) by adding equal volumes of zygote suspension to 12% glutaraldehyde in MBL formula sea water, pH 7.6. The fixative was prepared by adding 24 ml of 50% glutaraldehyde (EMS, Fort Washington, Pa.) to 33.3 ml of 3X MBL stock solution and after adjusting the pH to 7.6, adding enough distilled water to make a total volume of 100 ml. After 1.5 hr of fixation, the cells were washed twice in MBL sea water and once in 0.1 M phosphate buffer, pH 7.2. They were then postfixed in 1% osmium tetroxide in 0.1 M phosphate buffer, pH 7.2 for 30 min. Other methods of fixation were tried (Table 3) but did not result in the same quality of fixation. These methods included some without

TABLE 2  
ALL CELLS EXAMINED BY ELECTRON  
MICROSCOPY AT EACH MITOTIC STAGE

<u>Type of Study</u>	<u>Stage Examined</u>	<u>Numbers of Cells</u>
<u>In situ</u>	Unfertilized	3
	Streak	2
	Prophase	1
	Metaphase	2
	Anaphase	4
Hexylene glycol isolates	Metaphase	0
	Anaphase	3
Modified polymerization media	Metaphase	2
	Anaphase	1

TABLE 3  
VARIOUS FIXATION METHODS TRIED

<u>Glutaraldehyde Primary Fixative (followed by) OsO<sub>4</sub> Postfixation</u>	
2.5% in 70% MBL sea water	2% in MBL sea water
2.5% in 100% MBL sea water	1% in distilled water
2.5% in 100% MBL sea water	None
6% in 0.5% M sodium acetate, pH 6.1*	None*
6% in 100% MBL sea water	None
6% in 100% MBL sea water**	1% in phosphate**

\*Harris, 1965

\*\*Tilney and Gibbins, 1969

osmium tetroxide in an attempt to prevent the eggs from becoming opaque. In addition, to supplement glutaraldehyde fixation when osmium tetroxide was not used, solutions of 2% uranyl acetate in either 70%, 95%, or 100% ethanol at 60°C were used to stain the eggs before complete dehydration. In all cases, controls showed this to be of no help.

The osmium tetroxide was pipetted off and after 3 washes in distilled water, the cells were dehydrated in ethanol (50%, 70%, 95%, 100%), followed by propylene oxide, and infiltrated with Epon (R.P. Cargille Laboratories, Inc., Cedar Grove, N.J.). BEEM capsules or hemihyperboloid SPB capsules (BEEM, Inc., Bronx, N.Y.) were used for embedding. Polymerization was effected by heating at 60°C for 3 days.

The Epon blocks were trimmed to faces of about 1 mm on a side and thick sectioned by either glass or diamond knives on a Sorvall Porter-Blum MT-2 ultramicrotome. Sections of 5 to 10  $\mu$ m thickness were placed in immersion oil on a slide and viewed with a Zeiss phase contrast microscope (Fig. 3). When a cell of the desired mitotic stage and orientation was found, it was photographed through a Nikon M-35s camera back attached to the phase contrast microscope through a Zeiss adapter.

The section was then re-embedded for thin sectioning by washing off the immersion oil in 2% MICRO solution (International Products Corp., Trenton, N.J.), rinsing with water, air drying, and washing with Epon. The section in a drop of Epon was picked up by a Pasteur pipette and placed either on the tip of a BEEM capsule embedment blank or on top of a Chang flat embedding mold embedment blank (EMS, Fort Washington, Pa.) prepared previously by polymerizing Epon without

FIGURE 3. Use of thick sections.

3A. Typical thick section through a pellet of streak stage cells embedded in Epon. These sections were viewed to single out cells of desired stage and orientation. They were then re-embedded for thin sectioning and electron microscopy.

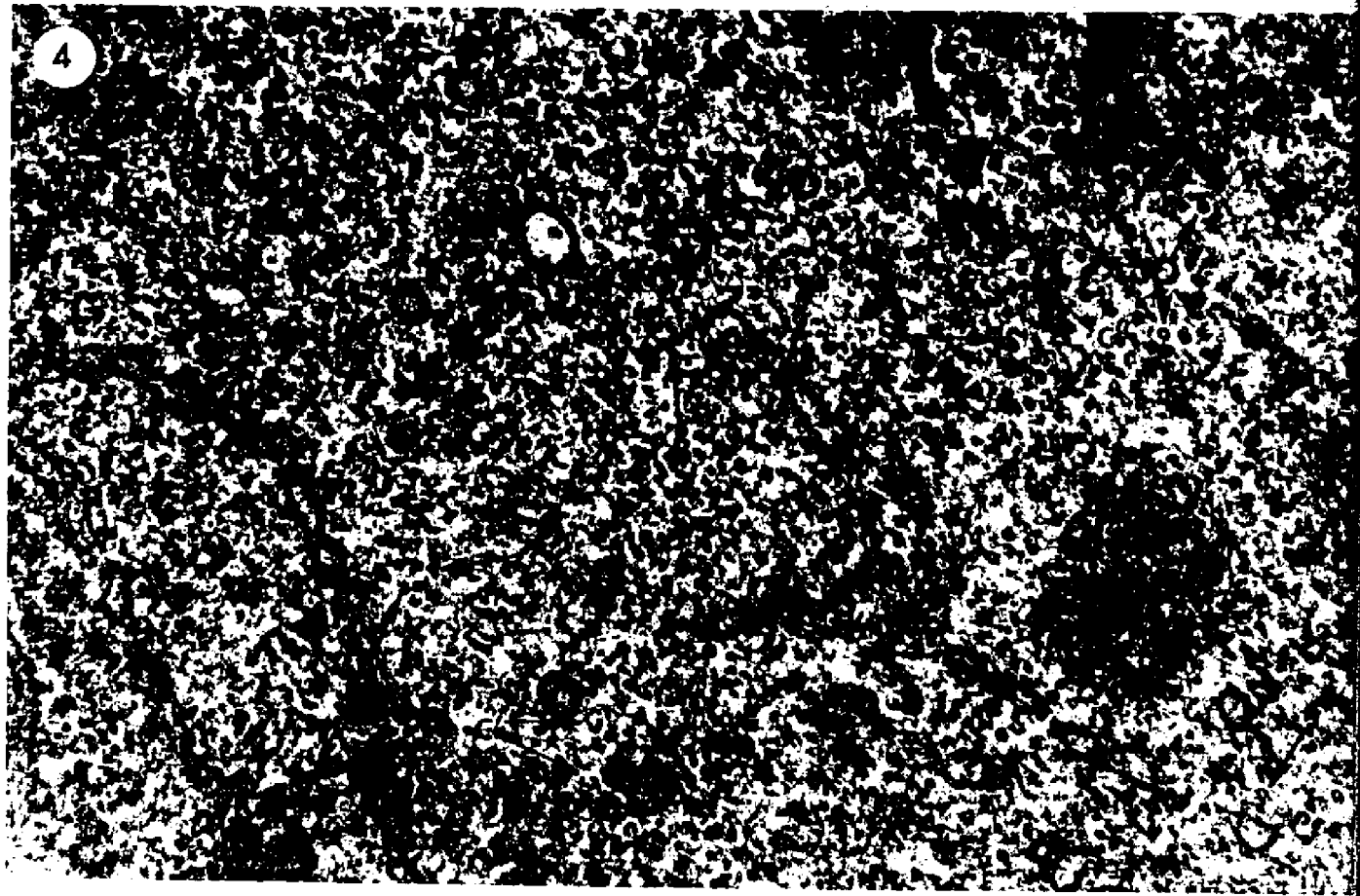
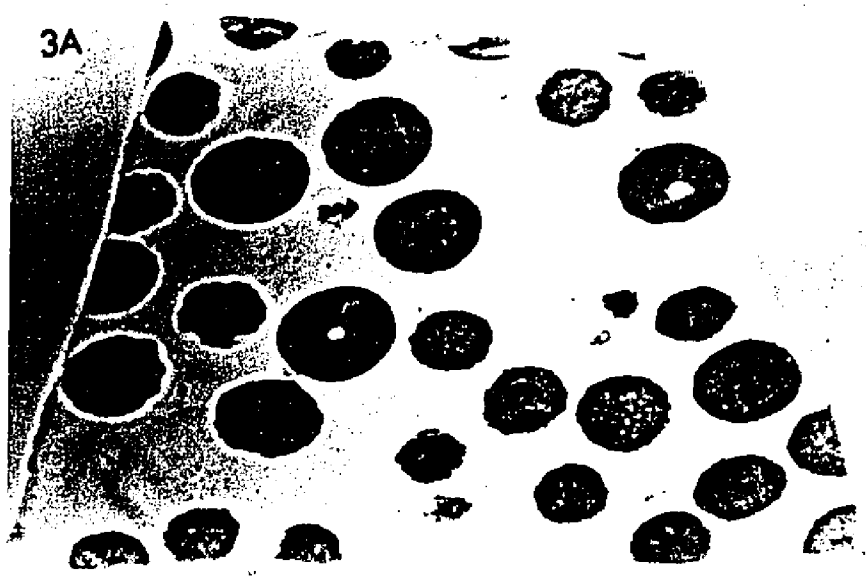
Phase Contrast. X180

3B. Typical trimmed face of a BEEM block with a re-embedded thick section. The face is approximately 200  $\mu\text{m}$  X 100  $\mu\text{m}$ . The cell on the right is the streak stage cell of Fig. 15. Note the irregular, trapezoidal shape of the face.

Dissecting Scope. X100

FIGURE 4. Interzone of early anaphase cell. Note the many C-MTs (C-arrows). Normal MTs (O-arrows) are easier to distinguish since some C-shaped structures are ambiguous (?-arrows). Openings between the ends of C-MTs may vary in length from fairly large (C'-arrows) to fairly small (C''-arrows). Sometimes, 2 C-MTs may join together to form an S-shape (S-arrow). Sometimes 2 normal MTs are connected by a short, line-like structure bridging the distance between them (B-arrow). See page 42.

EM. X58,500



a specimen in the proper mold. In the case of the Chang mold, the underside is "scratched" so that it is translucent but not transparent. If the section is added to this side and a drop of Epon spread to fill in the scratches, the blank becomes transparent and the section easily seen. The blanks with their sections in a drop of Epon were placed in an oven at 60°C for 2 to 3 days for polymerization.

Trimming for thin sectioning the thick section longitudinally, i.e., parallel to the spindle axis, was done by placing the BEEM capsule re-embedments under a Bausch and Lomb stereoscopic zoom dissecting microscope equipped with 33X eyepiece lenses which make it capable of 99X total magnification. By matching phase contrast photomicrographs to the view of the sections in the dissecting microscope, it was possible to locate and identify a desired cell. Judicious trimming isolated the cell from its neighbors. Although this often meant trimming a block face to as little as 200  $\mu\text{m}$  in length (Fig. 3B), it makes it possible to distinguish this zygote easily from any neighbor in the electron microscope.

Trimming for cross-sectioning the thick section, i.e., perpendicular to the spindle axis, was even more difficult. The phase contrast photomicrographs were examined to see how the desired zygote in the flat embedment should be oriented for trimming. A line was drawn on the print perpendicular to the zygote's spindle axis a little in front of where sectioning of the actual cell should begin. The cells through which this line passed served as markers. Under the dissecting microscope, an industrial razor blade was pressed deeply into the Epon along the corresponding cells and then hammered

until the embedment split. The part with the desired cell (whose "new" side now corresponds to the line) was placed in a vise-type holder and further trimmed under the dissecting microscope using a China marker to mark the edge of the plastic to be removed. This is difficult because the cell could not be seen on edge while trimming. Reliance on the marks made on the edge while viewing the cell (section) broadside and from other angles is therefore necessary. This results in the desired cell isolated at the tip in correct orientation for thin sectioning.

The faces of all blocks were made as irregular trapezoids, with one side making a more acute angle with the base than the other side. This differentiates each corner and permits identification of the desired cell as well as the direction of sectioning when viewing with the electron microscope.

Serial sectioning was done with a DuPont diamond knife on a Sorvall Porter-Blum MT-2 ultramicrotome. Sections were either silver-grey (60 nm) or silver (90 nm) depending upon whether they would be collected on formvar-coated loops or on copper mesh grids (200 or 300 mesh; Pelco, Tustin, Cal.). The number of sections cut, as well as their color, was recorded for later use in determining the location of each section within the cell. Silver-grey sections were picked up as a ribbon on wire loops coated with formvar (Monsanto Corp.). Uncoated, acetone-washed, slot grids (Pelco) were placed on a peg of similar diameter covered with parafilm (American Can Co., Neenah, Wisc.) which keeps them from shifting position. While viewing through the dissecting microscope, the sections on the formvar-coated loops were placed directly

over the slot in the grid and passed down over the grid and peg, breaking the formvar connection to the loop and draping the formvar over the grid. Jewelers forceps removed excess formvar so that it could not be peeled off accidentally.

Staining was done for 20 min in saturated uranyl acetate in 50% ethanol (Dawes, 1971) followed by 5 to 7 min in lead citrate (Reynolds, 1963). Mesh grids were floated on drops of stain placed on parafilm in a Petri dish. The bottom of the Petri dish was lined with a filter paper soaked with either 50% ethanol for uranyl acetate or sodium hydroxide for lead citrate. Since handling tended to break the formvar, slot grids were often stained by the Hiraoka method (Polysciences, Inc., Rydal, Pa.) which resulted in slightly more contamination. In this method the grids are made to stand upright by placing an edge of each grid in special slots cut into a flexible, slow-to-relax plastic sheet. The sheet with its attached grids is then turned upside-down over a well of stain so that the grids are all submerged and stained at one time. Washing is done in the same way so that handling of grids with jewelers forceps is minimized.

All sections were viewed with an Hitachi HS-8 electron microscope operating at 50 kV.

### C. Mitotic Apparatus Isolation

#### 1. Hexylene glycol

For isolation of mitotic apparatuses in hexylene glycol (after Kane, 1962), eggs were collected, washed and fertilized as above except that 50 ml of sperm suspension was added to 50 ml of egg suspension gently stirring magnetically. The eggs and all solutions were kept at 20°C. To soften and swell the fertilization membrane prior to its removal, 100 ml of a

fresh 2 mg/ml mercaptoethylgluconamide solution (CycloChemical Corp., Los Angeles, Cal.) was added to the eggs 30 sec after fertilization (Mazia et al., 1961). The solution is made by dissolving the mercaptoethylgluconamide in Moore's (MBL Formulae and Methods V, 1956) calcium-free sea water (Table 1) and adjusting the pH to 8.2 with NaOH. This solution must be made up fresh and used immediately.

After 10 min of stirring, the cells were poured through a fine silk mesh (Dufour bolting) stretched across a syringe barrel (end removed) to strip off the fertilization membranes (Harris, 1965). After settling, the cells were washed twice in calcium-free sea water and gently stirred until asters became apparent. At this point the zygotes were washed twice in monovalent salt solution consisting of 19 parts 0.5 M NaCl and 1 part 0.5 M KCl which removes divalent cations facilitating lysis. Washing was done by gentle, hand centrifugation sedimenting zygotes in conical centrifuge tubes.

Lysis was accomplished by suspending the cells in isolation medium consisting of 1.0 M hexylene glycol (2-methyl-2,4,-pentanediol; Matheson, Coleman, and Bell, East Rutherford, N.J.) in 0.1 M potassium phosphate buffer, pH 6.3. After 30 sec the pigmented supernatant was discarded and the cells resuspended. Swirling on a vortex mixer resulted in release of the mitotic apparatuses from the cells. Gentle centrifugation separates the suspended mitotic apparatuses from the pelleted cellular debris. The isolated mitotic apparatuses were then stored on ice. An equal volume of 0.006 M  $MgCl_2$  in isolation medium at 0°C was added to make a final concentration of 0.003 M. This helps to preserve the structure of the

mitotic apparatus (Goldman and Rebhun, 1969). From this point on, the isolation medium contained 0.003 M  $MgCl_2$ . Five washes in isolation medium with  $Mg^{++}$  at 0°C was followed by suspension in the same medium at room temperature. This was required to prevent the tannic acid from precipitating in the next step.

The mitotic apparatuses were fixed by adding an equal volume of 5% glutaraldehyde and 16% tannic acid (Sigma, St. Louis, Mo.) in isolation medium with  $Mg^{++}$ , pH 6.3, making a final concentration of 2.5% glutaraldehyde and 8% tannic acid (Mizuhira and Futaesaku, 1971; Tilney et al., 1973). The solution was prepared by adding the tannic acid to hot, concentrated stock solutions and continued heating in a water bath. The glutaraldehyde was added, the pH adjusted to 6.3 with 3 N KOH, and diluted to the proper volume just before use. The stock solutions used were 0.5 M potassium phosphate buffer, 0.06 M  $MgCl_2$ , and 50% glutaraldehyde (EM grade from EMS, Fort Washington, Pa.).

After 1 hr fixation at room temperature, the mitotic apparatuses were washed twice with isolation medium and post-fixed with 1% osmium tetroxide in isolation medium, pH 6.3. 45 min later the osmium was removed by Pasteur pipette and the mitotic apparatuses washed twice with distilled water. Dehydration and infiltration was as described above. The apparatuses were flat-embedded directly in Chang molds (EMS) and polymerized at 60°C for 3 days. Afterwards, a light coat of Epon was applied to the translucent bottom surface, inverted, and returned to the oven for 2 to 3 days more, resulting in transparency for phase contrast microscopy.

The flat embedments were taped by their edges to a glass

slide and viewed by phase contrast microscopy to find mitotic apparatuses of the proper stage and condition. When such a mitotic apparatus was seen, its location was marked with a Sanford Sharpie felt-tipped marker pen. At least four dots were placed on the surface of the Epon around the maximally-narrowed cone of light coming from the condenser. A "scratcher" could not be used because it moved the block; other types of markers and pens would not write on the Epon. The mitotic apparatus was then photographed through the microscope.

Using an additional 2X objective lens (Bausch and Lomb) on the 99X dissecting microscope, the mitotic apparatuses could be seen and the dots used as a guide to the selected one. A razor blade was pushed through the Epon deep into the embedment perpendicular to the spindle axis where sectioning of the desired mitotic apparatus was to begin. A hammer was used to split the block, which was further trimmed as described above, using marker dots and the high-powered dissecting microscope to remove excess plastic and isolate the desired mitotic apparatus at the tip. Further work was done as described above for the mitotic apparatus in situ.

## 2. Modified polymerizing medium

For isolation of mitotic apparatuses in PIPES (piperazine-N,N'-bis [2-ethane sulfonic acid]), buffer (after Rebhun et al., 1974), eggs were collected, washed, fertilized, and handled as in the hexylene glycol isolation until the desired mitotic stage was reached. The zygotes were then washed in Moore's calcium-free sea water 3 times in order to remove  $Ca^{++}$  which destroys MTs in these preparations (Rebhun et al., 1974). Two different EGTA concentrations were used in the isolations, 20 mM and 50 mM (Rebhun, 1976) to chelate endogenous calcium.

All solutions contained 0.1 M PIPES buffer (P; Sigma), 10 mM TAME (T; p-tosyl arginine methylester HCl) which is an inhibitor of proteolytic enzymes (Sigma), 0.25 mM  $MgCl_2$  (M), and either 20 mM EGTA (E-20) or 50 mM EGTA (E-50). The isolation media are thus designated PTME-20 and PTME-50 below. Wash solutions included either 0.6 M glycerol (G-PTME-20) in the lower and 0.5 M glycerol (G-PTME-50) in the higher EGTA concentration. This ensures isotonicity and prevents early cell lysis. Sucrose was not as good as glycerol for this purpose, resulting in deformed cells and inhibition of division.

After removal of fertilization membranes and the 3 washes in Ca-free sea water, the cells were washed in either G-PTME-20 or G-PTME-50, pH 6.85 (by KOH). Isolation was effected by suspension of the zygotes in 3X their volume of either PTME-20 or PTME-50 to which 0.5% Triton X-100 (Sigma) was added. Vortexing lysed the cells releasing their mitotic apparatuses. These were fixed with 2.5% glutaraldehyde in either PTME-20 or PTME-50, pH 6.85 at room temperature because the MTs are cold-labile in these solutions just as they are in vivo (Rebhun et al., 1974). Three washes in distilled water were followed by postfixation in 1% osmium tetroxide for 1 hr at pH 7. No tannic acid was used because it forms precipitates in these media. The isolated mitotic apparatuses were then handled as described above for hexylene glycol isolates.

#### D. Counts of Microtubules

MTs were counted by viewing prints of MTs at magnifications of about 50,000X and tabulating them with two hand counters, one for 0- or normal MTs and one for C-MTs. Each MT was crossed out with a China marker so that none could be

counted twice. Since serial sectioning was done, the exact location of the cross section within the cell was known. In these counts, only obvious C- and O-MTs were tabulated (C- and O-arrows, Fig. 4) while ambiguous ones were not (?-arrows, Fig. 4). On the other hand, when two C-MTs were viewed attached by their ends to form an S-shape, they were counted as two C-MTs (S-arrow, Fig 4). In general, C-MTs were more difficult to recognize with certainty than O-MTs. Although usually shaped like the letter "C", the openings between the ends of the "C" may vary in size (compare C'-arrow with C''-arrow, Fig. 4). Also, small C-MTs of only a few protofilaments may appear as short, straight segments rather than curved ones and the rough background conceal it. Despite these problems, many C-MTs were obvious and easily tabulated.

#### E. Polarization Microscopy

Polarization microscopy was performed on Lytechinus variegatus zygotes because pigment present in the Arbacia punctulata egg prevents such viewing in that species. A Zeiss microscope equipped for polarization microscopy was used to detect birefringence. The sea urchins were obtained from the Bermuda Biological Station and eggs collected by injection of 0.5 M KCL solution (Harvey, 1956). Sperm were obtained by removing the testes and gametes were then treated like those of Arbacia punctulata.

### III. RESULTS

#### A. Fine Structure of the Mature, Unfertilized Arbacia Egg

When viewed with the electron microscope, the mature, unfertilized Arbacia egg reveals a cytoplasm filled with organelles, granules, and vacuoles.

##### 1. Endoplasmic Reticulum

The mature egg does not have the usual type of ER, i.e., it does not form a reticulum in the cell. Rather, there are numerous vesicles of assorted sizes and many irregular in shape (v, Fig. 5). Some are about 1.0  $\mu\text{m}$  in diameter, although most are smaller than mitochondria. They are bounded by a 100  $\text{\AA}$  thick membrane and a few have a fuzzy material within (v1, Fig. 6).

The vesicles of this ER are often found in contact with other organelles and granules, so they may shuttle among them and play a role in intracellular transport. Yolk granules (Y1, Fig. 5), pigment vacuoles (P, Fig. 5), Golgi apparatuses (G, Fig. 5, inset), annulate lamellae (A, Fig. 7), and mitochondria (Mi1, Fig. 5) are all seen in contact with ER vesicles.

Most of the vesicular ER appears to be smooth. Where ribosomes are seen to abut the vesicles, it is difficult to determine whether they are really on the membrane and not just part of the great number of free ribosomes dotting the background. In any case, there is no obvious extensive rough ER.

##### 2. Yolk

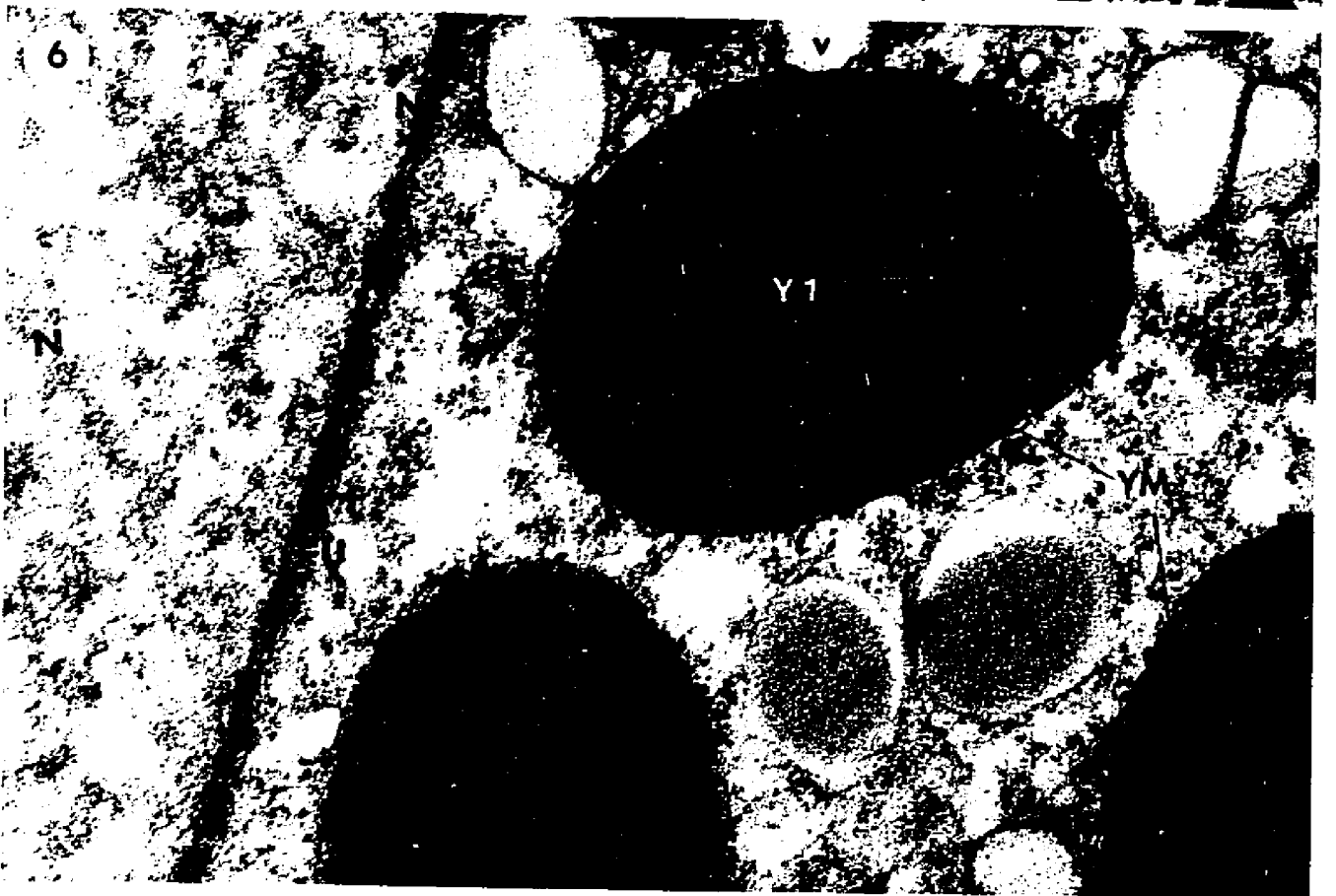
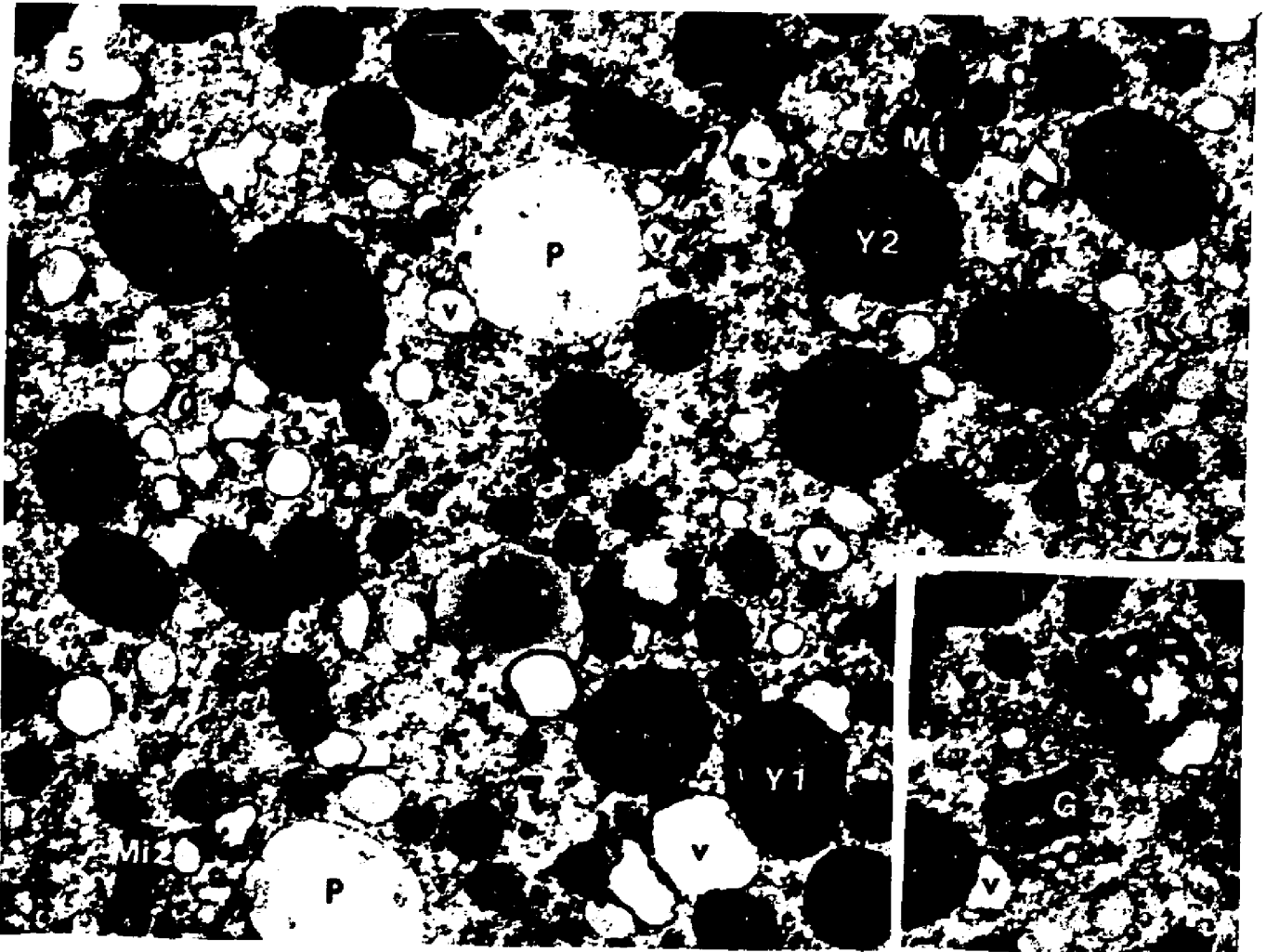
Yolk granules (Y, Fig. 5) are perhaps the most striking feature. There are a great many of these large, electron-dense granules distributed throughout the cytoplasm. In sec-

FIGURE 5. Cytoplasm of the mature unfertilized egg. The large, electron-dense yolk granules (Y) are the most obvious feature. The ER is all smooth and vesicular (v). It is often associated with yolk (Y1) and mitochondria (Mi1). Mitochondria also seem to be associated with yolk (Y2). Although most mitochondria are round, some are elongated (Mi2). Lipid droplets (L) can be distinguished from yolk by the membrane closely apposed to the lipid as well as their greyish color since lipid is less electron-dense than yolk. Mitochondria do not associate with lipid at this stage. Pigment vacuoles (P) are seen throughout the cytoplasm until after fertilization when most migrate to the cortex. EM x 16,400.

Inset. Golgi apparatus (G). They are small, widely scattered, and few in number in the mature egg. Vesicles of ER (v) are often found in contact with them.

EM x 16,400.

FIGURE 6. High magnification of nuclear area of egg. Nucleus (N) is surrounded by nuclear envelope (NE). The envelope is composed of two membranes coated on the cytoplasmic side with fuzzy material (F) interrupted by uncoated areas (U). The nucleus has interconnected fibers of various diameters in the nucleoplasm. Membranes around yolk granules (YM) and amorphous material in the vesicular ER (v1) are obvious. Part of an ER vesicle (v) adjacent to a yolk granule (Y1) is shown. EM x 48,100.



tions they usually appear round, ellipsoid, or pear-shaped, and may be over 1.5  $\mu\text{m}$  long. These differences are probably due to the various planes of section through the granule. Higher magnification reveals a thin, 60 to 80  $\text{\AA}$  thick irregular membrane (YM, Fig. 6) around the yolk.

Many of the yolk granules appear to be in intimate contact with small, apparently smooth vesicles of ER. Also, mitochondria (Mi) are often found in contact with yolk (Y2, Fig. 5). Although the large majority of yolk granules exhibit a homogeneous electron density, a few are heterogeneous (Y3, Fig. 8). These few are seen to be in contact with mitochondria and suggest that the yolk is being metabolized.

### 3. Pigment Vacuoles

Pigment vacuoles are another prominent feature of the Arbacia egg. They appear as large, circular, electron-transparent vacuoles (P, Fig. 5). In the living egg they contain the reddish "echinochrome" pigment. This pigment is lost during the preparation of the cells for electron microscopy so that except for a few wisps of material, the vacuoles exhibit little internal structure (Tilney and Marsland, 1969). Their identification was made easy by the fact that although dispersed throughout the unfertilized egg, at fertilization most migrate to the cortex, forming a highly pigmented layer around the entire zygote. Although sometimes difficult to distinguish from ER vesicles, in most cases their size and wispy content differentiate them. In fact, the pigment vacuoles are often found in contact with ER vesicles (P, Figs. 5 and 9).

### 4. Lipid Droplets

The lipid droplets (L, Fig. 5) are not as abundant as

FIGURE 7. Annulate lamellae (A) of unfertilized egg. They are coated with an amorphous fuzzy material (F). What is possibly a pore in face view (Po) is seen nearby. An interaction with vesicular ER (v) is suggested by its proximity and apparent connection. EM x 20,600.

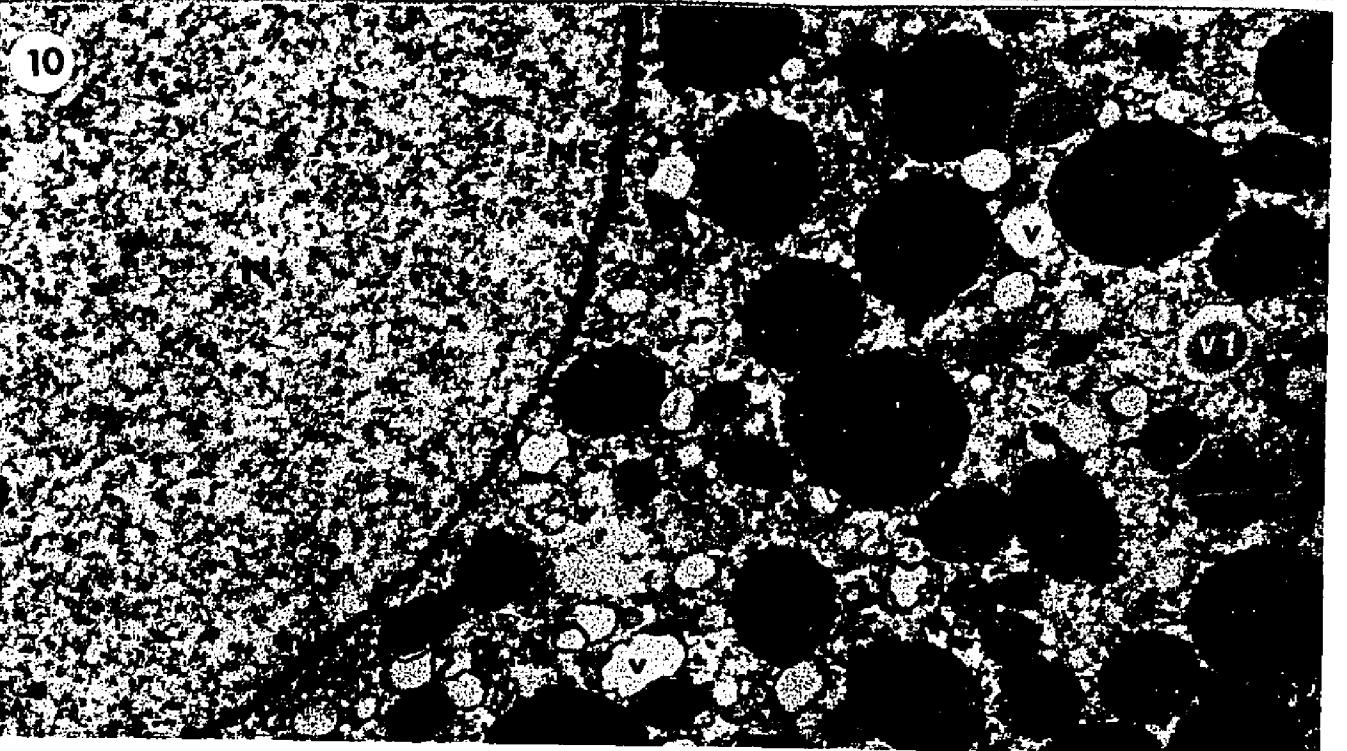
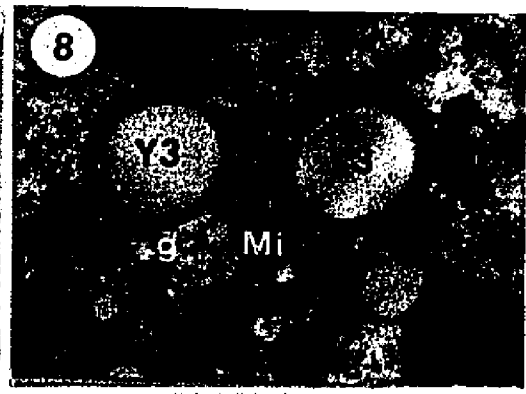
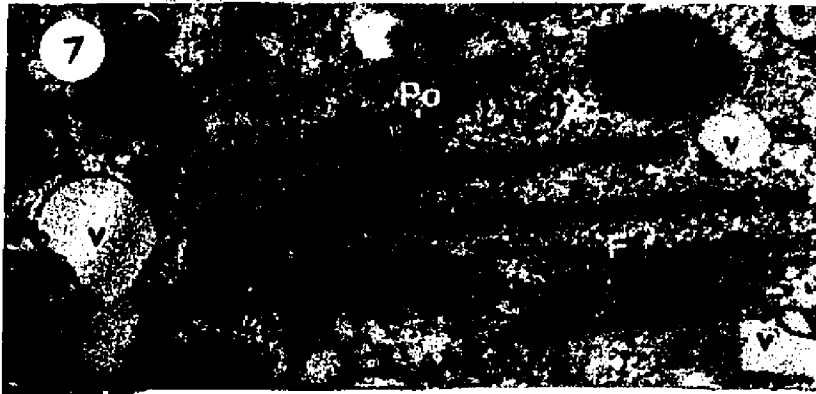
FIGURE 8. Heterogeneous form of yolk granules (Y3) in the egg. They have an electron-transparent center and are surrounded by mitochondria (Mi). Note mitochondrion with a dense granule (g). EM x 20,600.

FIGURE 9. Cortical region of egg. Except for the cortical granules (C), all other granules, particles, and organelles are randomly distributed. Note association of pigment vacuole (P) with ER vesicle (v). The egg membrane has short microvilli (mV) except over cortical granules. Lipid (L), mitochondria (Mi), and yolk (Y) are seen. EM x 14,200.

Inset. Higher magnification of the cortical granule (C).

Its periphery is less electron-dense than its core of fine granules. Note the typical trilaminar appearance of the cell membrane (CM). EM x 41,900.

FIGURE 10. Nuclear region of unfertilized egg. Nucleus (N) is spherical and surrounded by nuclear envelope (NE) with few pores. Nucleoplasm has a fibrous, homogeneous network. Note the presence of the same types of particles and organelles as in the rest of the cytoplasm: lipid droplets (L), mitochondria (Mi), and vesicular ER (v). One of the vesicles is filled with an amorphous material (v1) distinguished from lipid droplets (L) by its irregular membrane which is not closely apposed to the contents. EM x 15,200.



yolk granules but their electron-dense appearance and circular profile in electron micrographs make them hard to distinguish from the latter. Fortunately, upon centrifugation of eggs, they migrate to the centripetal pole, making their identification easier. There, it can be seen that they appear as a lighter grey than yolk granules and can thus be distinguished from the latter (Anderson, 1970). Also, the lipid droplets are generally smaller, about 0.5 to 0.8  $\mu\text{m}$  in diameter, and are usually round. Their membrane is more obvious than that of the yolk granule and closely adheres to the lipid. This latter feature distinguishes them from ER vesicles containing amorphous material (v1, Fig. 6).

#### 5. Mitochondria

Mitochondria are found throughout the egg. They often appear in groups of two or three (or more) and sometimes alone (Mi, Fig. 5). As mentioned above, they are often contiguous with yolk granules (Y2, Fig. 5 and Y3, Fig. 8). Many have small, irregular blebs (b, Fig. 9) but only rarely is one found with a granule. These granules are very small when they do occur (g, Fig. 8).

Most mitochondria are round or slightly ellipsoid. They are about 0.5  $\mu\text{m}$  in diameter. A few are elongated to about 0.9  $\mu\text{m}$  and may represent mitochondria in the act of division since they usually have a central constriction (Mi2, Fig. 5).

#### 6. Golgi Apparatus

Unlike the immature oocyte which has much Golgi to assist in cortical granule production (Anderson, 1968), the mature egg has only a few scattered Golgi apparatuses (G, Fig. 5, inset) and these are small. They are composed of the usual stack of membranes and vesicles, the latter presumably fusing

with or budding from the stack.

## 7. Cortex

Close observation of the cell membrane (CM, Fig. 9, inset) reveals its trilaminar nature. The membrane is irregular because of the short microvilli (mV, Fig. 9) which project only about 0.2  $\mu\text{m}$  from the egg surface.

Although cortical granules (C, Fig. 9) can be found throughout the cytoplasm of the immature oocyte (Anderson, 1968), they are restricted to the cortex of the mature egg. There, they are barely separated from the cell membrane. (The cortical granule in Fig. 9 is 40  $\text{\AA}$  from the plasma membrane at its closest point.)

Arbacia cortical granules are bounded by a membrane, have a circular profile, and are about 1.0  $\mu\text{m}$  in diameter. They have a bipartite structure. The periphery has a more even and less electron-dense appearance than the grainy, electron-dense center. Such granules are not found directly under a microvillus.

The cortex also contains yolk (Y), lipid (L), ER vesicles (v), mitochondria (Mi), and pigment (P, Fig. 9).

## 8. Annulate Lamellae

Patches of annulate lamellae are found in the mature egg, especially near the cortex (A, Fig. 7). They have also been reported in the immature oocyte (Anderson, 1968) and as part of another organelle, the heavy body (Harris, 1967). (This study could not confirm the existence of heavy bodies in the mature egg. Of the small number of heavy bodies that may be present, none appeared in the few sections surveyed. Only a limited number of sections were examined because this stage

was not critical, being used only for comparison. They are commonly found during the streak stage (HB, Fig. 19), however.)

Coating the lamellae and easily seen between the stacks of lamellae is a "fuzzy" material (F, Fig. 7). This material is regularly interrupted by uncoated areas. The lamellae often appear to be continuous with vesicles of the ER (v, Fig. 7). Face views of what may be a pore of the annulate lamellae are often seen nearby (Po, Fig. 7).

#### 9. Microtubules

No unequivocal MTs are seen although MTs of meiotic apparatuses had been present previously during polar body formation.

#### 10. Nucleus

The nuclear envelope is circular with no irregularities (NE, Fig. 10). The nucleoplasm is fibrous and evenly distributed throughout the nucleus (N, Fig. 10). Higher magnification of the nuclear envelope (NE, Fig. 6) shows that it is coated on the cytoplasmic side with a fuzz similar to that of the annulate lamellae (F, Figs. 6 and 7). Like the annulate lamellae fuzz, the nuclear envelope fuzz is discontinuous, leaving many areas uncoated (U, Fig. 6). The early oocyte nucleus is reported to have many pores (Anderson, 1968), but the mature egg nucleus does not appear to have as many (Figs. 6 and 10). The perinuclear area (Fig. 10) contains many yolk granules (Y), lipid droplets (L), mitochondria (Mi), and ER vesicles (v).

#### B. Fine Structure of the Streak Stage

From phase contrast light micrographs of serial longitudinal sections through a representative streak stage cell (Fig. 11, A to I), a clay model may be constructed showing

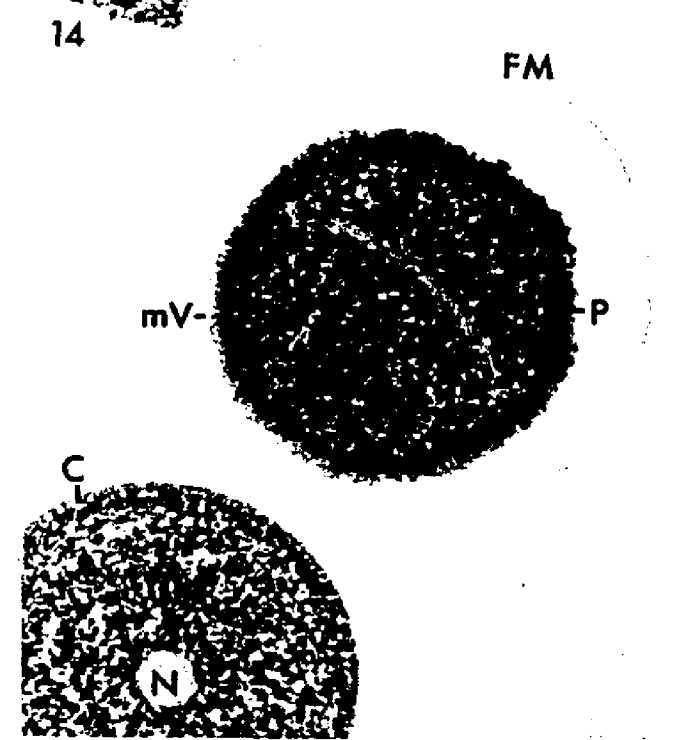
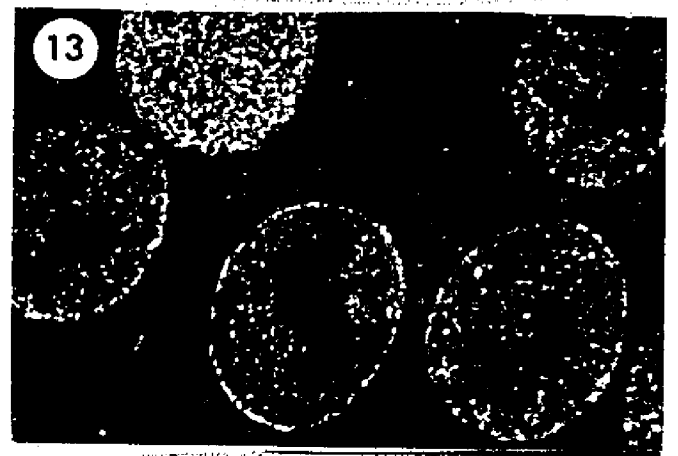
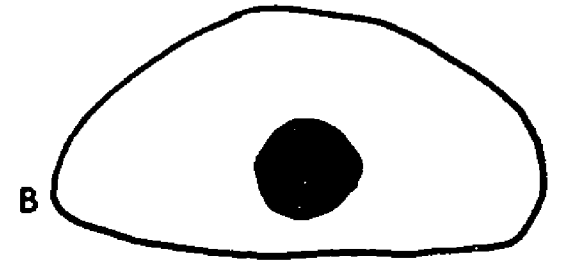
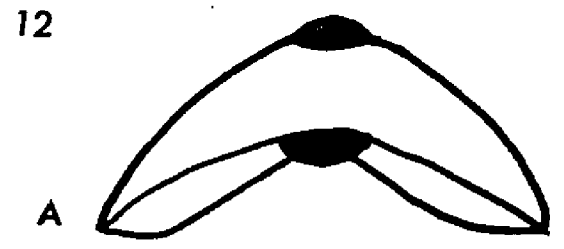
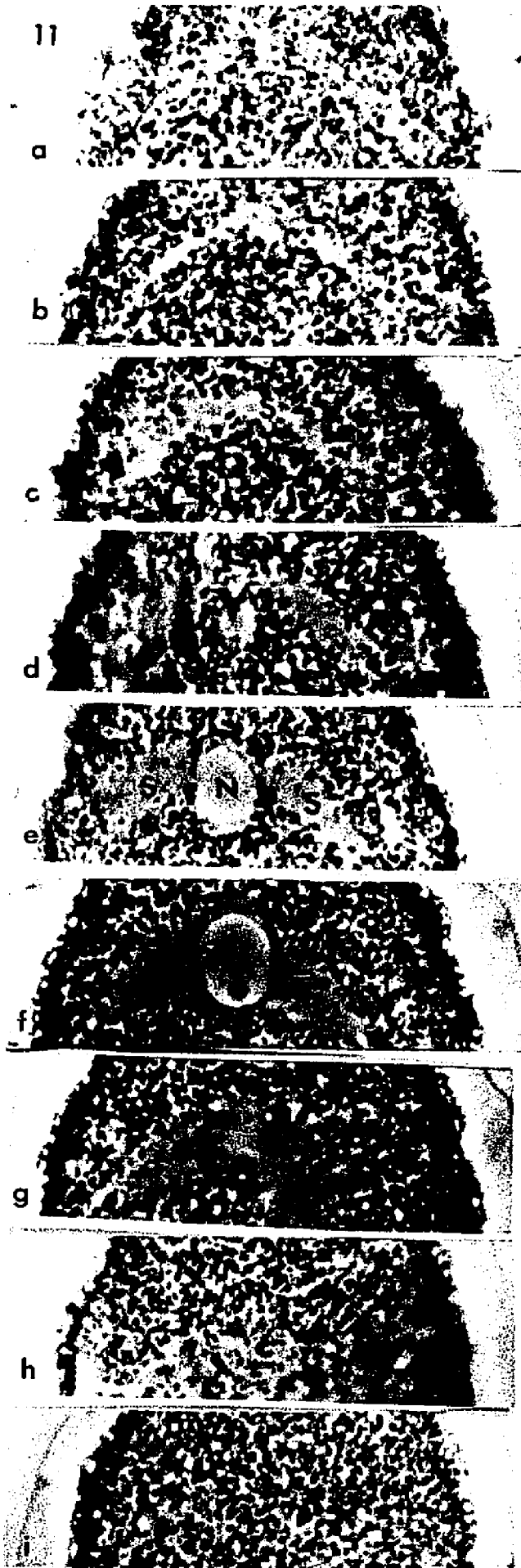
FIGURE 11. Serial sections through the streak stage cell. The sections were cut at  $4\ \mu\text{m}$ . Note the lack of large particles in the streak zone (S). The nucleus (N) and nucleolus (Nu) are clearly visible. In Fig. f the nucleus can be seen to protrude both above and below the plane of the streak. The lower limit of each micrograph corresponds to an equator of the cell. Phase contrast x 1050.

FIGURE 12. Diagram of the relationship between the nucleus (filled in) and the surrounding streak based on a clay model reconstruction of the serial sections of Fig. 11.

- A. Side view. The nucleus protrudes less above than below the streak. Note how the streak bends downward along its long axis.
- B. Viewed from top. The nucleus is eccentric with respect to the shorter axis. Along this axis, the side away from the nucleus is rounder and its edge thinner than the side closer to the nucleus.

FIGURE 13. Thick section of streak stage cells viewed by darkfield illumination. There are no refractile particles in the streak zone. Darkfield LM x 365.

FIGURE 14. Thick section comparing an unfertilized mature egg to a streak stage cell. The cell with the streak zone (S) is surrounded by a fertilization membrane (FM) and has a deeply pigmented layer (P) just under its surface, "ruffled" by numerous, long microvilli (mV). Occasionally, side channels (SC) of streak zone can be identified. No fertilization membrane surrounds the unfertilized egg (UN) but small cortical granules (C) can be seen as white particles just under its smooth surface. Its nucleus (N) is round. The nucleus of the streak stage cell does not appear in this section. Phase contrast x 620.



the 3-dimensional structure of the streak and its relationship to the nucleus. The model (diagrammed in Fig. 12) reveals that the streak resembles a donut elongated and bent downward along one axis, its hole eccentric, especially with respect to the other, shorter axis. The nucleus occupies the hole, protruding only barely above but more so below the streak.

Light and electron microscopy show that the streak is an area from which most organelles are excluded. In fact, dark-field illumination (Fig. 13) clearly demonstrates the exclusion of nearly all refractile particles. Phase microscopy reveals not only the absence of particles in the zone, but also the presence of side channels (SC) as discussed below.

The cell in the streak stage is very different from the unfertilized egg (Cell UN, Fig. 14). The latter cell has no fertilization membrane but it has a vitelline membrane closely apposed to its surface (not visible here). The fertilized cell, on the other hand, has a prominent fertilization membrane. The egg has a smooth surface with light cortical granules (C) just under it. The streak stage cell has an irregular surface due to its many long microvilli (mV) and has lost its cortical granules by exocytosis shortly after fertilization. Also, the pigment vacuoles, found throughout the unfertilized egg, have largely migrated to the cortex of the fertilized cell, forming a dark layer just under the surface all around the cell (P, Fig. 14). These differences in the cortex can be more easily seen by electron microscopy (compare Fig. 15 with Fig. 9).

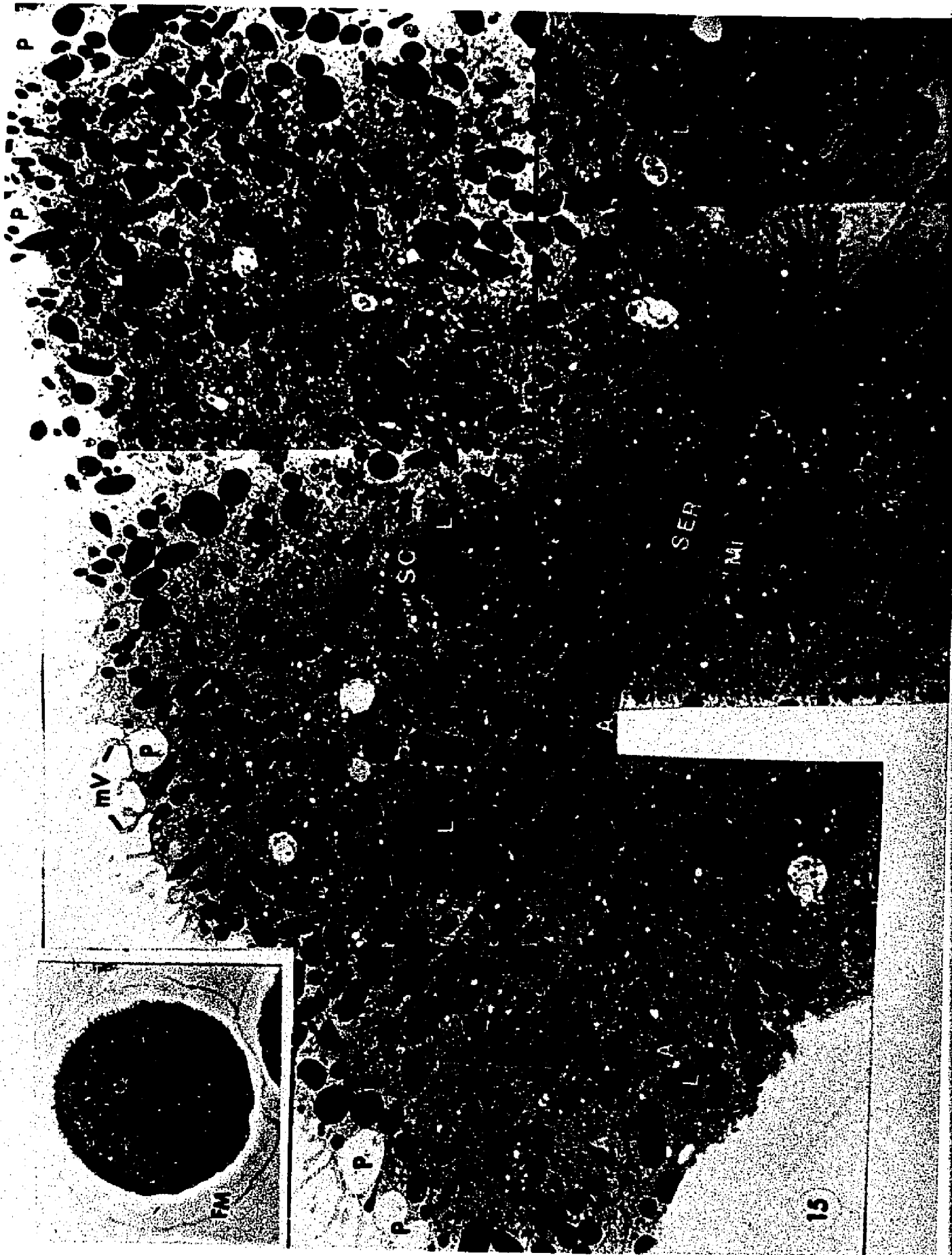
Electron micrographs of the streak reveal that the streak zone is full of intracellular membranes, the most obvious ones

FIGURE 15. Low magnification view of portion of streak stage cell. The streak zone has few particles and consists mostly of saccular ER (SER) and annulate lamellae (A). Part of a side channel (SC) is visible which also contains ER. Vesicular ER (v) is much reduced both in amount and size of vesicles but is still randomly distributed throughout. Mitochondria (Mi) are also scattered throughout and now display an affinity for lipid droplets (L) rather than the more plentiful yolk. The plasma membrane has long microvilli (mV) which are also more numerous than those of the unfertilized egg. The cortex is rich in pigment vacuoles (P), leaving the rest of the cytoplasm less pigmented. Cortical granules are no longer seen, having exocytosed after fertilization. The Nucleus (N) has prominent nucleoli (Nu) abutting a mostly regular nuclear envelope (NE). Surrounding the nucleus is saccular ER (SER).

EM. X4,100

Inset. The same cell as it appeared in thick section before being longitudinally sectioned for electron microscopy. The nucleus (N) with nucleolus (unlabelled), the fertilization membrane (FM), and the streak zone (S) are clearly visible.

Phase contrast. X500



being long cisternae of mostly rough ER and annulate lamellae (SER and A, Figs. 15, 16, 17, and 18). Although numerous mitochondria line the streak zone's periphery (Mi, Figs. 15 and 16), only occasionally are they found in the central area of the streak. Except for such mitochondria and heavy bodies (HB, Figs. 16 and 19), all other large organelles and particles like yolk, lipid, and pigment are generally excluded from the streak, resulting in their absence in phase contrast micrographs (Figs. 13 and 14).

#### 1. Endoplasmic Reticulum

There are two types of ER in the streak stage. The minor component is similar to that of the unfertilized egg, i.e., it is vesicular (v, Fig. 16) but the larger vesicles are no longer present (compare Fig. 16 with Fig. 5). This form is found throughout the whole cell including the streak zone (v, Figs. 15 and 16). Small vesicles are often found in association with mitochondria and are about 0.3 to 0.4  $\mu\text{m}$  in diameter (Figs. 16 and 18, inset). The vesicular ER is always smooth.

The major component seems to be flattened cisternae of mostly rough saccular ER, the ribosomes distributed somewhat unevenly and often showing preference for one side of a sacculus (SER', Fig. 17). The cisternae appear to be discontinuous but align in parallel rows (SER, Fig. 17 and 18). These rows run for such long distances that they are easy to see at low magnification (Fig. 15) coursing throughout the cell even in the cortex, but especially gathered in the streak zone. The cisternae may contain an amorphous material with fine grains (GER, Fig. 18).

Although saccular ER tends to run in all directions outside the streak zone, inside the zone they generally run parallel to the axis of the streak and extend around the nucleus (Figs. 15 and 16). Occasionally, some ER from the streak periphery bends away from the zone into the general cytoplasm forming side channels (SC) that can be seen not only in electron micrographs (Fig. 15) but even in light micrographs (Fig. 14) as well. Wherever an ellipsoid (or any other assymmetric shape) yolk granule abuts saccular ER, the granule's long axis is always parallel to that of the ER (Figs. 15 and 17). Finally, ER saccules are often continuous with annulate lamellae (AER, Fig. 17).

## 2. Annulate Lamellae

Annulate lamellae are usually seen in stacks of 2 or 3 but stacks of 4 or 5 are not uncommon (A, Figs. 16, 17, and 18). A fuzzy material can be seen to coat the lamellae both intracisternally (F) and along the surface, often between lamellae (F', Fig. 18). There are spaces between the fuzzy material (U and U', Fig. 18) which generate a railroad track appearance. Such spaces often contain one or two granules (g and g', Fig. 18) about  $175 \text{ \AA}$  in diameter. Sometimes, what appears to be a C-MT is also present, always between lamellae, never intracisternally (c-arrows, Figs. 17 and 18). The intracisternal space varies between  $300$  and  $500 \text{ \AA}$ . Two lamellae may lie as close to each other as  $850 \text{ \AA}$ , although appearing to be closer because of the fuzzy coating.

Tangential sections through the annuli (Fig. 17, inset) reveal the pores to be hexagonally packed. A center to center spacing of only  $1400 \text{ \AA}$  reveals how tightly they are packed. Often, a granule of about  $200 \text{ \AA}$  appears in the center

FIGURE 16. Streak zone of cell shown in Fig. 14. It consists of saccular ER (SER) and vesicular ER (v) as well as annulate lamellae (A). Annulate lamellae are also part of the heavy body (HB) in the center of the micrograph. Much of the saccular ER is rough (rER). Mitochondria (Mi) line the streak and contain dense granules (g). They are sometimes associated with vesicular ER (v). A pigment vacuole (P) is also at the streak zone's periphery. Although difficult to see at this magnification, a few MTs can be resolved (arrow).

EM X15,600

FIGURE 17. Higher magnification of another part of the same streak zone. The saccular quality of the ER is readily apparent (SER). Sometimes ribosomes attach to only one side (SER'). Annulate lamellae (A) are often continuous with ER (AER). C-MTs are barely visible among the annulate lamellae (c-arrows). Normal MTs are present in the streak zone (arrows). A V-shaped Golgi apparatus (G) is present at the periphery. Note that the long axis of the yolk granules (Y) is parallel to the long axis of the saccular ER. A dense granule (g) is found in the mitochondrion.

EM. X30,400

Inset. Tangential section through the pores of (an) annulate lamella(e). The pores (Po) are tightly packed in a hexagonal array. A central granule (g) can be seen in each one.

EM. X47,300

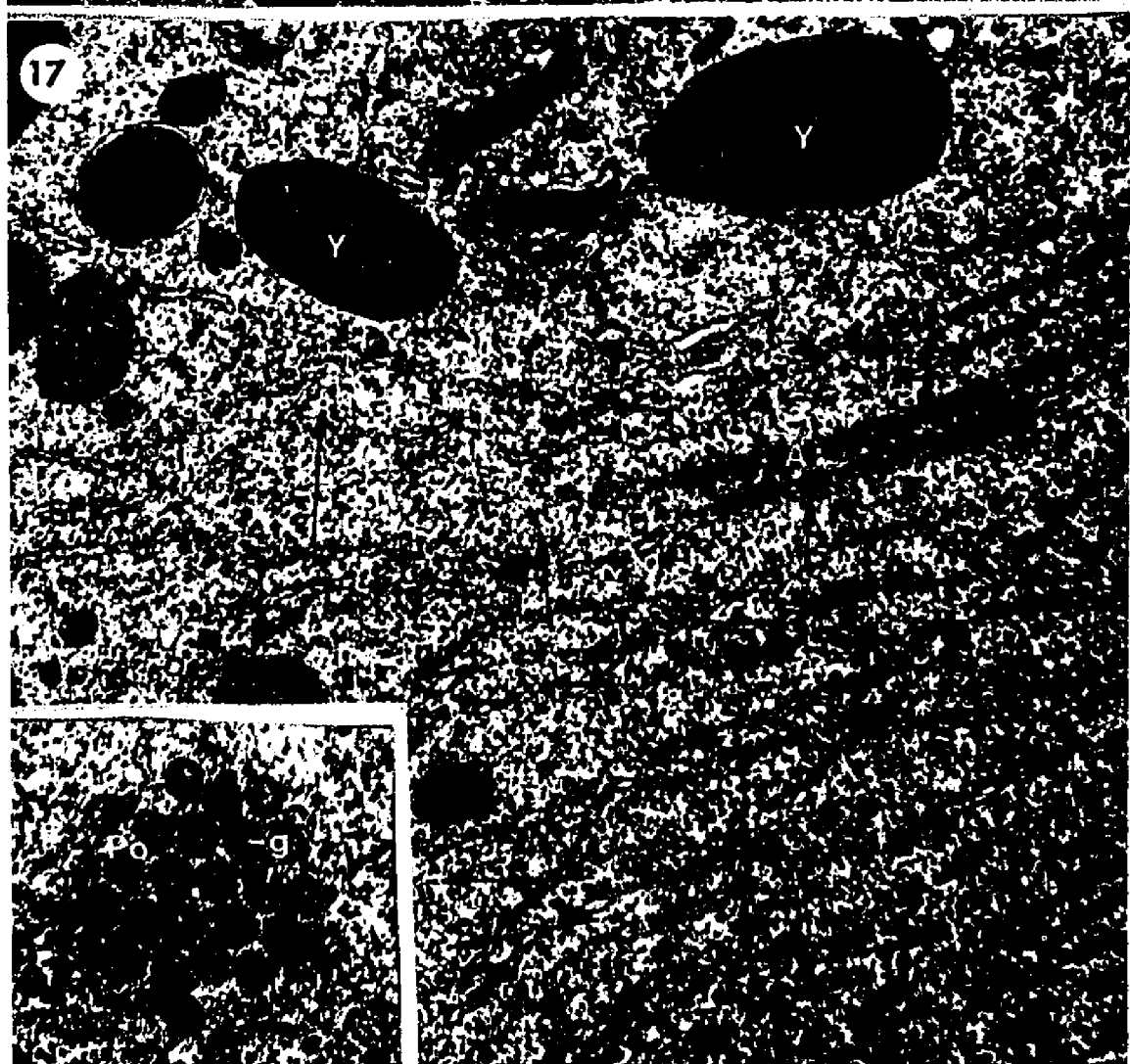
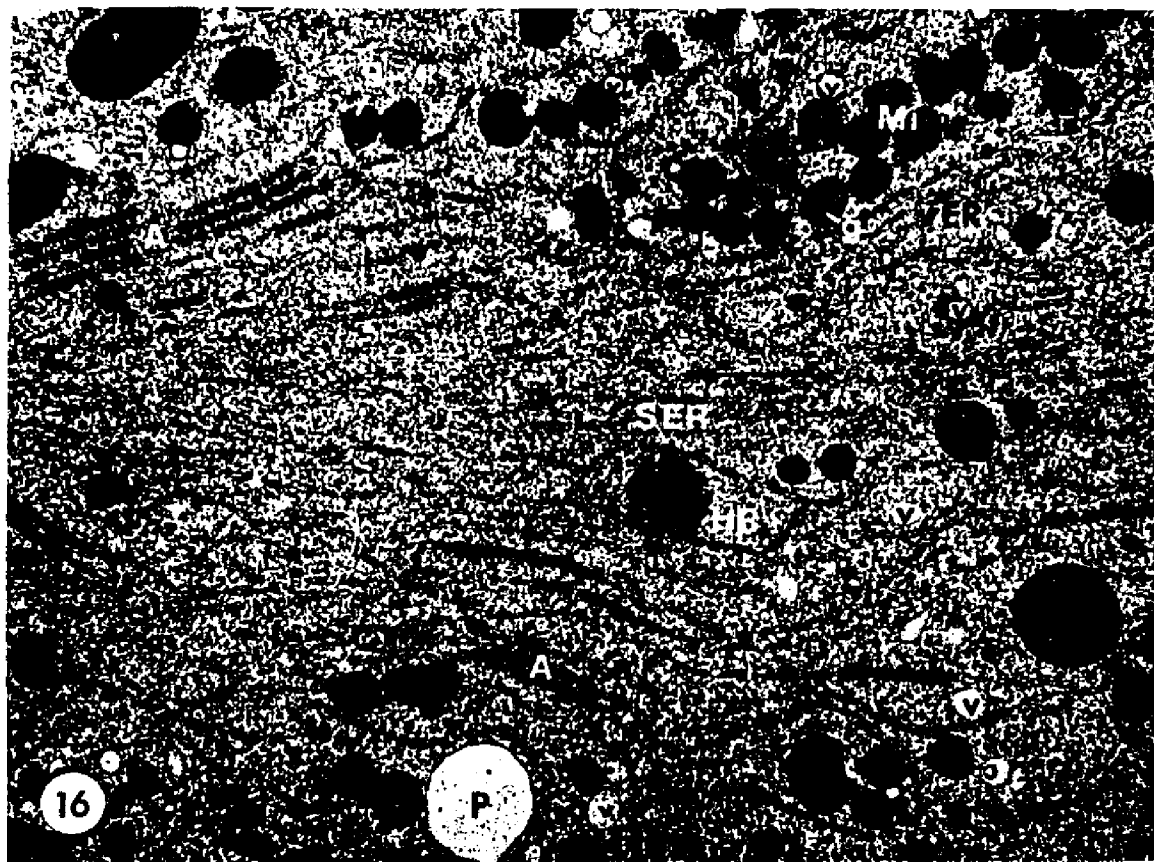
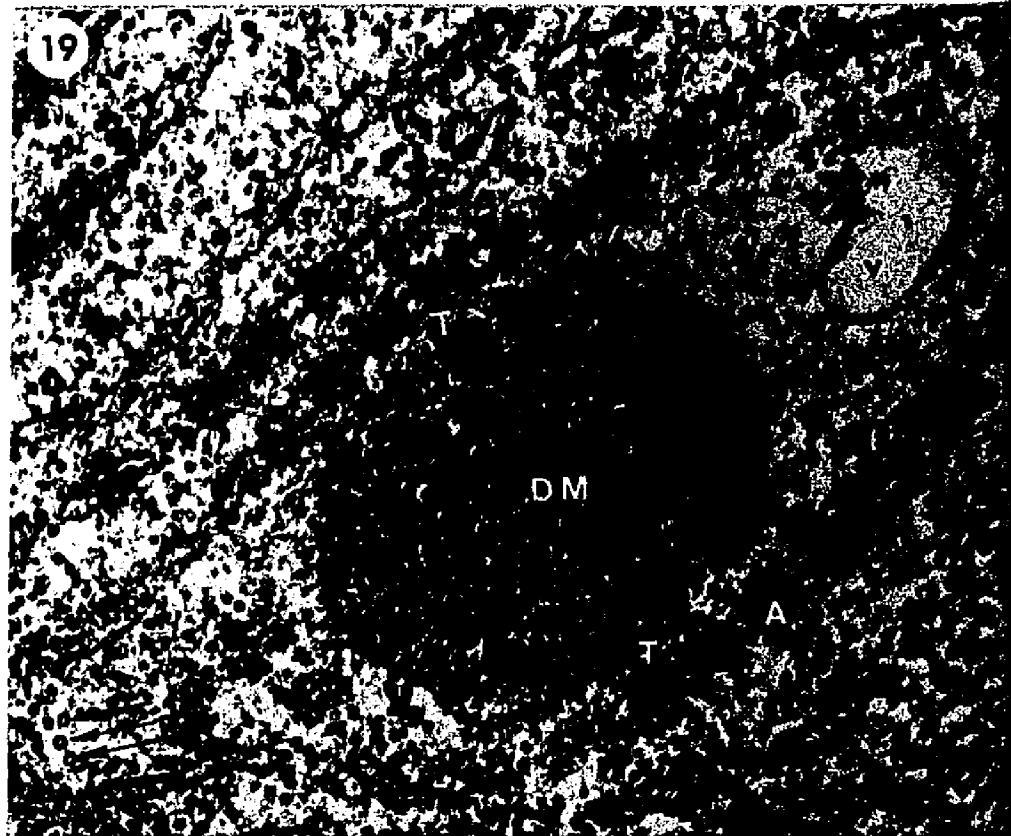
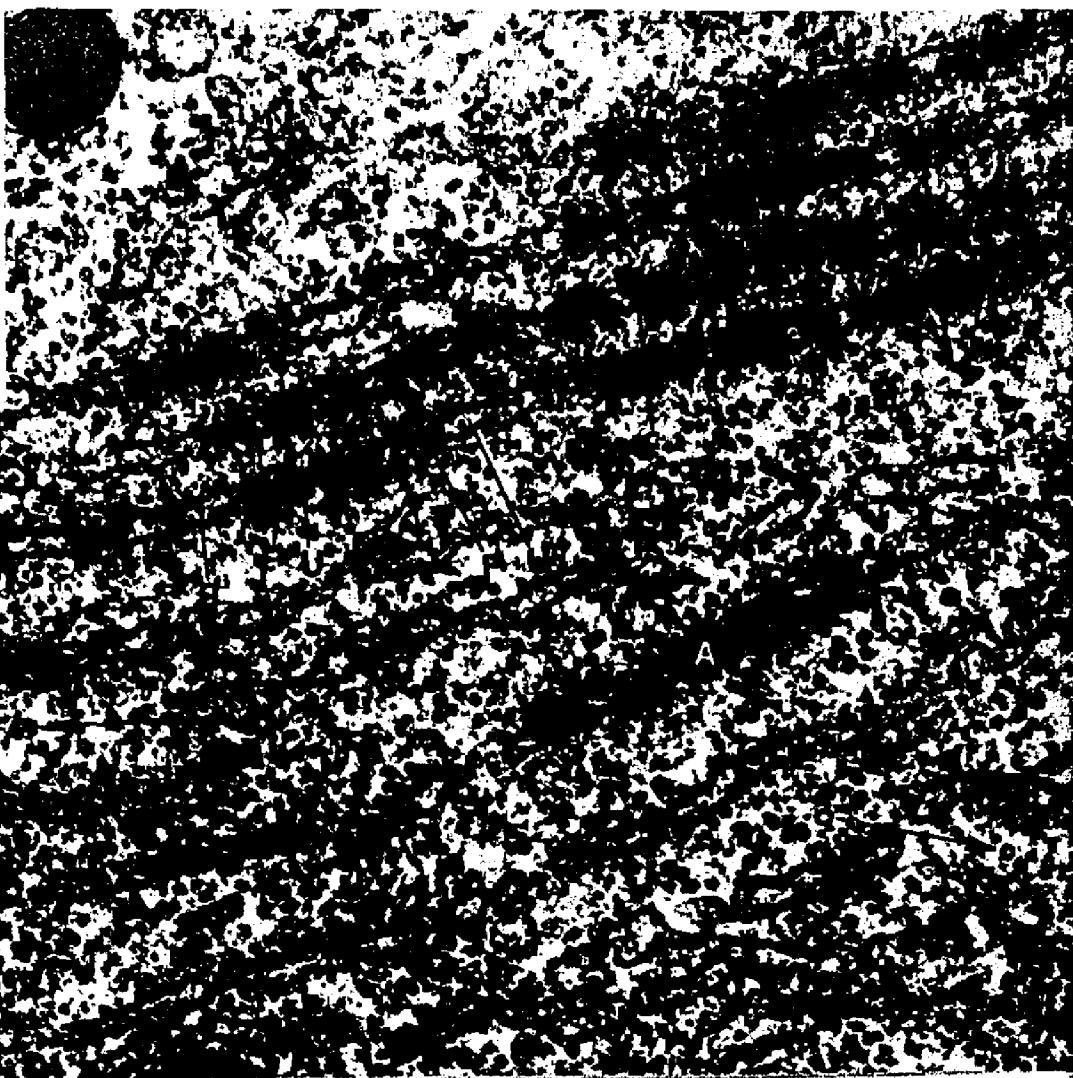


FIGURE 18. Annulate lamellae from cell of Fig. 14. Patches of fuzzy, amorphous material are seen both within the lamellae (F) and between the lamellae (F'). Clear areas separate such patches (U and U' respectively). Small dense granules are found in such areas within lamellae (g) and between lamellae (g'). What appears to be C-MTs can be observed between lamellae (c-arrows) and perhaps in the general area of the streak zone (C-arrow). Normal MTs (O-arrows) and saccular ER (SER) are commonly observed in the streak zone. Much of this ER contains granular material (GER). EM x 71,500.

Inset. A nearby mitochondrion (Mi) with attached vesicle (v).  
EM x 58,800.

18A. Higher magnification of upper right area of annulate lamellae of Fig. 18. The 3 C-MTs (c-arrows) and a few possible ones (?-arrows) are shown. EM x 88,000.

FIGURE 19. Heavy body (HB) from the same cell. It consists of a dense mass (DM) surrounded incompletely by annulate lamellae (A) which are continuous with saccular ER (AER). The incompleteness of the bounding membrane makes it impossible to define its exact boundaries. Thus, whether the MTs (arrows) or vesicle (v) are actually in the heavy body or not is completely arbitrary. They are, however, in an area where the lamellae are uncoated, resembling saccular ER (AER). Two of the MTs (B-arrow) are connected by a bridge-like structure. Some interaction between the dense mass and annulate lamellae may be occurring where they are closest through a transfer of material (T) between the two. Other annulate lamellae are in the streak zone near the heavy body. EM x 70,000.



of the pore (g, Fig. 17, inset).

In location, the annulate lamellae are found in the same places as the saccular ER. They are close to and often parallel the nuclear envelope (A, Fig. 21). They are present in the streak zone (Figs. 15, 16, 17, and 18), in the side channels (SC), and at the periphery of the streak near the cortex (Fig. 15). Annulate lamellae are generally aligned parallel to the ER and the long axis of the streak.

### 3. Golgi Apparatus

The streak stage cell seems to have more Golgi than the mature, unfertilized egg. Although some Golgi apparatuses appear throughout the cell, most are found either just inside or just outside the borders of the streak zone (G, Fig. 17). Stacks of Golgi saccules are often found in pairs at an acute angle to each other (G, Fig. 17).

### 4. Mitochondria

Mitochondria are ubiquitous and may be seen even in the streak zone which excludes most everything else. (Figs. 15 and 16). They are often found in large groups along the boundary of the streak zone (Mi, Figs. 15 and 16). Mitochondria are sometimes found associated with vesicular ER as mentioned above, and occasionally seem to incorporate the vesicles within their outer membranes (Fig. 18, inset).

In the streak stage, mitochondria are almost never associated with yolk. Instead, many can be found associated with lipid droplets (L, Fig. 15). Also, more of the streak stage mitochondria have dense granules in them than those of the unfertilized egg (g, Figs. 16 and 17).

## 5. Heavy Bodies

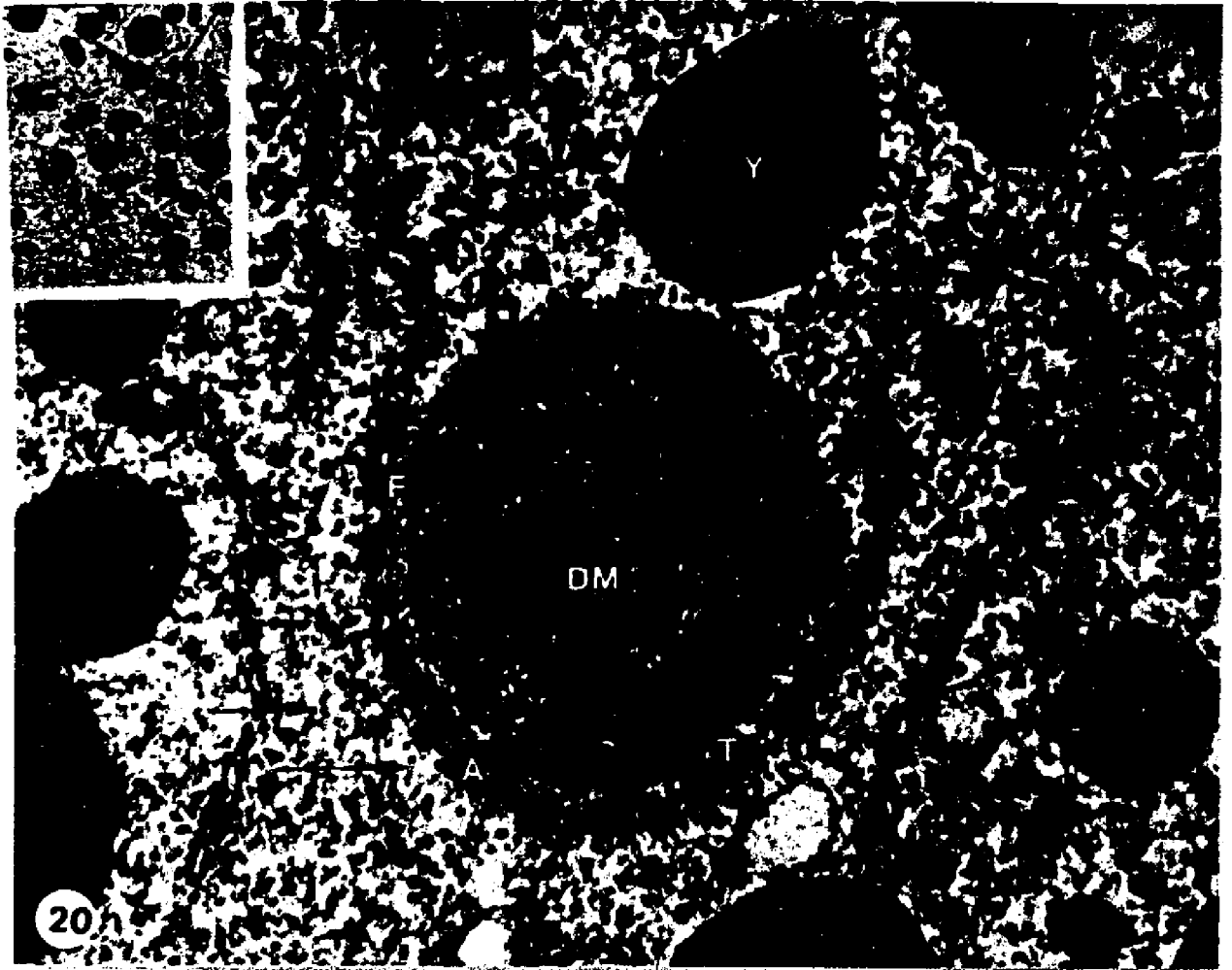
Although heavy bodies have been reported in the Arbacia oocyte (Anderson, 1968) scattered throughout the cytoplasm, in the streak stage they seem to gather in or near the streak zone (HB, Fig. 16 and 18). The heavy body consists of a dense mass (DM) of material surrounded at least partially by annulate lamellae (Figs. 16, 19, and 20). The dense mass is composed of a heterogeneous collection of electron-dense granules and an amorphous fuzz (Figs. 19 and 20). There may be some interaction between the dense mass and the annulate lamellae. Areas where transfer of material might be occurring are readily found (T, Figs. 19 and 20). Annulate lamellae nearest the dense mass are coated most heavily, while those further away may be even uncoated. In addition, fuzzy, amorphous material is found between the dense mass and annulate lamellae but is not seen in areas where the heavy body lacks annulate lamellae (F, Fig. 20). Such material might also be responsible for heaviest coating of the nearest lamella. Further away, the lamellae seem to become part of the cisternae of the ER (AER, Fig. 19).

Heavy bodies of the streak stage are always found with at least one MT nearby and usually more (arrows, Figs. 19 and 20). Elements of the vesicular ER (v, Fig. 19) and even yolk granules (Y, Fig. 20) are sometimes observed in the heavy bodies. Like other annulate lamellae in the streak zone, those of the heavy bodies also line up parallel to the saccular ER and the long axis of the streak zone. There may be more than one annulate lamella around any one side of the dense mass (Fig. 19) but this may simply be an accidental proximity to annulate lamellae normally found in the streak zone. In

FIGURE 20. Heavy body located in a side channel outside the streak zone (see inset). A yolk granule (Y) is near the dense mass (DM) but the annulate lamellae (A) bounding the mass does not extend to the granule. A fuzzy, amorphous coating (F) is found between the annulate lamellae and dense mass. Its similarity to material in the dense mass suggests transfer of material between the two (T). MTs (arrows) are always present near heavy bodies even when such bodies are outside the streak zone. EM x 52,100.

Inset. Low magnification micrograph showing relationship of heavy body (bracketed) to the streak zone (S) and its side channel (SC). EM x 4,100.

FIGURE 21. Perinuclear area of streak stage cell. The nucleus (N) is bounded by an intact nuclear envelope (NE). Surrounding this envelope are saccular ER (SER) and annulate lamellae (A). As usual, the annulate lamellae appear to be continuous with ER (AER). In the nucleoplasm some chromatin fibers seem to be condensing. EM x 39,300.



addition, it is interesting to note that all the heavy bodies shown are from the cell of Fig. 14, none being seen in the cell shown in Fig. 15. Whether this is due to the plane of section (which is most likely), the amount of time into the streak stage, or some other variable remains unknown.

#### 6. Microtubules

There are MTs in the streak stage cell but they are few and confined to the streak zone (arrows, Figs. 17, 18, and 19). No particular orientation is readily apparent. They may occur alone or in groups of 2 or 3 (arrows, Figs. 17 and 19). In favorable sections, a few C-MTs may be discerned (C-arrows, Figs. 17 and 18). C-MTs are also seen frequently near or among annulate lamellae (Figs. 17, 18, and 18A). As mentioned above, some MTs are always found near (perhaps within) heavy bodies (Figs. 19 and 20).

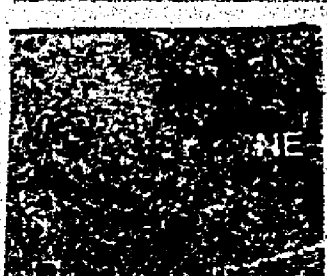
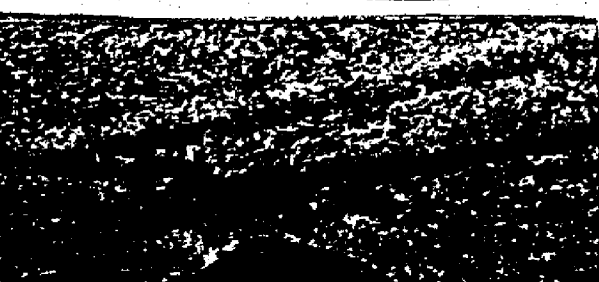
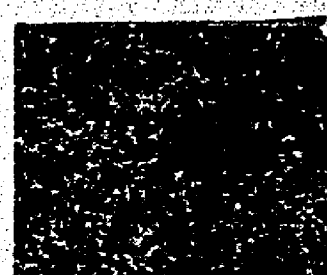
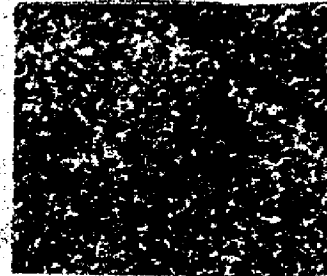
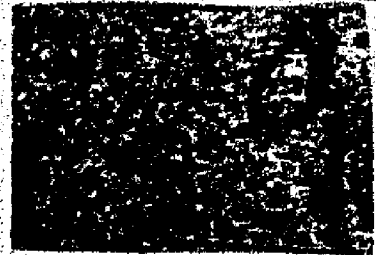
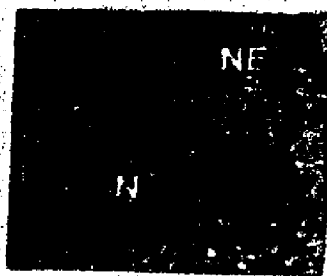
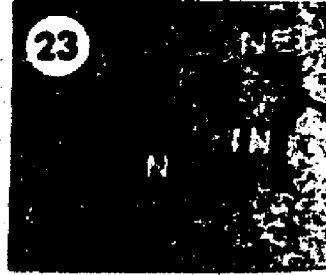
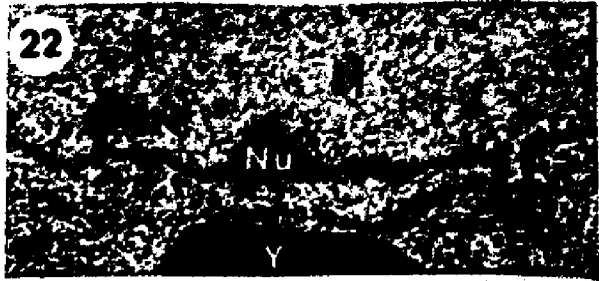
#### 7. Nucleus

The nucleus of the streak stage cell is different from that of the unfertilized egg. Its nucleoplasm (Fig. 21) is more granular and less wispy than the unfertilized egg nucleus (Fig. 6). Furthermore, the nuclear envelope has developed both evaginations (EV) and invaginations (IN, Figs. 22, 23, and 24), never seen in the mature, unfertilized egg. The evaginations of membrane appear to be too few in number to explain the large amount of ER and annulate lamellae in the streak zone. The nuclear invaginations are interesting because they may result in intranuclear annulate lamellae. Such structures can be produced in at least three ways (Figs. 22, 23, and 24) but all form a sac-like structure bounded by invaginated nuclear envelope.

FIGURE 22. Series of sections through the streak stage nucleus (N). A small, heavily coated invagination (IN) and a small evagination (EV) of nuclear envelope are shown. What is probably a small nucleolus (Nu) can be seen. A yolk granule (Y) is in the nearby cytoplasm. The invagination resembles a delamination, the nuclear envelope seeming to remain intact throughout. EM x 22,000.

FIGURE 23. Serial sections through the streak nucleus (N) showing invagination of nuclear envelope (NE) by formation of an invaginating stalk (IN) which balloons out at its end (Figs. b, c, and d). The stalk has no central channel in it to allow the cytoplasm to come in. EM x 22,000.

FIGURE 24. Serial sections of invagination by "ballooning" of the streak stage nuclear envelope (NE) directly into the nucleus (N). Thus, again, although the irregularly-shaped "balloon" has much volume, no cytoplasm can come in. EM x 22,000.



### C. Fine Structure of Prophase

In most species, including Arbacia punctulata, prophase chromosome condensation begins prior to breakdown of nuclear envelope. Such cells look like streak cells except that the particle exclusion zones now appear short and wide rather than long and thin, and they no longer curve (S, Fig. 25).

Electron microscopy reveals changes of fine structure in the ER, annulate lamellae, Golgi apparatuses, mitochondria, heavy bodies, MTs, and nucleus.

#### 1. Endoplasmic reticulum

The saccular type of ER is now greatly reduced and is located primarily outside the exclusion zone and in the cell periphery (SER and rER, Figs. 26, 27, 28, and 29). In its place there is tubular smooth ER (TER, Figs. 26, 28, 30, and 31). Some of the remaining cisternae appear to be rough ER (rER, Figs. 26 and 27). The bands of saccular ER around the nucleus have also been largely replaced by tubular ER (Figs. 26, 30, and 31). The vesicular type of ER is still found except that it is rarely associated with the many mitochondria (v, Figs. 26, 28 and 29).

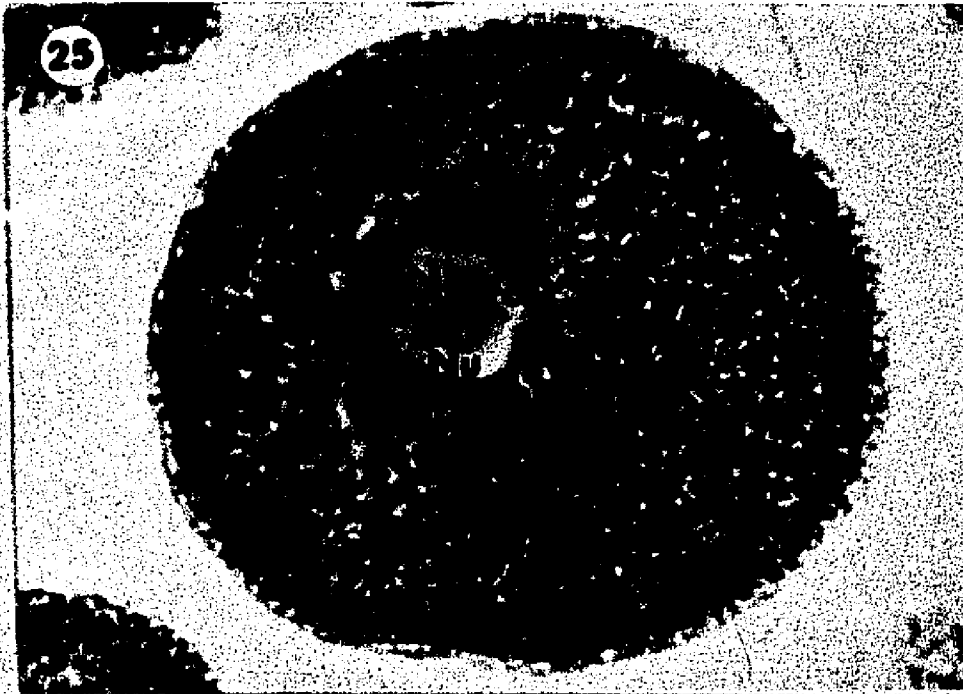
#### 2. Annulate Lamellae

Annulate lamellae have completely disappeared, even from the exclusion zone (Figs. 26, 28, 30, and 31). Occasionally, a few cisternae connected by a small amount of "fuzzy" material (A?) are seen near nuclear evaginations (EV) poking into the cytoplasm of the streak (Fig. 30) which are described more fully below. Also profiles of pores are found near the nucleus (Po, Figs. 31, 32, and 33). It is difficult to tell whether these are remnants of annulate lamellae or

FIGURE 25. Thick section of the late prophase cell. The nucleus (N) has a prominent, unattached nucleolus (Nu) surrounded by condensing chromatin (cc) beginning to form chromosomes. The exclusion zones (S) are shorter and wider than those of the streak stage. Phase contrast x 1,300.

FIGURE 26. The exclusion zone full of vesicular (v) and tubular (TER) smooth ER. Some saccular ER, both rough (rER) and smooth (SER) can be found at the zone's periphery. MTs (arrows) are easily found, some even seem to touch the nucleus (N). Mitochondria (Mi) with their dense granules (g) are still present in the zone but do not seem to associate with vesicles. EM x 28,600.

25



26

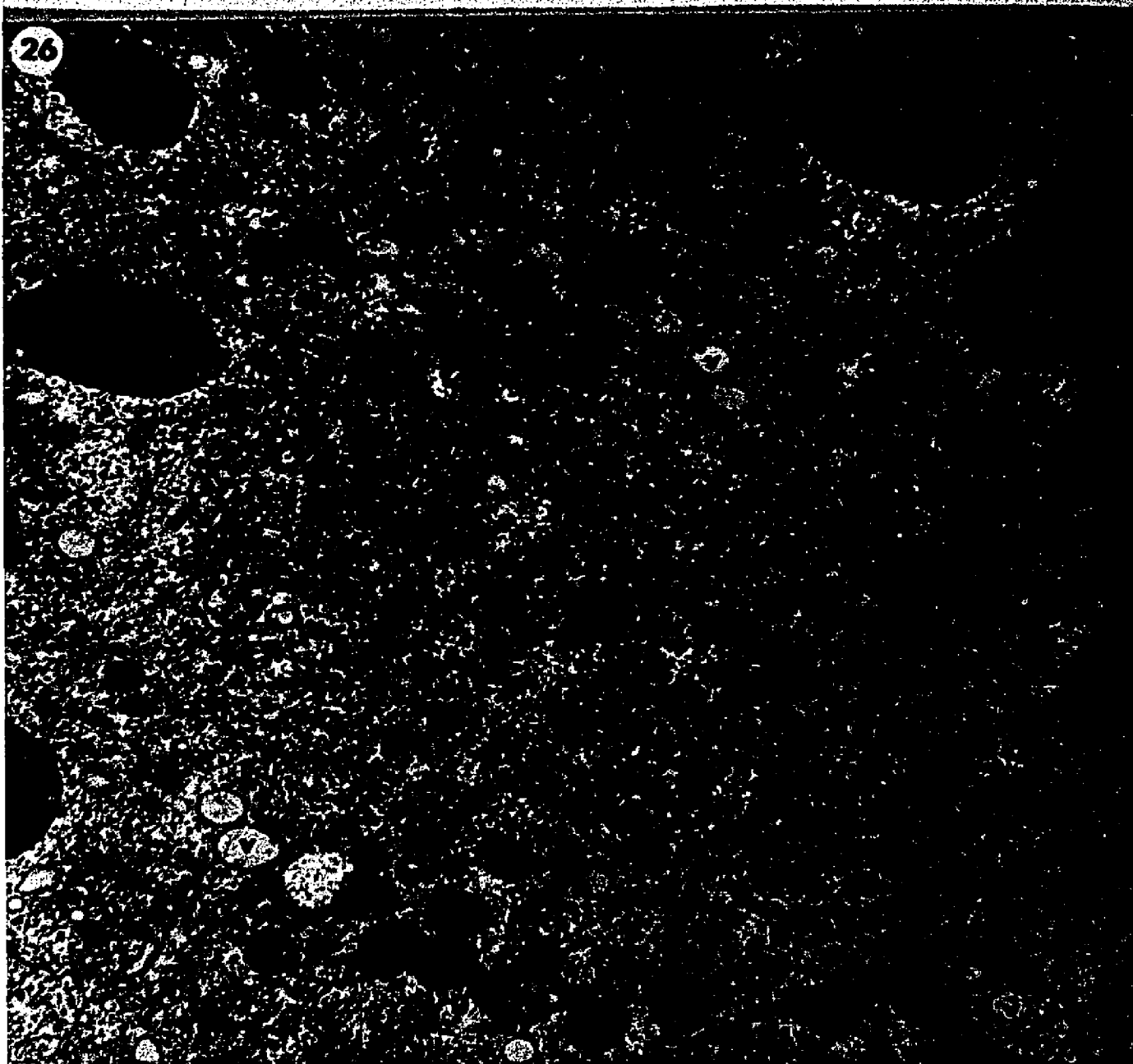


FIGURE 27. Cortical area of prophase cell. The cell surface still has many microvilli (mV) overlying a heavily pigmented layer (P). Lipid droplets (L) are still surrounded by mitochondria (Mi) whereas yolk granules (Y) are not. Rough saccular ER (rER) and vesicular ER (v) are present. The tubular type is not, confined entirely to the exclusion zone. EM x 16,200.

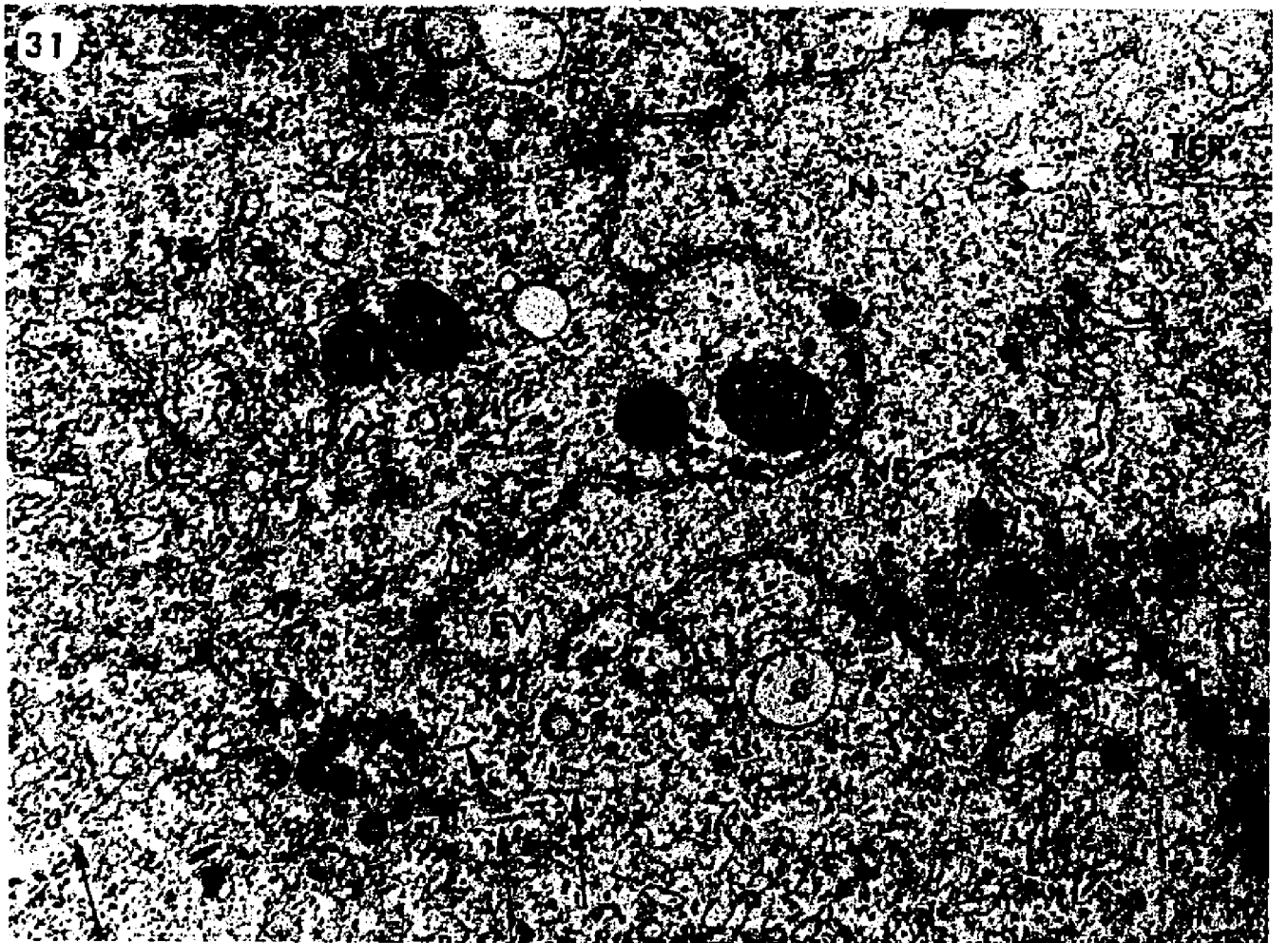
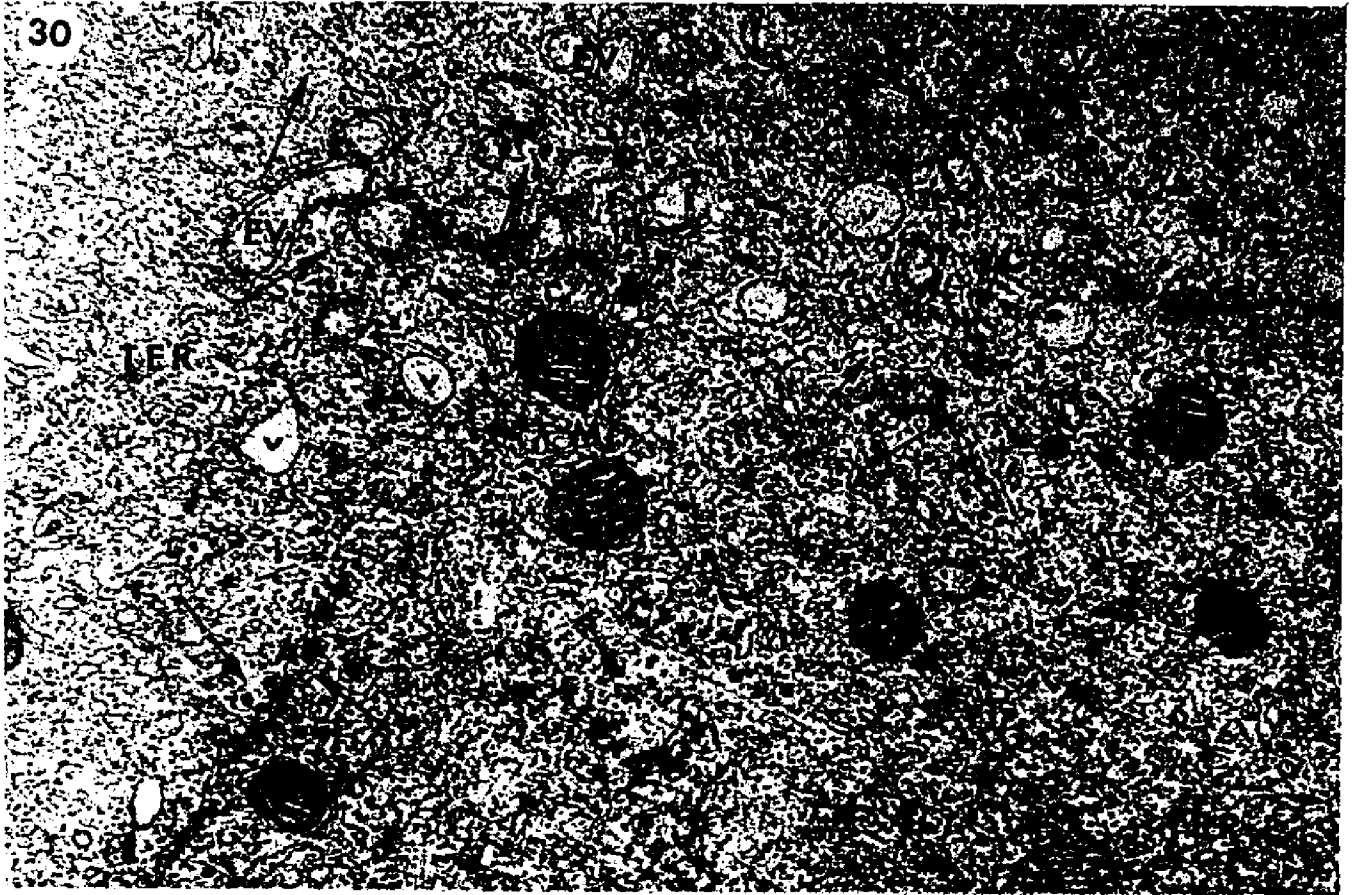
FIGURE 28. Golgi apparatus at periphery of prophase exclusion zone. The Golgi (G) has many vesicles around it suggesting that it is active. Saccular ER (SER) is found distal to it while tubular ER (TER) is found proximally, closer to the exclusion zone (S). Vesicular ER (v) and a mitochondrion with a dense granule (g) are also shown. EM x 41,000.

FIGURE 29. Area just outside of this exclusion zone (S) penetrated by MTs (arrows). Vesicular (v) and saccular (SER) ER are present. Mitochondria (Mi) with dense granules (g) surround lipid droplets (L) but not yolk (Y). EM x 25,600.



FIGURE 30. Area of prophase exclusion zone with evaginations (EV) from the nucleus clearly visible. They are easily recognized since the nuclear envelope is a "double" membrane, easily distinguished from the single membrane around vesicles and vacuoles. Subsequent sections show the evaginations enlarging and "fusing" to form the "whole" nucleus ( as in Fig. 36). This area has mitochondria (Mi), vesicular (v) and tubular (TER) ER, and many MTs (arrows), some of which are C-MTs (C-arrows). What may be the remnant of annulate lamellae (A?) is seen with some MTs (arrows) nearby. EM x 29,700.

FIGURE 31. Cross-section nearly tangential to the prophase nucleus (N) with nuclear envelope (NE) intact on left but not on right where tubular ER (TER) seems to mix with nucleoplasm (at \$ signs). The pores (Po) near the nuclear evagination (EV) may be from the nuclear envelope. Many MTs (arrows) are seen nearby. A fuzzy, amorphous material (F) and mitochondria (Mi) are also present. EM x 30,800.



part of nuclear envelope, perhaps being released during nuclear envelope breakdown. Serial sectioning demonstrates that such pores may exist independently in the cytoplasm, i.e., not attached to membranes (Po, Fig. 32). There may be some attachment or interaction with MTs (arrows, Figs. 30, 31, 32, and 33) which are always present among the pores. Serial sections reveal MTs above and below the pores as well as at the level of the pores (Figs. 32 and 33). One set of serial sections suggests that vesicles of either ER or Golgi extend through the area where the pores are (G?, Fig. 32B, C, and D).

### 3. Golgi Apparatus

Golgi apparatuses are found in abundance both near the exclusion zone and in the rest of the cell. Unlike the apparatuses of the previous stage, V-shaped saccular stacks are seen only occasionally. Since most stacks are straight rather than curved (G, Fig. 28), it is difficult to distinguish the forming face from the maturation face.

### 4. Mitochondria

Mitochondria are the same as before morphologically but appear to be more numerous, especially in the exclusion zone and around the nucleus (Mi, Figs. 26, 30, and 31). They are often in groups and still associate with lipid droplets (L) rather than yolk granules (Y, Figs. 27 and 29). Their association with vesicular ER has apparently ended, but more mitochondria have dense granules than before (g, Figs. 26, 28, and 29).

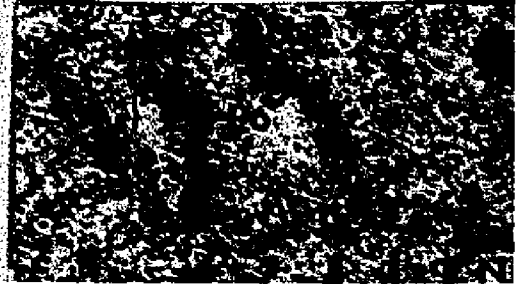
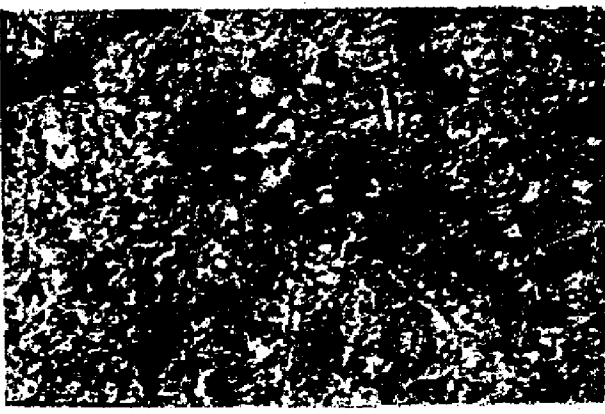
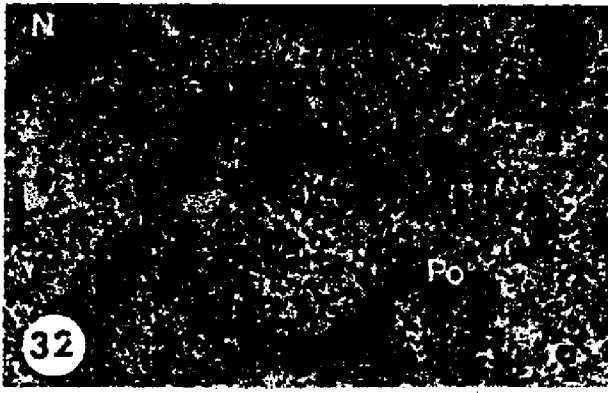
### 5. Heavy Bodies

Neither heavy bodies nor their recognizable remnants are seen.

FIGURE 32. Serial sections through prophase perinuclear region. The nucleus (N) and its nuclear envelope (NE) are in upper left. Fig. e is expanded to show general area. This region contains pores (Po) which seem to be "loose" in the cytoplasm, i.e., not connected to either the nuclear envelope or annulate lamellae. Many MTs (arrows, Figs. a, b, c, and d) are seen to course among them. Nearby are vesicles of what may be Golgi apparatus (G?, Figs. c, d, and e). In some instances, vesicles (v) near the nucleus (N) seem to have MTs (v-arrows, Figs. b, c, and f) connecting the two organelles together. This occurs in an area where there is some evidence of possible nuclear envelope breakdown (\$, Fig. d). Many other MTs might also make contact with the nucleus (arrows, Figs. e and f). Figs. a, b, c, d, and f: EM x 31,900.

Fig. e: EM x 33,000

FIGURE 33. Serial sections through a group of perinuclear pores from the same cell. The pores (Po) are in three rows perpendicular to the nucleus (N) on the lower right. Although the pores within each row seem to be held together by an amorphous material, which may be membrane cut tangentially, between rows no such material exists. MTs (arrows) can be seen among the pores. EM x 28,600



## 6. Microtubules

MTs are longer and in greater number than in the streak stage. Although the majority are found in the exclusion zone (Fig. 26), some extend into the surrounding cytoplasm (arrows, Fig. 29). Although many still seem to be random, most run toward the nucleus (Fig. 26). A few probably run along the nuclear envelope but do not penetrate it. This is suggested by the many oblique sections of MTs that seem to touch but not penetrate the nuclear envelope (arrows, Figs. 26 and 32E). MTs may also be responsible for pushing part of the nuclear envelope inward, forming invaginations containing MTs (IN, Figs. 34 and 35). These are described more fully below. A few C-MTs (C-arrows, Fig. 30) can be seen but normal MTs are the rule.

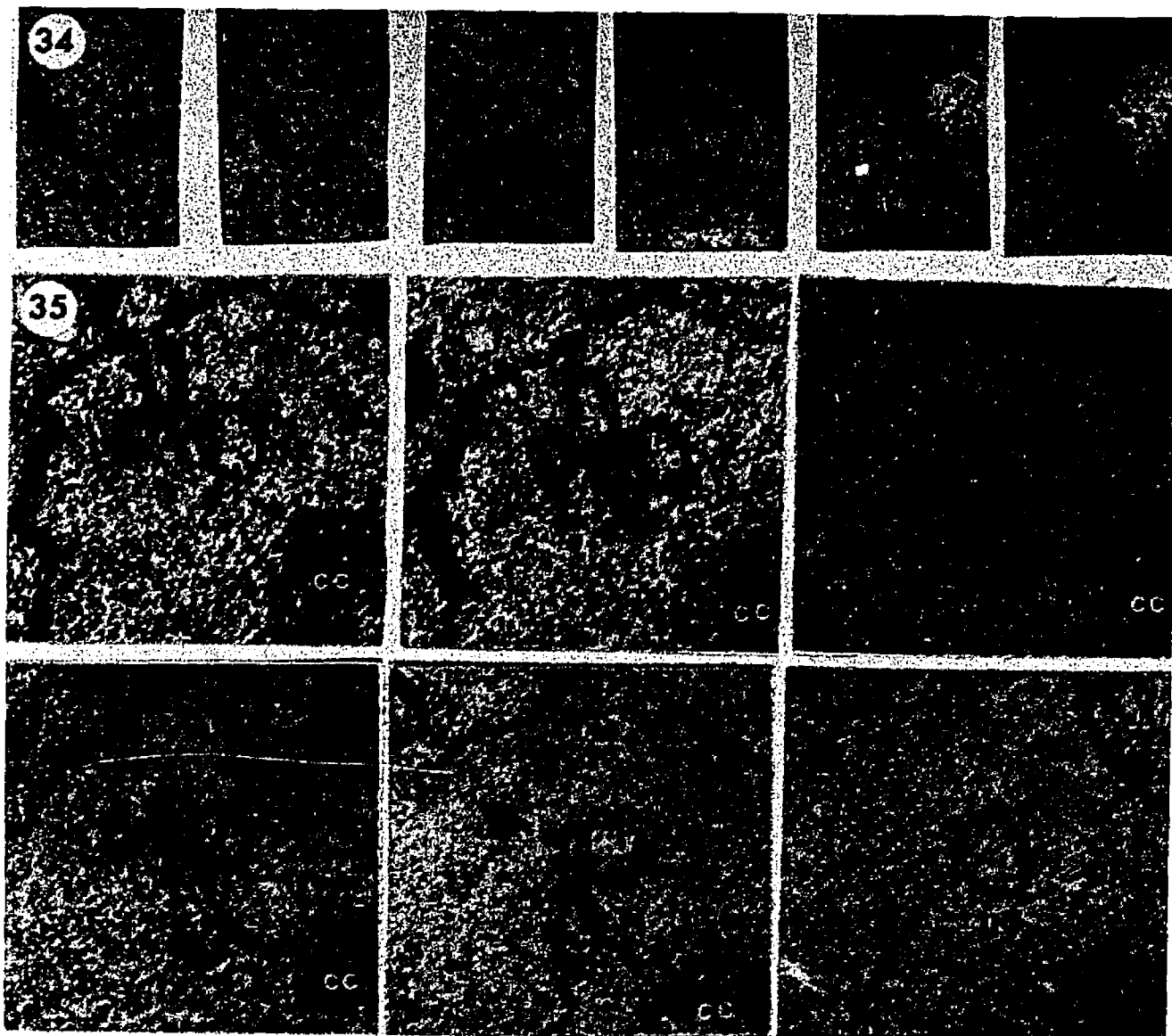
As noted above, many MTs are found near the pores of either annulate lamellae or nuclear envelope (Figs. 31, 32, and 33). Sometimes a vesicle appears to have a MT extending to the nuclear envelope but it may be an illusion (v-arrows, Fig. 32B and C). It is interesting that this is near an area possibly exhibiting nuclear envelope breakdown (§, Fig. 32D).

## 7. Nucleus

The nucleus, although still enclosed in the nuclear envelope, is irregular because it has bulges and indentations. Nuclear evaginations may extend for 3 to 4  $\mu\text{m}$  into the cytoplasmic exclusion zone (EV, Fig. 31). In cross section, these evaginations resemble irregular vesicles enclosed by two membranes (EV, Fig. 30). They are most prominent on the sides of the nucleus presumably facing the centrioles, and MTs can be seen among them (arrows, Fig. 30). No condensed chromatin is found within such evaginations.

FIGURE 34. Serial sections through an area of the prophase nucleus (N) showing how a single MT (arrow) can be associated with a nuclear invagination (IN). In this way, part of the cytoplasm as well as nuclear envelope (NE) are brought into the nucleus. Two sections are missing between Fig. d and Fig. e. EM x 44,000.

FIGURE 35. Serial sections of prophase nucleus showing relationship of MTs with the nuclear invaginations (IN<sub>1</sub>, IN<sub>2</sub>, and IN<sub>3</sub>). MTs (arrows, Figs. a, b, and d) seem to push the nuclear envelope (NE) inward to form an invagination (IN<sub>2</sub>, Figs. a and b) which ends just after the MT seems to terminate (arrow, Fig. d). Such invaginations may make contact with the chromatin condensing to form chromosomes (cc). The ends of such MTs may be C-MTs (c-arrow of IN<sub>1</sub>, Fig. c) especially just before the termination of the invagination (IN<sub>1</sub>, Fig. d). In general, the more MTs present, the larger and deeper the invagination (IN<sub>3</sub>, Fig. f). Some extend for 4  $\mu$ m which is one-quarter of the way through the nucleus. EM x 29,400.



Conversely, invaginations of nuclear envelope containing cytoplasm and MTs are seen in the nucleus (IN, Figs. 34, 35, and 36). Serial sectioning reveals that such cytoplasmic "fingers" may extend for over  $4\ \mu\text{m}$ ,  $\frac{1}{4}$  of the way through the nucleus, before they disappear (IN, Fig. 36). Although it is obvious that the invaginations do not overlap at this time, their growth toward the center of the nucleus from opposite sides suggests that overlap and interaction may be possible slightly later in prophase. At their deepest penetration in this one prophase cell studied, they are only about 3 or 4  $\mu\text{m}$  from the middle of the  $15\text{-}\mu\text{m}$  nucleus. Most of the invaginations, however, do not penetrate as deeply (IN<sub>2</sub>, Fig. 35).

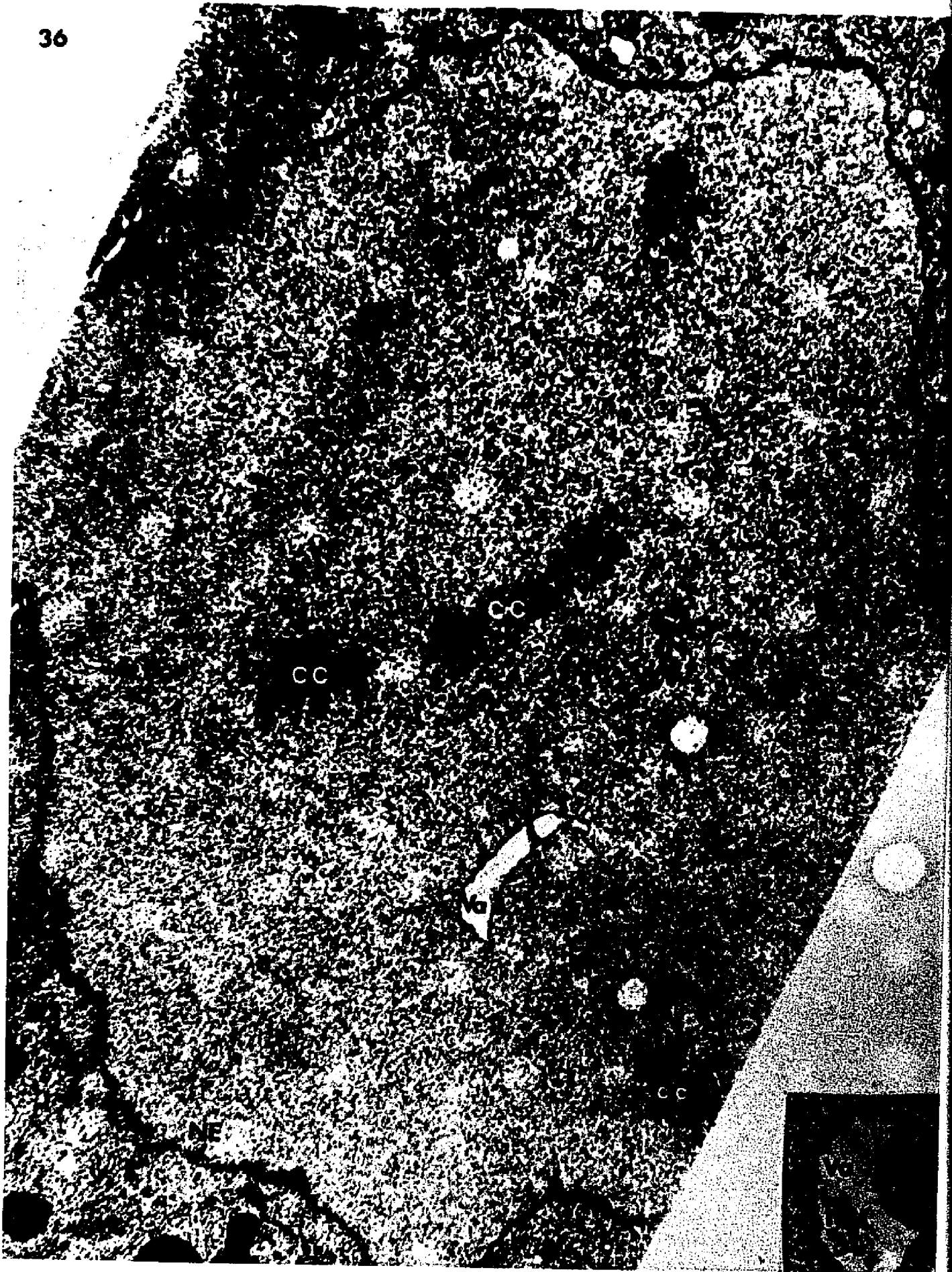
One feature common to most of these invaginations are MTs. In fact, MTs terminate just before the invagination does. (IN<sub>1</sub> and IN<sub>2</sub>, Fig. 35). The invagination may begin with many MTs in a relatively wide area and by attrition terminate with one MT in a narrow tube. Occasionally, only one or two MTs can be found in the invagination (Fig. 34) which then remains a narrow tube throughout its length. Such tubes are about  $0.25\ \mu\text{m}$  in diameter. In rare instances, a narrow invagination may occur without any MT apparent. Some "intranuclear" MTs may be short, longitudinal ones (Arrows, Fig. 35) or even C-MTs (C-arrow, Fig. 35). Such C-MTs usually occur just before MT termination.

Serial sections reveal a possible connection between the invaginations and the condensing chromosomes (CC) since the former seem to be growing toward the latter (IN<sub>2</sub>, Fig. 35). As noted above, although MTs appear to touch the nuclear envelope, in no instance do they penetrate it (Arrows, Figs. 26 and 32E). Rather, the presence of so many oblique MTs near

FIGURE 36. Section through the prophase nucleus. Its envelope (NE) is intact but irregular. Condensing chromosomes (cc) appear as electron-dense clumps of material. MT-containing invaginations (IN) can still be seen in this section about 4  $\mu$ m into the nucleus. A small amount of intranuclear membrane (IM) which resembles saccular ER is present. A conspicuous intranuclear vacuole (Va) is one of several seen in other sections. Another appears in the inset. The section is supported by a formvar film visible in the upper left and lower right. Since the prophase thick section (Fig. 25) was cross-sectioned, this section's width is the same as the thickness of the original thick section. EM x 19,800.

Inset. Another intranuclear vacuole. It appears to be surrounded by a double membrane. In this respect, it resembles the nuclear envelope. Intravacuolar membranes (IVM) are visible within the vacuole. EM x 34,600.

36



the nucleus (Fig. 32) suggests that they course along the nuclear surface.

Evidence of nuclear envelope breakdown is difficult to find but is present nevertheless. Small gaps in the envelope (\$, Fig. 32D), although rarely seen, probably grow wider and more numerous with time. Also, some mixing of cytoplasm with nucleoplasm may already be seen but interpretation is difficult (\$, Fig. 31).

The nucleoplasm has condensed into chromosomes easily visible as electron-dense clumps by electron microscopy (CC, Figs. 35 and 36), or as rather broad threads by phase microscopy (CC, Fig. 25). Few are seen at the periphery of the nucleus; many are grouped about the centrally-located nucleolus (Nu, Fig. 25) which at this stage has lost its connection to the nuclear envelope just prior to its disappearance.

Another interesting feature peculiar to the prophase nucleus is the presence of amorphous, electron-transparent vacuoles (Va, Fig. 36). These may be surrounded by a single (Fig. 36) or double (Fig. 36, inset) membrane. Sometimes, they enclose other membranous elements (IVM, Fig. 36, inset). Occasionally, intranuclear membranes resembling the nuclear envelope are seen (IM, Fig. 36). These do not enclose part of the cytoplasm and do not form circular profiles. They are, therefore, very different from the nuclear invaginations.

#### D. Fine Structure of the Metaphase Cell.

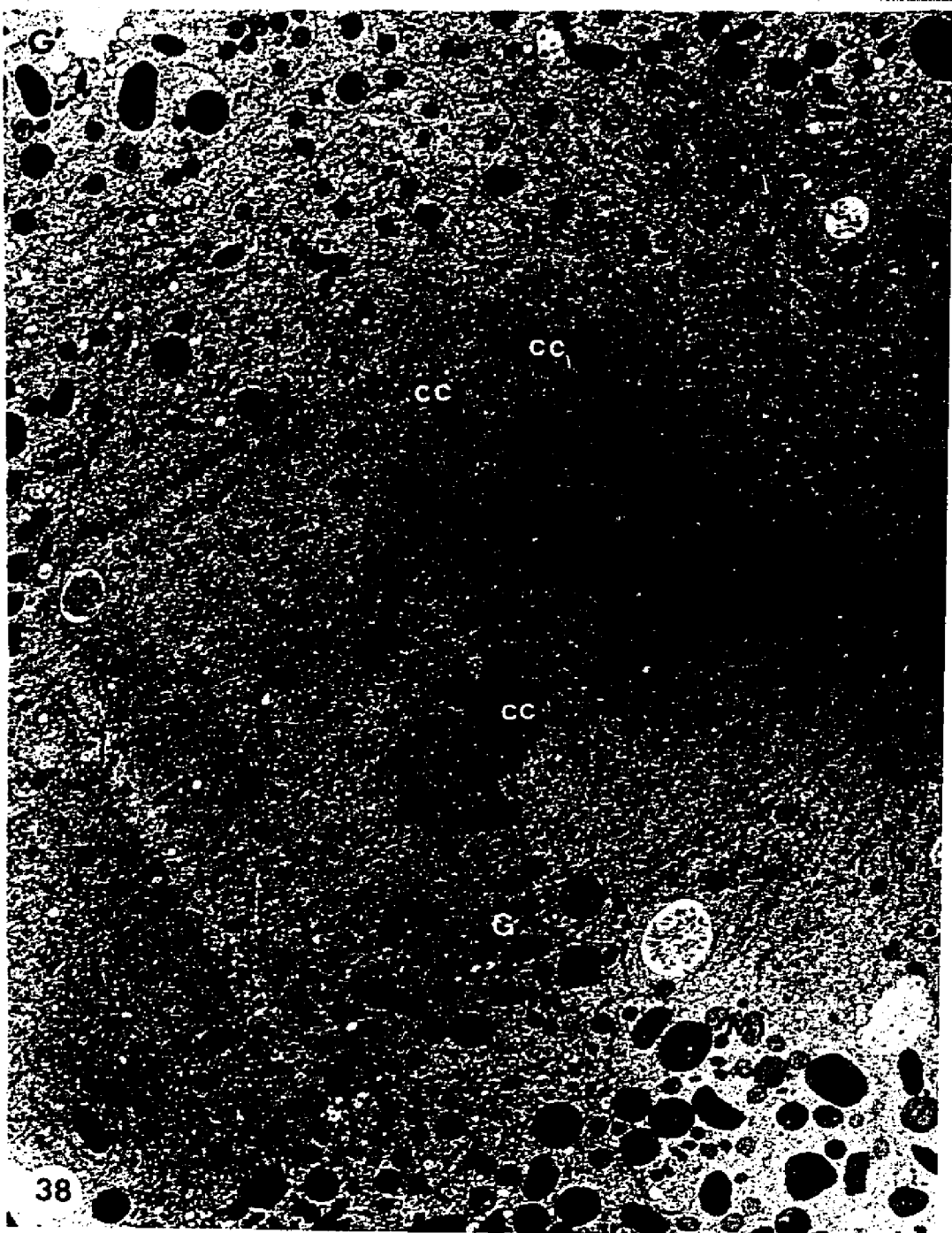
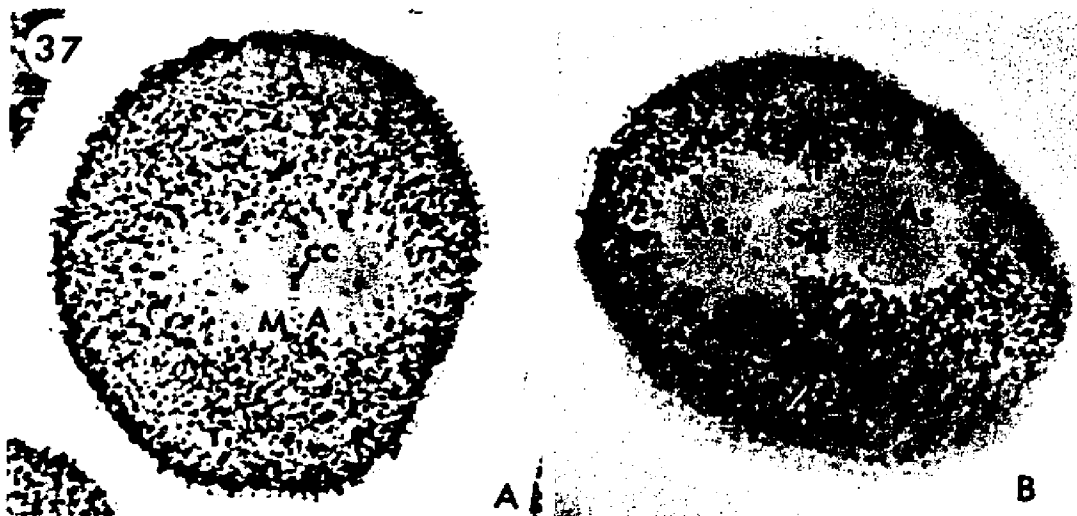
At metaphase the nuclear envelope has already disappeared, the chromosomes (CC) are aligned on the metaphase plate (MP), and the mitotic apparatus (MA) has been assembled (Fig. 37A and B). The mitotic apparatus has the appearance of two spheres adhering to each other along the metaphase plate.

FIGURE 37. Thick sections of metaphase cells.

37A. The mitotic apparatus is fully formed (MA). The chromatin has fully condensed into many small chromosomes (cc) aligned in the center of the apparatus. Phase contrast x 725.

37B. The mitotic apparatus consists of two large, spherical asters (As) separated by a narrower spindle region (Sp). The center of the spindle where the chromosomes are aligned forms the metaphase plate (MP). Phase contrast x 725.

FIGURE 38. Longitudinal section through the metaphase spindle of Fig. 37A. A line of chromosomes (cc) are at the center of the spindle. A small Golgi apparatus (G) is at the periphery aligned with the chromosomes (see Fig. 44 for higher magnification). Another (G') is just outside the mitotic apparatus. The entire spindle is surrounded by saccular ER (SER) but most of the ER in the spindle itself is tubular (TER). Some ER forms loops (LER). Spindle MTs (arrow) can be resolved even at this low magnification. Mitochondria (Mi) surround the spindle, being found both among the saccular ER and beyond but not within the spindle itself. Other granules, organelles, and particles are excluded. EM x 6,300.



### 1. Endoplasmic Reticulum

Electron microscopy reveals smooth saccular ER in the mitotic apparatus, most of it forming a thick band around the spindle and especially along edges of the metaphase plate (SER, Fig. 38). The inner area of the spindle, near the chromosomes has mostly tubular ER although saccular ER is also present. Thus, spindle cross sections through chromosome-to-pole (Fig. 39) or metaphase plate (Fig. 40) regions have tubular ER (TER).

In the aster there is a little tubular ER near the centriole (Ce, Figs. 41 and 42) and saccular ER (SER) radiating from more distal regions, especially toward the spindle (Sp, Fig. 41). Often, loops of saccular ER (LER, Fig. 41) can be found. In general, aster ER radiates outward from the centriolar region much as MTs do. Vesicular ER is present in both spindle and asters, and is distributed peripherally (v, Fig. 41). In this respect it is similar to the saccular ER which is also at the periphery. Thus, the overall pattern seems to be one in which the saccular and vesicular ER is found at the periphery while the tubular ER is found in the internal areas of the mitotic apparatus. This difference may be seen in cross-section at the border of the mitotic apparatus where the peripheral saccular ER gives way to the internal tubular ER even before the MTs of the spindle are seen (Fig. 43).

### 2. Annulate Lamellae and Heavy Bodies

No annulate lamellae or heavy bodies are seen during metaphase.

### 3. Golgi Apparatus

An active Golgi apparatus is found at metaphase just

FIGURE 39. Cross-section through the metaphase chromosome-to-pole region near the chromosomes. This section is from the cell shown in Fig. 37B. Among the numerous MTs (arrows) are a few C-MTs (C-arrows). Much smooth tubular ER (TER) is also present. EM x 45,000.

FIGURE 40. Cross-section through the metaphase plate of the cell shown in Fig. 37B. There are many C-MTs (C-arrows) relative to the number of normal MTs (arrows). Chromosomes (CC) and smooth tubular ER (TER) are also present. EM x 33,600.

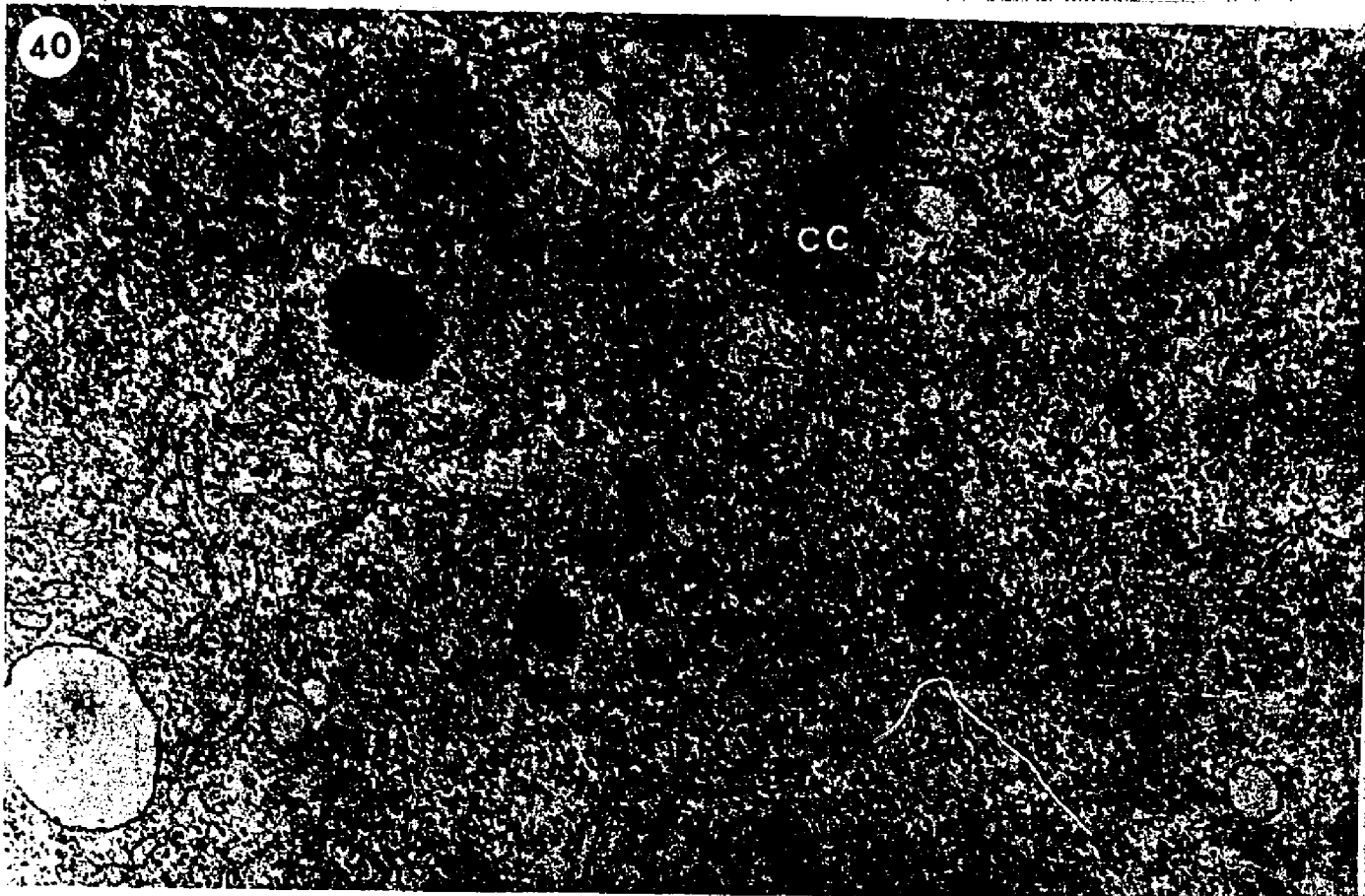
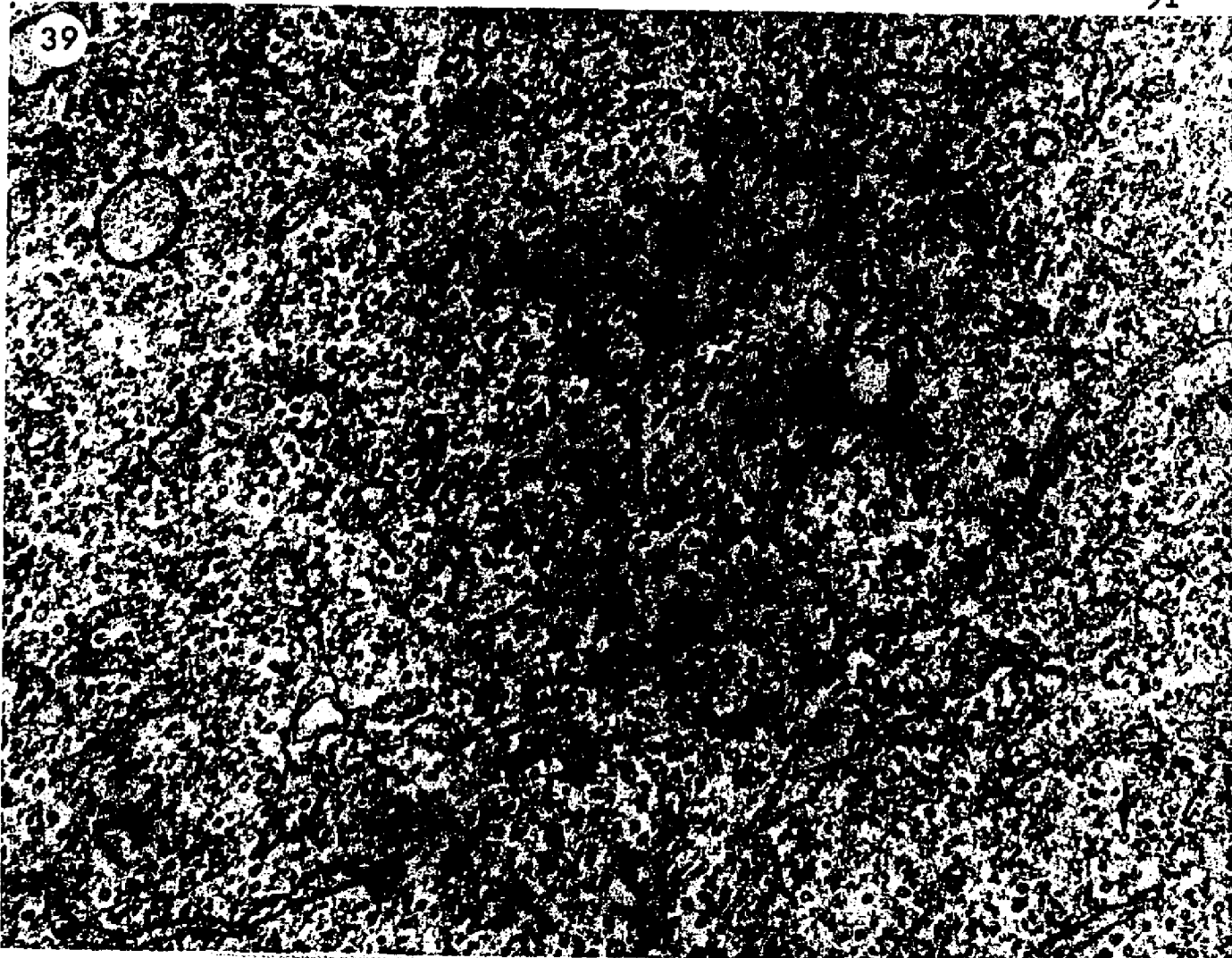
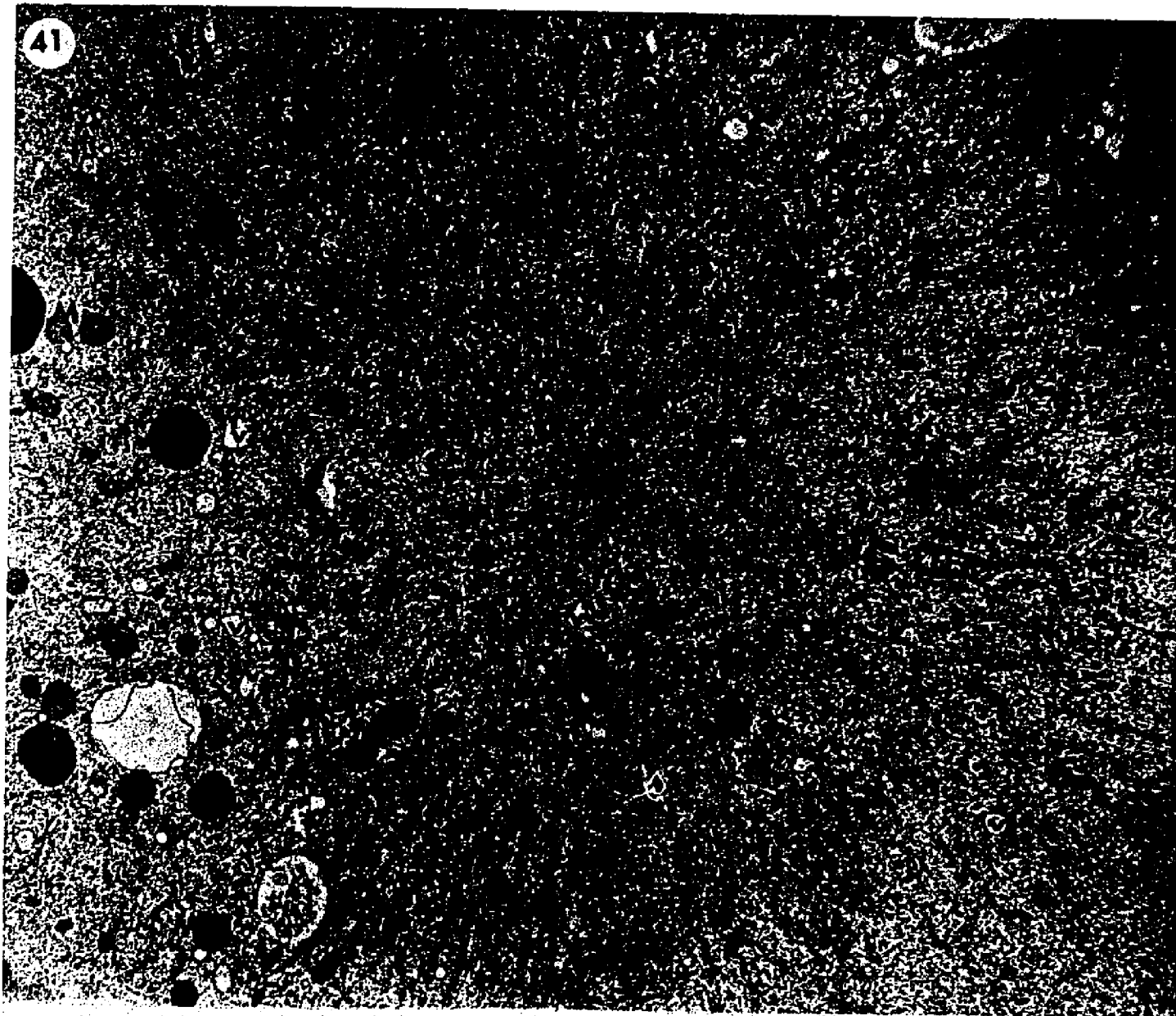


FIGURE 41. Longitudinal section through the metaphase aster of the cell shown in Fig. 37A. At the center of the aster (As) is a single centriole (Ce), i.e. no daughter centriole is present. MTs (arrows) radiate from the vicinity of the centriole but do not touch it. ER also seems to radiate from the centriolar region, most of it tubular (TER) although some saccular ER (SER) is found at the periphery. Looped ER (LER) can also be found, especially on the side where the spindle (Sp) is located. Vesicular ER (v) is mostly peripheral as are the mitochondria (Mi). Some mitochondria (Mi-1) are still associated with vesicles. EM x 14,300.

FIGURE 42. Higher magnification of the centriole in Fig. 41. The tubular nature of the centriole (Ce) is observed. Although it is sectioned obliquely, the MTs of its walls can be distinguished (arrowheads). Many other MTs of the mitotic apparatus (arrows) surround it but none actually touch the centriole. EM x 82,500.



peripheral to the line of chromosomes on the metaphase plate (G, Figs. 38 and 44). It has vesicular swellings on both faces indicating its active state. Whether its distribution is random or nonrandom throughout the cell could not be determined, but similar patches are found just outside the mitotic apparatus (G', Fig. 38). Also, anaphase seems to have a Golgi apparatus at the chromosome line, too (see anaphase section).

#### 4. Mitochondria

Mitochondria are largely excluded from the spindle and metaphase plate (Mi, Fig. 38) as well as from the centriolar region (Mi, Fig. 41) but are found all over the periphery of the mitotic apparatus, especially in the band of saccular ER at the border of the metaphase plate (Mi, Fig. 38). They are also found near the cell cortex (Mi, Fig. 45). As before, the mitochondria are often contiguous to lipid droplets (L, Figs. 43 and 45) and display small dense granules (g, Fig. 43). Vesicular connections can be observed (Mi-1, Figs. 41 and 43).

#### 5. Mitotic apparatus

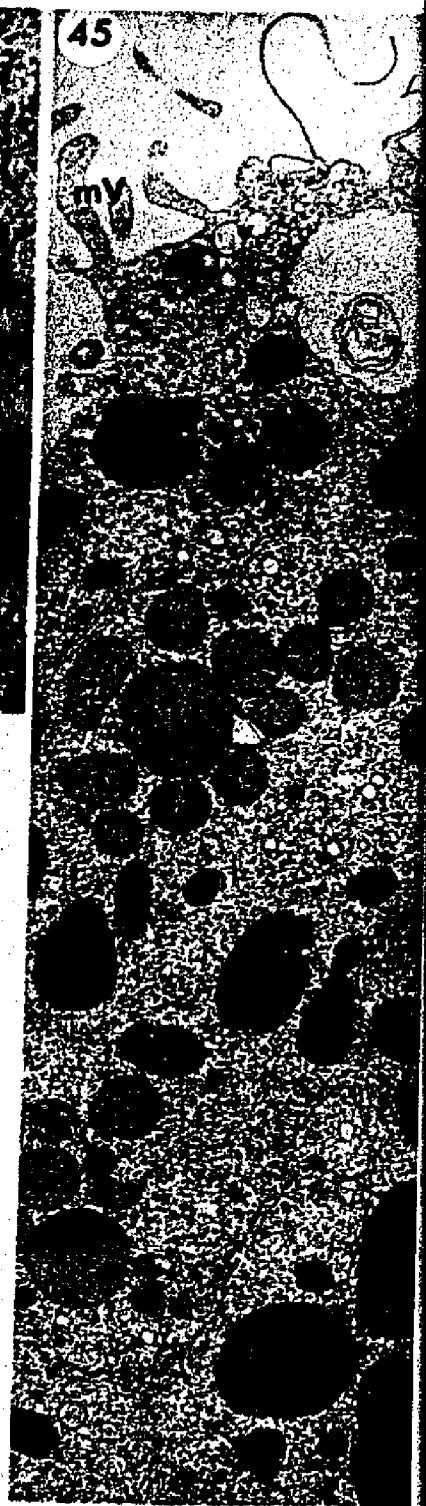
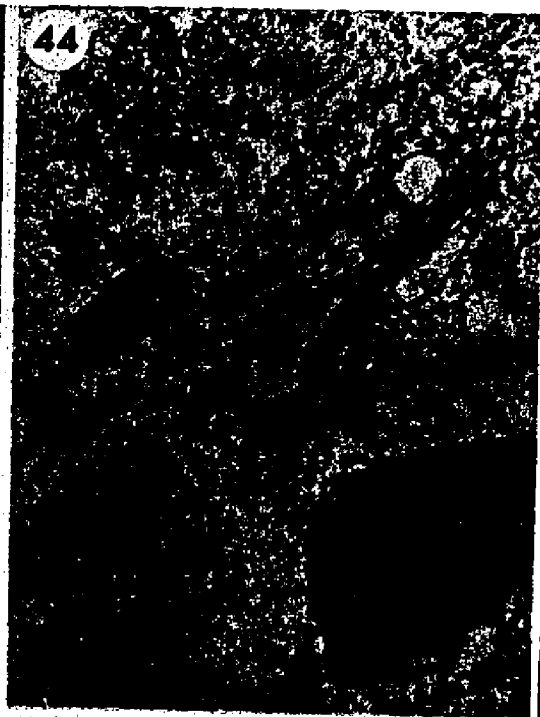
The mitotic apparatus is fully formed, consisting of centrioles (Ce, Figs. 41 and 42), asters (As, Figs. 37 and 41), spindle (Sp, Figs. 37B and 38), and chromosomes (cc, Figs. 37A and 38) aligned on the metaphase plate (MP, Fig. 37B).

The centriole (Ce, Figs. 41 and 42) is 0.2  $\mu\text{m}$  in diameter. It is in the center of the aster and is the focal point of both the MTs (arrows) and ER (Fig. 41). These run parallel to each other and are the major structural elements of the aster. Mitochondria are not found near the centriole. Rather, they remain several micrometers away, loosely surrounding the

FIGURE 43. Continuity of metaphase mitotic apparatus ER with that of the general cytoplasm. ER continues from the spindle where it is mostly tubular (TER) through the periphery where it is saccular (SER) into the surrounding cytoplasm. Little rough ER can be found. Mitochondria still surround lipid droplets (L) and contain dense granules (g). They still seem to contain vesicles (Mi-1). EM x 18,000.

FIGURE 44. Golgi apparatus aligned with the chromosomes of the metaphase plate. This is the same Golgi apparatus (G) of Fig. 38 at higher magnification. Its proximity to the chromosomes (CC) makes it noteworthy. The numerous vesicles of various sizes along both faces of the apparatus suggests that it is active. EM x 50,700.

FIGURE 45. The cortex of the metaphase cell. Numerous microvilli are still present. Many mitochondria (Mi), especially surrounding lipid droplets (L) can be seen. Elements of ER (ER) and vesicles (v) are found near the cell surface. EM x 14,350.



centriole (Mi, Fig. 41). Higher magnification of the centriole (Ce, Fig. 42) helps reveal its own microtubular substructure. Serial sectioning did not reveal a daughter centriole. Although many MTs originate near the centriole, none actually touch it (arrows, Fig. 42).

As noted above, the aster surrounds the centriole and is composed of ER and MTs radiating from it (Fig. 41). Much of the ER near the centriole is tubular. Toward the spindle, sacular ER may be seen and is often found as continuous loops or circles (LER, Fig. 41). Vesicular ER (v) is found mostly in the periphery of the aster. (Fig. 41).

The spindle is composed of many MTs and much ER (Fig. 39). In the chromosome-to-pole region near the chromosomes (Fig. 39) approximately 90% of the MTs are normal (arrows, Fig. 39). The other 10% are C-MTs (C-arrows, Fig. 39). In the metaphase plate region, however, the ratio of C-MTs to normal MTs changes. Thus, only about 50% of the MTs are complete while the other 50% are C-MTs (Fig. 40 and Table 4). Both normal and C-MTs are surrounded by a clear zone devoid of background ribosomes and other small particles. (Figs. 39 and 40).

TABLE 4

## TABULATION OF METAPHASE SPINDLE MICROTUBULES

<u>REGION OF SPINDLE</u>	<u>NUMBERS OF MTs</u>		<u>PER CENT C-MTs</u>
	<u>C-MTs</u>	<u>O-MTs</u>	
Metaphase plate	328	306	51.70

Chromosome-to-pole  
near the chromosomes      41      383      9.67

The data was collected from one metaphase cell by combining the counts from several sections. The absolute values cannot be compared as they reflect only the number of sections counted.

In longitudinal sections C-MTs are difficult to distinguish. It is thought that they are formed when a MT has less than the usual 13 protofilaments. This prevents the MT from closing up so that it forms a "C" in cross-section rather than an "O". From model analysis, Cohen and Gottlieb (1971) felt that in longitudinal section they may appear as a widened area of the MT, i.e., as greater than the usual 250 Å diameter because they are lying flat rather than rounded up (W-arrows, Fig. 46). Alternatively, they may appear as an extension of one edge of the MT while the other edge stops (1-arrow, Fig. 46). Although such areas of MTs have been found, it is impossible to equate them definitively with longitudinal views of C-MTs. Their location at the metaphase plate, however, is supportive.

#### E. Fine Structure of the Anaphase Cell

The chromosomes separate with the onset of anaphase and remain aligned in sets during their poleward movement. As they move apart, the chromosomes (CC) define an interzonal area (I, Figs. 47, 48, and 49) between them. Naturally, as the chromosome sets move further apart, this interzone grows longer. Simultaneously, the spindle elongates so that the poles grow 15% further apart (Harvey, 1956). In addition, the anaphase aster (As) is larger (Harvey, 1956) and projects rays into the surrounding cytoplasm (Figs. 47 and 48).

##### 1. Endoplasmic Reticulum

The distribution of ER at anaphase resembles that of metaphase. From the centriolar region saccular ER radiates in all directions as a major structural element of the aster (As, Fig. 49). On the spindle side of the asters, tubular ER mixing with some saccular ER extends to the chromosomes (SER',

FIGURE 46. Possible C-MTs in longitudinal section at the metaphase plate. It is thought that if the protofilaments of a C-MT were just lying flat without curling, it would resemble a straight line if viewed edge-on in longitudinal section. Such single lines continuing from normal MTs can be seen (1-arrows). Alternatively, if the flattened protofilaments were viewed broadside, it should form an image resembling a widened MT since flattened protofilaments cover a greater area than those folded up to form the normal MT cylinder. They may also appear lighter since only one layer of protofilaments rather than two is being viewed. Such widened areas of MTs are also observed (W-arrows). Their appearance among the chromosomes (CC) of the metaphase plate is supportive because this region of the spindle has the highest percentage of C-MTs. EM x 45,000.

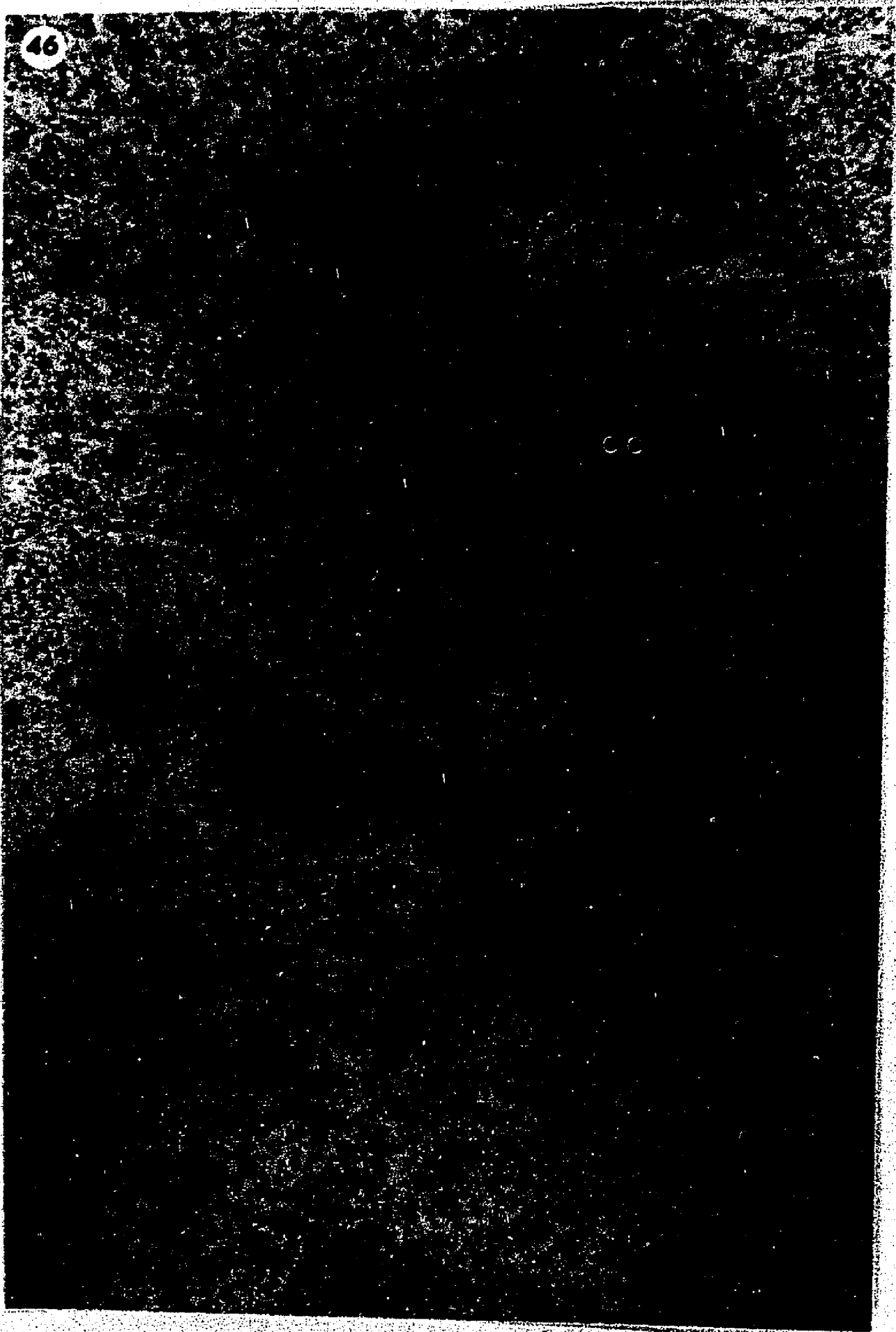


Fig. 49). Saccular ER forms a band around the entire spindle (SER, Fig. 49) with continuity into surrounding cytoplasm in some places (SER, Fig. 50). Small amounts of rough ER (rER, Fig. 50) are sometimes seen here but the rest is smooth. Vesicular ER also surrounds the mitotic apparatus but most of it is within the asters (v, Fig. 49). As before, the vesicular ER is often associated with mitochondria. The interzone (I, Fig. 49) has much less ER as comparisons of cross sections of chromosome-to-pole regions (Fig. 51) with interzone regions (Fig. 52) demonstrates. Interzone of early anaphase, however, does have more ER (ER, Fig. 53) than mid-anaphase (Fig. 51).

## 2. Annulate Lamellae and Heavy Bodies

No annulate lamellae or heavy bodies appear during anaphase.

## 3. Golgi Apparatus

Small patches of Golgi apparatus with few lamellae are located in the periphery of the mitotic apparatus and near where the chromosomes are found (G, Fig. 49). They are also found away from the mitotic apparatus in the general cytoplasm (G, Fig. 50).

## 4. Mitochondria

Anaphase mitochondria are like the metaphase ones. They surround the mitotic apparatus and are associated with vesicular ER and lipid droplets (Mi, Fig. 49). Small granules within mitochondria are still present (g, Fig. 50).

## 5. Microtubules

MTs radiate from the centriolar region as a major structural component of the aster. Within the spindle, radiating MTs intermingle with MTs coming from the chromosomes them-

FIGURE 47. Thick section of early anaphase cell. The sets of chromosomes (CC) have begun to move apart, leaving a small region, the interzone (I) between them. The spindle (Sp) is easier to distinguish from the asters (As) than in the case of the metaphase mitotic apparatus. Phase contrast x 1,100.

FIGURE 48. Thick section of mid-anaphase cell. The interzone region (I) has grown larger as the sets of chromosomes (cc) move further apart, still aligned, toward the poles. The spindle (Sp) is defined between the two asters (As). Phase contrast x 1,200.

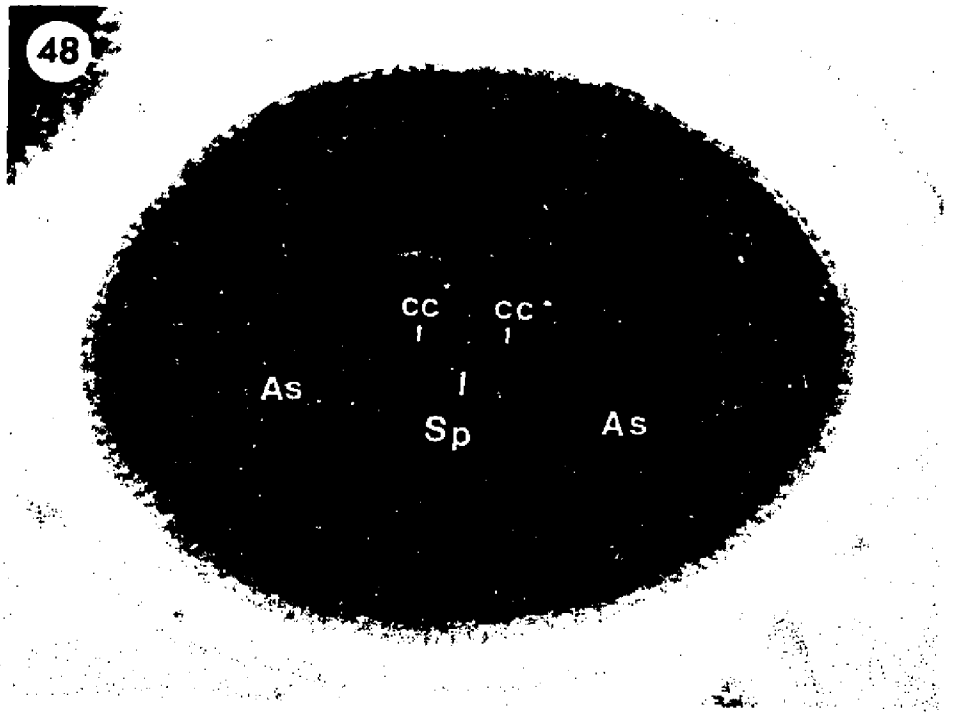
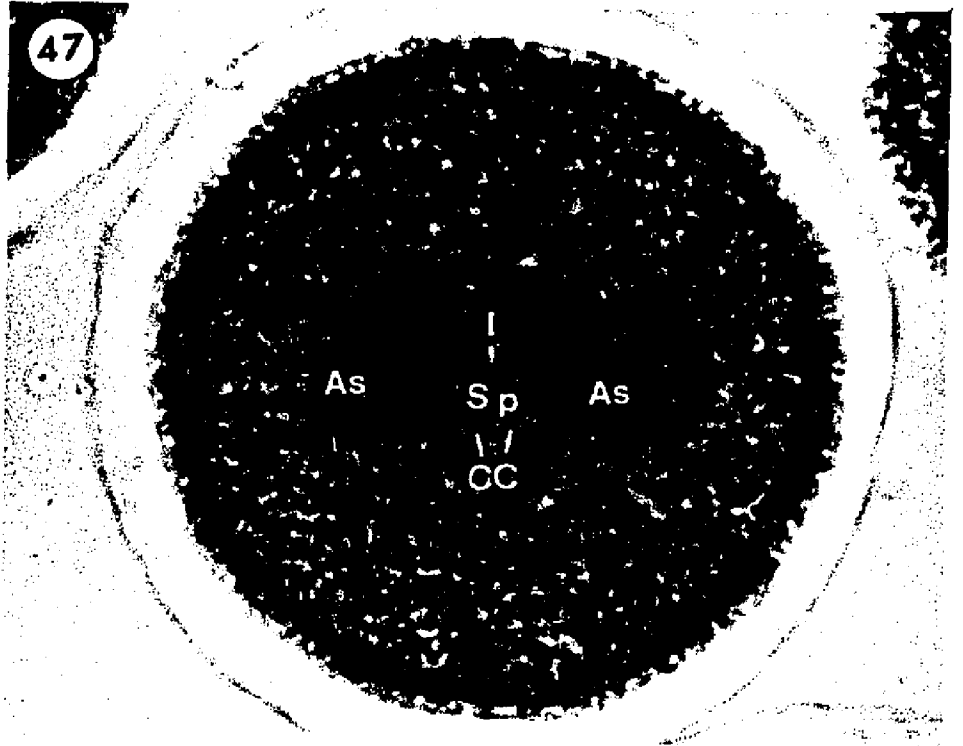


FIGURE 49. Longitudinal section through the mitotic apparatus of the mid-anaphase cell of Fig. 48. The spindle is surrounded by mostly smooth saccular ER (SER) which seems to radiate from the poles in the aster (As). Smooth ER, mostly tubular but with some cisternae (SER') extend to the chromosomes (cc). Only some of this ER extends into the interzone (I). There, the ER does not run in any particular direction as is the case with the radiating ER of the asters and the inter-polar ER that surrounds the spindle (SER). Vesicular ER (v) surrounds the mitotic apparatus but is not found in quantity in the spindle itself, and this is especially true of the interzone. Numerous mitochondria (Mi) continue to surround the mitotic apparatus. They are still associated with lipid droplets (L). Like the metaphase cell (Fig. 38), the anaphase cell has a Golgi apparatus (G) in alignment with the chromosomes at the periphery of the spindle. EM x 5,600.



FIGURE 50. Continuation of anaphase mitotic apparatus ER into that of the general cytoplasm. Smooth ER from the mitotic apparatus (white SER) seems to continue into the general cytoplasm (black SER). Rough ER (rER) is sometimes seen but in very small amounts. A Golgi apparatus (G) in the general cytoplasm, having few vesicles, is probably not very active. Mitochondria around lipid droplets (L) are a common sight. A mitochondrion may have one (g) or more (g') dense granules. EM x 11,000.

FIGURE 51. Cross-section through the chromosome-to-pole region of a mid-anaphase cell. Although most of the MTs are normal ones (arrows), several C-MTs (C-arrows) can be found. A small amount of smooth ER (ER) is also present. This section is representative of the area near the chromosomes. EM x 44,800.

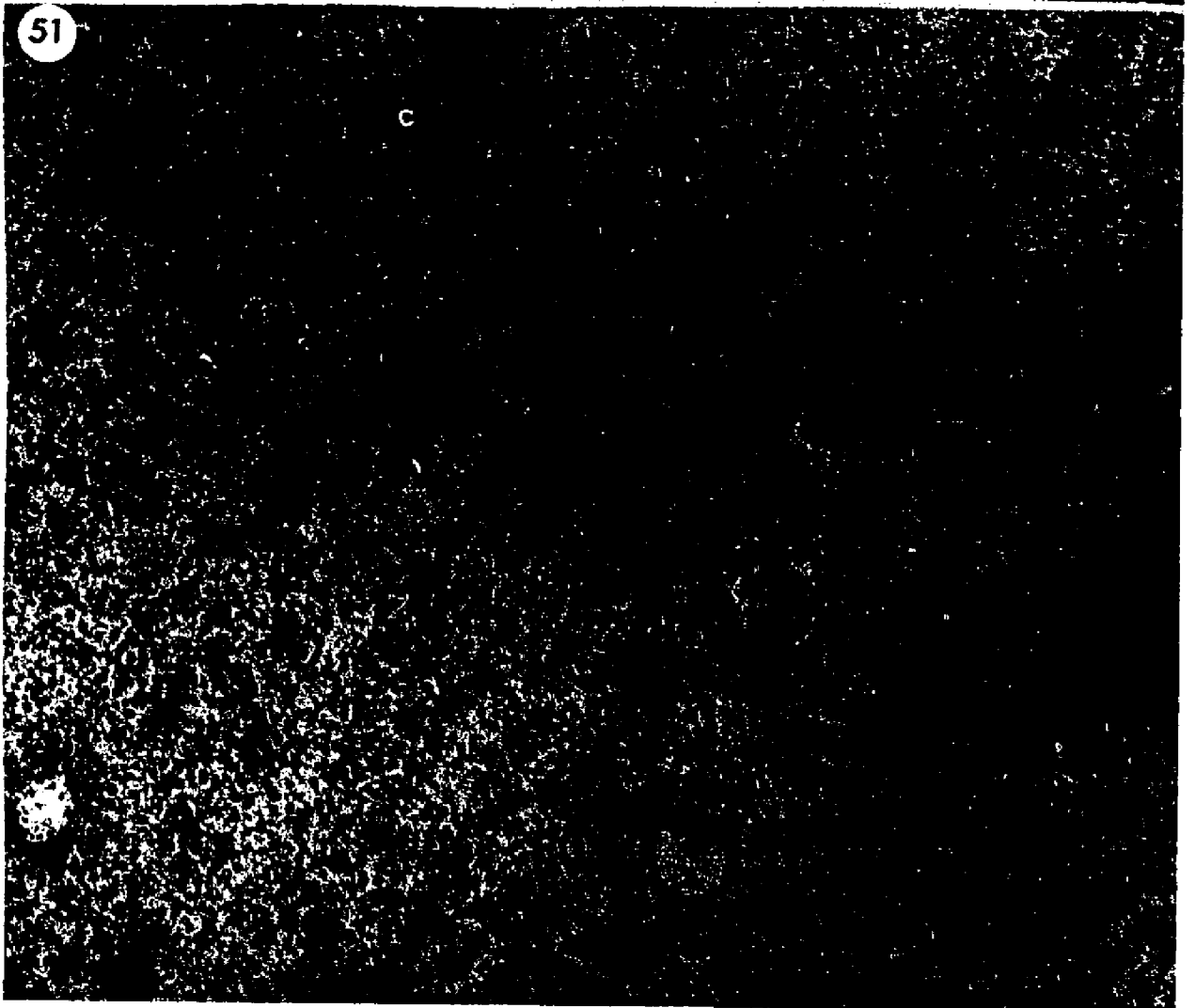
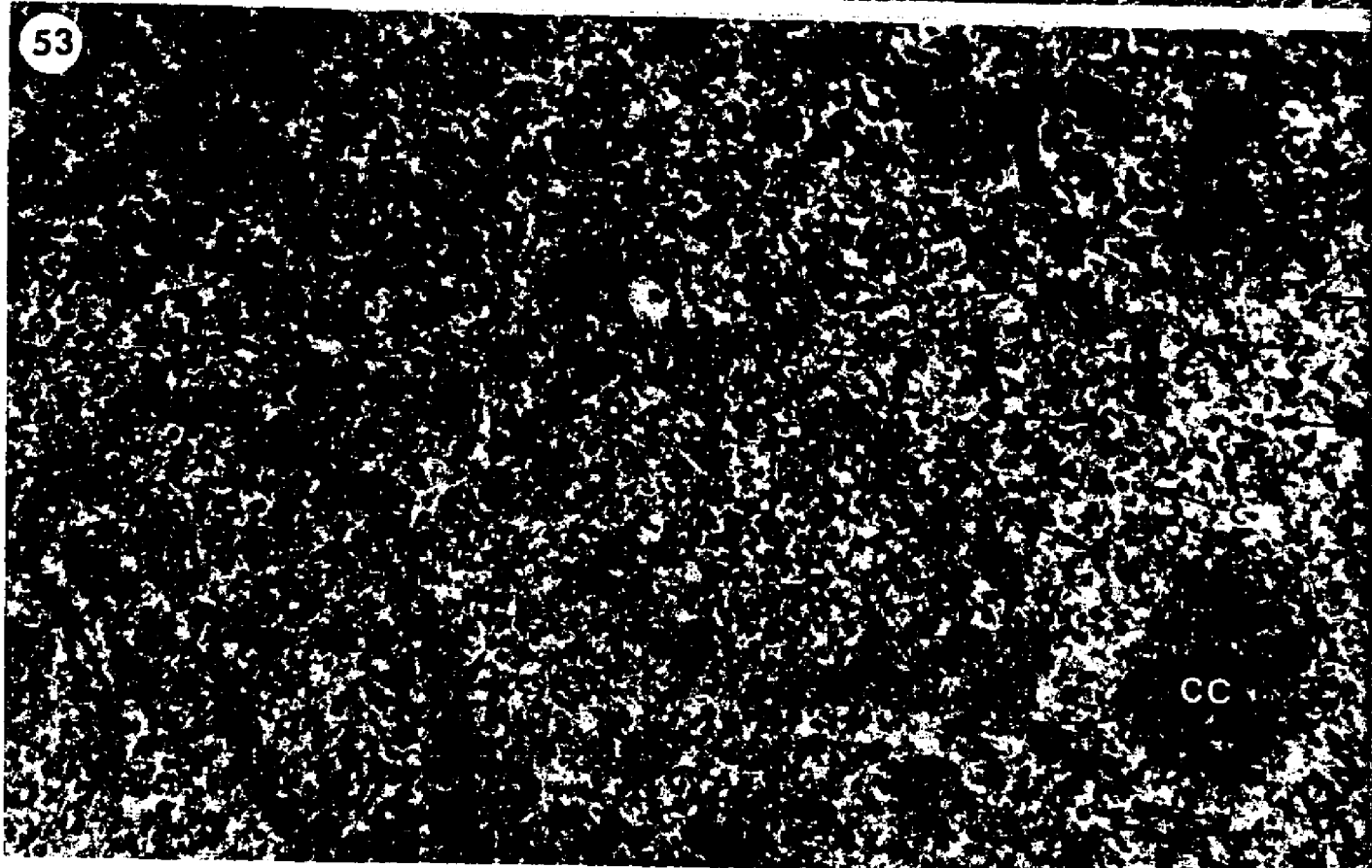
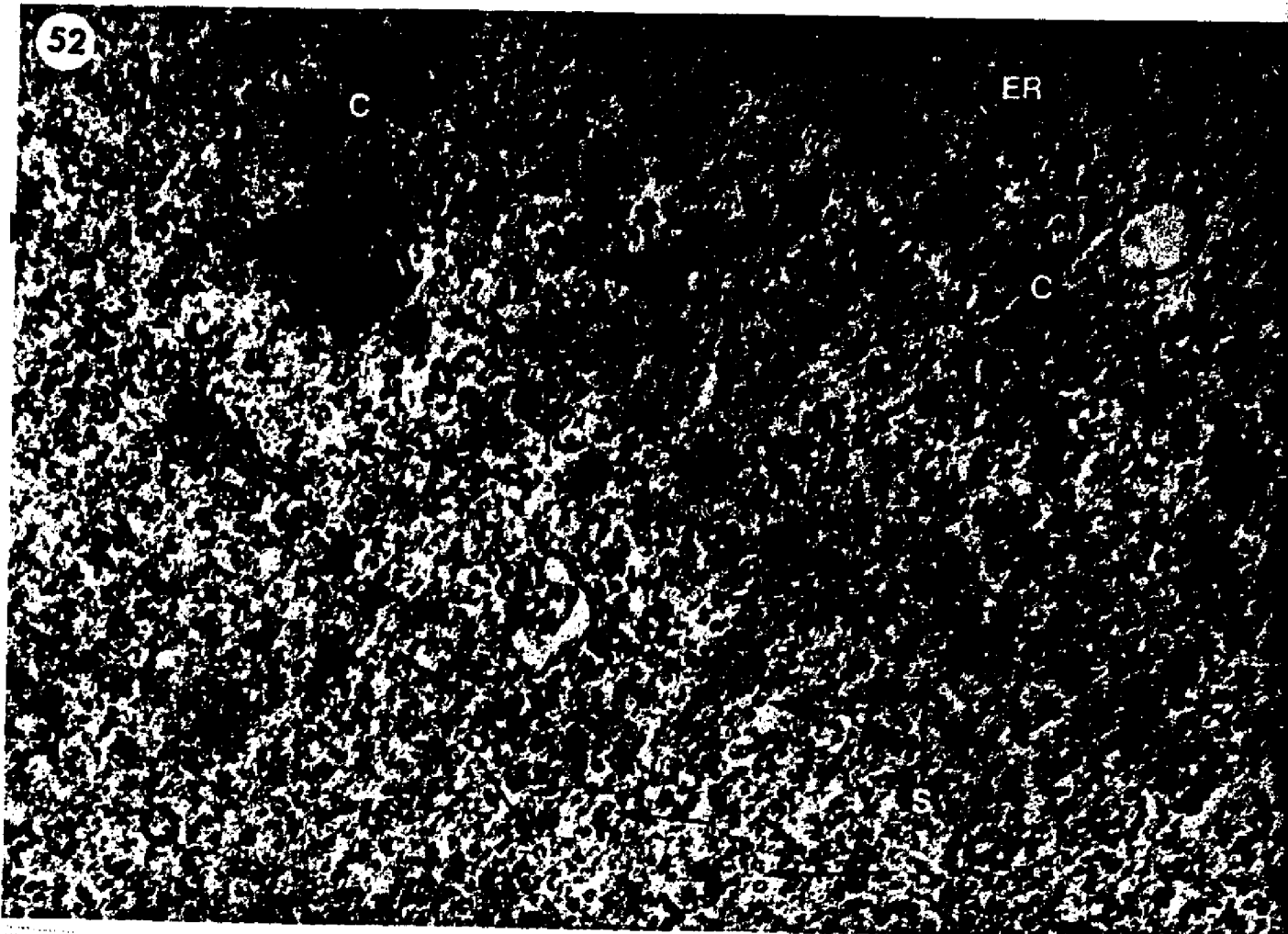


FIGURE 52. Cross-section through the middle of the interzone of the same mid-anaphase cell as Fig. 51. There are obviously fewer MTs than in Fig. 51, mainly because the interzone has only interpolar MTs whereas sections from the chromosome-to-pole region include chromosomal MTs in addition to the interpolar ones. Since over half the interzonal MTs are C-MTs (C-arrows), normal ones (arrows) are harder to find. An S-shaped MT (S-arrow) probably consists of two C-MTs that are joined together. ER is sparse and difficult to recognize but is present nevertheless (ER). EM x 75,000.

FIGURE 53. Cross-section through the interzone of the early anaphase of Fig. 47. Because it was sectioned slightly oblique, a chromosome (CC) is present. There are more MTs (arrows) than in the interzone of the mid-anaphase above (Fig. 52) but part of this is due to extra chromosomal MTs from the slightly oblique cut. Nevertheless, the many C-MTs present (C-arrows) suggests that it is mostly interzone. Two MTs attached to each other through a bridge-like structure (B-arrow) and an S-MT (S-arrow) are present. It is also easy to see that there is more smooth ER (ER) than in the mid-anaphase. EM x 58,500.



selves. Such chromosomal MTs are obviously missing from the interzone resulting in fewer MTs in this region. Thus, a comparison of spindle cross sections shows many more MTs in the chromosome-to-pole region (Fig. 51) than in the interzone (Fig. 52).

Another major difference between the interzone and the rest of the spindle involves the structure of the MTs themselves. C-MTs are at least 6 or 7 times more prevalent in the interzone than in the chromosome-to-pole region. In fact, well over half the MTs of the interzone are C-MTs while only 10% or less of the MTs of the chromosome-to-pole region are (Table 5; also compare Figs. 52 and 53 with Fig. 51).

Like normal MTs, C-MTs are usually surrounded by an electron-transparent clear zone. Yet, S-MTs (S-arrow, Fig. 53) and perhaps even bridged MTs (B-arrow, Fig. 53), which seem to be connected to each other through a bridge-like structure, are formed through this zone so at least these structures are not restricted by it.

It is impossible to attach any significance to the apparent increase in interzone C-MTs between early and mid-anaphase (Table 5). The early anaphase interzone is so narrow that all sections have some chromosomes in them. It is likely, therefore that the chromosomal MTs are included and increase the count of normal O-MTs. This has the effect of decreasing the percentage of C-MTs. The absolute numbers cannot be compared because the area counted, as well as the numbers of ambiguous MTs, differ. It is interesting to note, however, that the percentage of C-MTs in the chromosome-to-pole regions did increase from early to mid-anaphase.

TABLE 5  
 TABULATION OF ANAPHASE SPINDLE MICROTUBULES

<u>REGION OF SPINDLE</u>	<u>NUMBERS OF MTs</u>		<u>PERCENT C-MTs</u>
	<u>C-MTs</u>	<u>O-MTs</u>	
Early Anaphase			
Interzone	146	141	50
Chromosome-to-pole near the chromosomes	19	282	6
Mid Anaphase			
Interzone	86	47	65
Chromosome-to-pole near the chromosomes	69	617	10

This data was collected from one early and one mid-anaphase cell. The numbers of MTs are combined counts from several sections in the region indicated. Since the absolute values reflect only how many sections and how large an area was counted, they cannot be directly compared.

## F. Fine Structure of Isolated Spindles

C-MTs were found in large numbers at the metaphase plate and interzone of A. punctulata spindles after isolation in hexylene glycol (Cohen and Gottlieb, 1971), and in situ as reported in the present work. Their substructure must, therefore, be established.

### 1. The Substructure of C-MTs

Spindles isolated in hexylene glycol and fixed with glutaraldehyde in the presence of tannic acid present a negatively-stained image of C-MTs when thin sections are viewed in the electron microscope. High magnification (Fig. 54A and B) reveals that they have less than the 13 protofilaments normally found in A. punctulata spindle MTs (Fig. 54C and Tilney et al., 1973). No obvious C-MT with 13 protofilaments is observed, although some with 12 exist (Fig. 54B). Some have as few as 4 or 5 but since they resemble straight lines, it is not certain that they are indeed MTs. Also, C-MTs with few protofilaments are most usually seen as slightly oblique making it difficult if not impossible to count the actual number of subunits. Thus, C-MTs are probably not as stiff as normal MTs or even C-MTs with 10 or more subunits which are not as prone to appear slightly oblique in cross-section (Compare the clarity of subunits in Fig. 54).

Because it was often difficult to count the number of subunits, another method based on curvilinear measurements (Table 6) was developed. A flexible wire was placed around the circumference of prints ( $\times 270,000$ ) of normal MTs of 13 subunits (Tilney et al., 1973), and measured to obtain an average curvilinear subunit length of 62.6 Å. Using the same

method, the numbers of subunits in C-MTs which cannot be directly counted may be approximated (Table 6). The center to center distance between subunits averages 35 Å. In general, the more subunits, the more curvature so that 9 protofilaments (Fig. 54A) do not curve as much as 12 (Fig. 54B) or 13 (Fig. 54C).

## 2. Spindles Isolated in Modified MT Polymerization Medium

Isolation of spindles in the modified MT polymerization medium (Rebhun et al., 1974) reveals that in the medium containing only 20 mM EGTA, C-MTs almost totally disappear although a few are still present (C-arrows, Figs. 55 and 56). They are distributed in the same way, i.e., they are easier to find in the metaphase plate (Fig. 56) or interzone than in the chromosome-to-pole region (Fig. 55) where there are practically none. Morphologically they are the same as those found in situ and after isolation in hexylene glycol.

Due to the action of Triton X-100 detergent, isolates in modified polymerization medium do not preserve any membranous structures (Figs. 55 and 56) although ER is a major structural component in situ. Isolates in hexylene glycol, however, have smooth membranous vesicles similar to microsomes (Kane, 1962b; Goldman and Rebhun, 1969). Thus, although the ordered structure of ER as seen in situ disappears, the membranes do not.

Another difference between isolates in modified polymerization medium and isolates in hexylene glycol is the presence of a filamentous material in the former but not the latter. This filamentous material forms a network in the background (F1, Fig. 55). This network is more obvious in sections from chromosome-to-pole regions (Fig. 55) than those from

TABLE 6  
CURVILINEAR MEASUREMENTS OF C-MT CROSS SECTIONS

<u>MEASURED CIR-</u> <u>CUMPERENCE (mm)<sup>1</sup></u>	<u>ACTUAL CIR-</u> <u>CUMPERENCE (Å)<sup>2</sup></u>	<u>LINEAR</u> <u>SUBUNITS<sup>3</sup></u>	<u>PROBABLE</u> <u>SUBUNITS<sup>4</sup></u>
9.0	333	5.43	5
10.0	370	5.91	6
11.9	440	7.02	7
12.0	444	7.09	7
12.3	455	7.27	7
13.4	496	7.92	8
15.5	574	9.17	9
16.8	622	9.94	10
18.0	666	10.64	11
O-MT: 21.3	788	12.59	13

1. Measured by carefully overlaying MTs as they appear in prints of 270,000 X magnification with a flexible wire and then measuring the length of the wire.
2. Measured by dividing the length obtained in "1" above by 270,000.
3. The actual circumference as obtained in "2" divided by 62.6 Å, the curvilinear length obtained for 1 subunit.
4. The nearest whole number.

FIGURE 54. MT subunits. The subunits were viewed with a JEOL 100CX electron microscope and appear to be negatively stained by being fixed in the presence of tannic acid after isolation in hexylene glycol. It is obvious that C-MTs (Figs. A and B) are composed of less than 13 subunits (protofilaments). Also, the more subunits present, the more curvature.

54A. A C-MT with 9 subunits.

54B. Two C-MTs of 12 subunits each. They are attached to each other in such a way that if one would twist around the attachment site, an S-MT would result.

54C. Two normal MTs for comparison. Note the increased curvature that occurs with the addition of the one subunit to make 13 and thereby closing the MT cylinder.

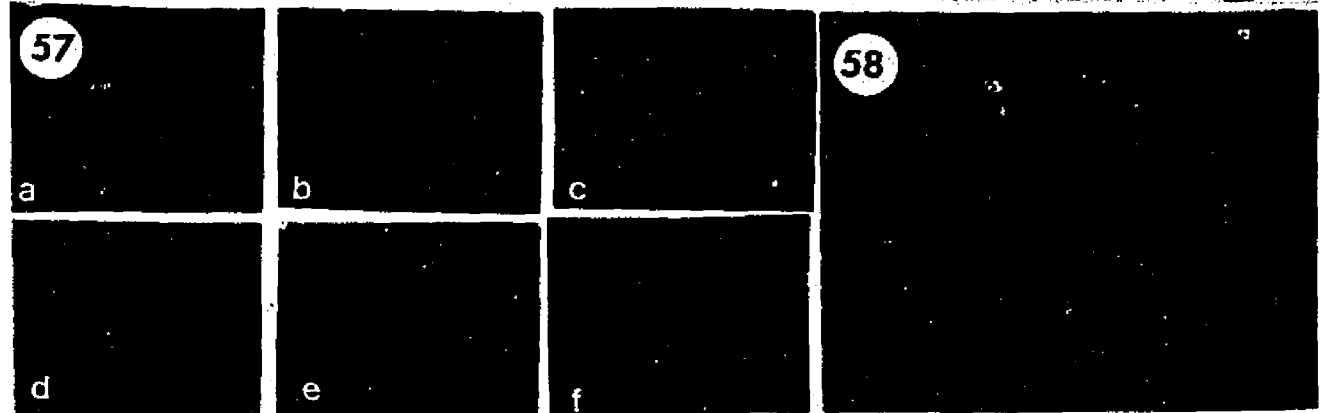
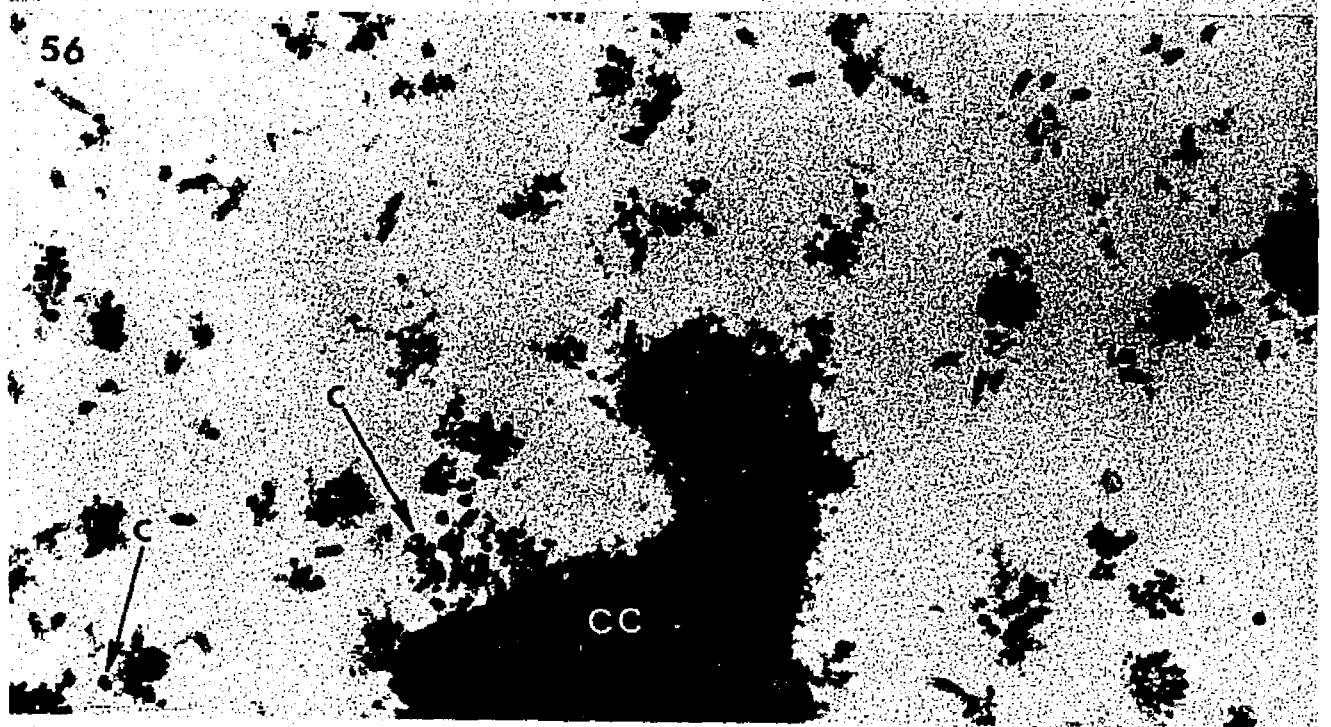
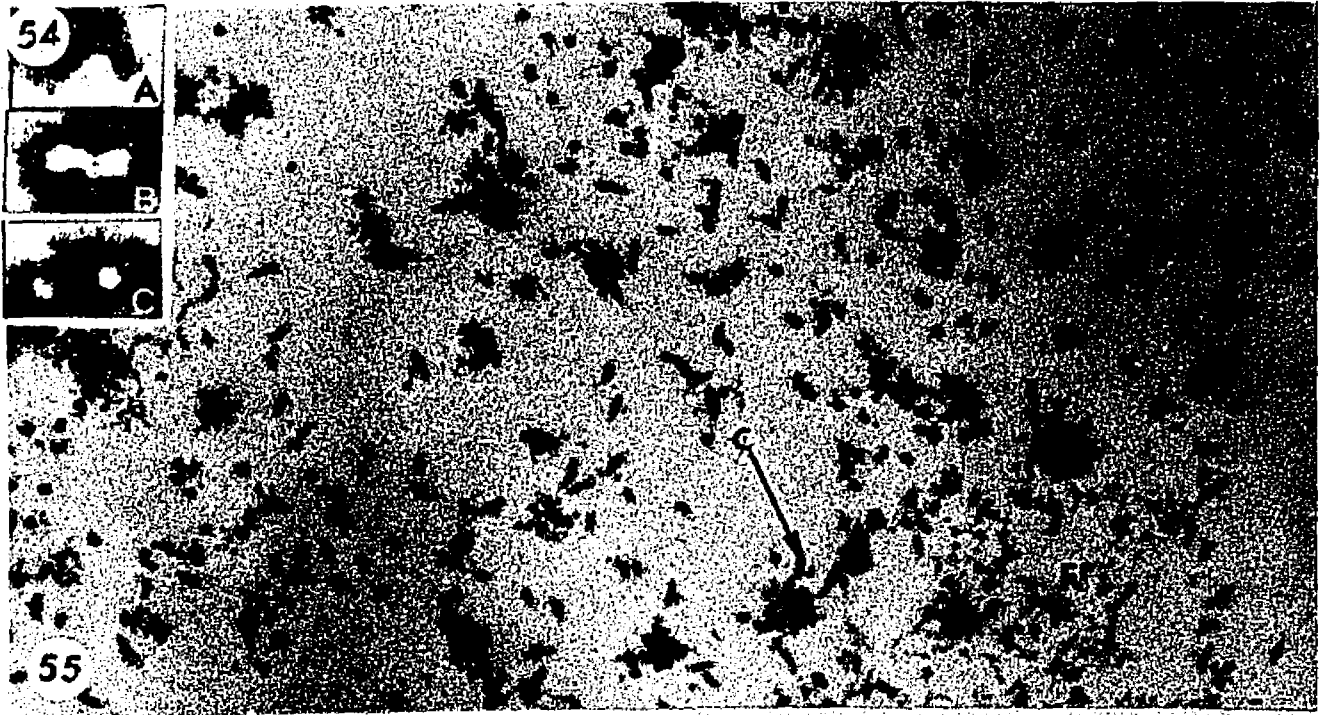
EM x 300,000.

FIGURE 55. Cross-section of the chromosome-to-pole region of an anaphase spindle isolated in the modified polymerization medium (20 mM EGTA). This section is located near the chromosomes. A rare C-MT is shown (C-arrow). A filamentous material (F1) is also present. Note the total absence of membranes, probably due to the action of the Triton X-100 detergent used during isolation. EM x 42,000.

FIGURE 56. Cross-section through the metaphase plate of a spindle isolated in modified polymerization medium (20 mM EGTA). In situ, this area is full of C-MTs (see Fig. 40) and ER. As above, there are no membranes from the ER and the number of C-MTs (C-arrows) is greatly reduced. In fact, this micrograph was chosen because it had more C-MTs than others. A chromosome (CC) is also present. EM x 49,500  
EM x 49,500.

FIGURE 57. Spindle birefringence during the first mitotic cycle of the Lytechinus variegatus zygote. Note that the interzone has little birefringence although MTs are known to be present in situ. Asters are not birefringent since their fibers are not parallel, radiating in all directions. a. metaphase; b to f. anaphase to telophase during the next five minutes. Polarization microscopy x 450.

FIGURE 58. Spindle birefringence during the third mitotic cycle of the Lytechinus variegatus zygote. Note the lack of birefringence in the four interzones. Polarization microscopy x 450.



metaphase plate (Fig. 56) or interzone. No such network is seen in situ.

### 3. Microtubule Clear Zones

Unlike MTs in situ which have a clear zone around them, MTs of isolated mitotic apparatuses lack such zones and are often seen to touch each other.

### G. Sea Urchin Spindle Birefringence

Using zygotes of Lytechinus variegatus which have little interfering pigment, polarization microscopy can be performed demonstrating changes in spindle birefringence from metaphase to telophase (Fig. 57). This reveals an almost total absence of birefringence in the interzone during the mitotic cycle. This lack of birefringence exactly correlates with the distribution of C-MTs in A. punctulata spindles. The same birefringence pattern continues at least into the 4-cell stage (Fig. 58). The slight decrease observed in birefringence at the metaphase plate during metaphase (Fig. 57a) is probably due to the presence of the non-birefringent chromosomes that are aligned there.

The absence of birefringence in the interzone is interesting because oriented MTs are known to be present and should be somewhat birefringent. While it is true that less birefringence is expected because of the fewer MTs present, nevertheless, some birefringence should be observed. Since the in situ study has shown that the area has a high percentage of C-MTs, it suggests that C-MTs may be exerting an influence on birefringence observable in vivo.

#### IV. DISCUSSION

##### A. Structural Changes In Situ Versus Biochemical Events During the First Mitotic Cycle

###### 1. Microtubules and Endoplasmic Reticulum

Electron micrographs presented in this study demonstrate that ER is a major part of the sea urchin cytoplasm at all stages and is particularly well-situated in and around the mitotic apparatus during its assembly and function. Since  $\text{Ca}^{++}$  is controlled by ER in muscle (Podolsky, 1968; Ebashi and Endo, 1968), it is natural to postulate a similar role for ER in A. punctulata zygotes. Indeed, careful control of  $\text{Ca}^{++}$  concentration is already known to be necessary for tubulin polymerization in vitro and that such MTs remain  $\text{Ca}^{++}$ -labile (Weisenberg, 1972).

Evidence that  $\text{Ca}^{++}$  is important in vivo comes from many systems. The calcium ionophore A23187, which raises intracellular  $\text{Ca}^{++}$  levels, was used to demonstrate reversible retraction and re-extension of Actinosphaerium axopodia, a process known to result from disassembly and assembly respectively of MTs (Schliwa, 1976). The same ionophore was used to depolymerize the cytoplasmic MT complex in cultured cells (Fuller et al., 1976).

Of more importance to this study, however, is the effect of  $\text{Ca}^{++}$  on the mitotic apparatus. Sisken and VedBrat (1977) found that HeLa metaphase can be prolonged by 40% when cells are exposed to drugs like nicotine, ionophore A23187, and caffeine which are all thought to increase cytoplasmic  $\text{Ca}^{++}$  concentration although by different mechanisms. A more direct approach was followed by Kiehart and Inoué (1976). As described

earlier (Introduction), they micro-injected  $\text{CaCl}_2$  into Echinoderm zygotes resulting in the loss of spindle birefringence only when injected near the spindle. After a while, the cell was obviously able to remove this  $\text{Ca}^{++}$  since spindle birefringence returned to normal. The ability of the cell to reverse all of these experiments suggests that the cell itself is capable of controlling local  $\text{Ca}^{++}$  levels.

As this study shows, three types of ER, most of it smooth, are found during the hour-long transition from unfertilized egg to cleavage: vesicular, saccular, and tubular. Each is dominant at different stages (summarized in Table 7), suggesting that they might have different functions. The available data suggest that of the three, tubular ER is likely to be the primary  $\text{Ca}^{++}$  regulator, although it may not be the only one. This is based on the fact that it is the dominant form when such regulation is thought to occur. Since the  $\text{Ca}^{++}$ -stimulated ATPase found by Mazia et al. (1972) and Petzelt (1972) is thought to be involved in pumping  $\text{Ca}^{++}$  like that of muscle sarcoplasmic reticulum, it is a good marker. Its activity, which peaks during prophase (just before nuclear breakdown) and again in metaphase (Petzelt and Von Ledebur-Villegger, 1973), focuses attention on tubular ER. This study has found such ER to occupy positions pertinent to  $\text{Ca}^{++}$  regulation during these stages (Table 7).

During prophase tubular ER surrounds the nucleus. Upon breakdown of the nuclear envelope, MTs of the mitotic apparatus polymerize within this region of tubular ER. Even before nuclear breakdown, however, MTs grow in number and length as asters form on either side of the nucleus (Wilson, 1895b).

TABLE 7

## BIOCHEMICAL EVENTS AND STRUCTURAL CHANGES DURING SEA URCHIN ZYGOTE MITOSIS

STAGE	BIOCHEMICAL EVENTS	SMOOTH ENDOPLASMIC RETICULUM			MITO-CHONDRIA	ANNULATE LAMELLAE	HEAVY BODIES	MICROTUBULES
		VESIC.	SACCULAR	TUBULAR				
MATURE UNFERT. EGG	Inactive	Through-out egg	None	None	Through-out egg	Few, dispersed	Present	None
STREAK	DNA Cycloheximide, puromycin, & x-Rayed sperm prolong or arrest it	Through-out cell & in streak zone	Mostly in the streak zone, side channels, & band around nucleus. But most is rough	None	Mostly in & around streak zone	Streak zone, side channels & around nucleus	In or near the streak zone	Few, dis-oriented; very few C-MTs
PROPHASE	First Ca-up-take peak, Ca-ATPase peak; critical tubulin conc.	Through-out cell incl. ex-clusion zone	Mostly at periphery of exclusion zone	Much, esp. around the nucleus	Many near nucleus & around zone	None seen	None seen	Surround nucleus; also inside invaginations of nuclear envelope
METAPHASE	Second Ca-up-take peak, Ca-ATPase peak	Asters, spindle & MA periphery	Radiates in aster, surrounds spindle periph. some in spindle	Center of spindle esp. near chromosomes & near centrioles	MA periphery & cortex	None	None	Highly ordered as elements of MA; C-MTs at metaphase plate
ANAPHASE	Ca-uptake peak of late metaphase declines	Mostly in asters & MA periphery	Radiates in aster, surrounds spindle periph. some mixes with TER in C-T-P spindle region	Some mixed in spindle with sac. ER in C-T-P region	MA periphery & cell cortex	None	None	Highly ordered as elements of MA; C-MTs in interzone

Some MTs are long enough to span half the distance to the center of the nucleus encased in folds of nuclear envelope (Figs. 34, 35, and 36) which have not previously been reported (discussed in greater detail in section 6 below).

At metaphase, tubular ER is found in the central part of the spindle among the MTs (Figs. 38 and 39) and in the centrosomal region (Fig. 41) of the aster known to be a MT nucleation site. Its position, therefore, satisfies the requirements of a  $\text{Ca}^{++}$  regulator controlling MT polymerization and corresponds with the time of mitotic apparatus assembly which is completed at metaphase. Recently, this dense mass of membranes at metaphase was viewed by scanning electron microscopy in specially isolated sea urchin mitotic apparatuses (Schatten and Schatten, 1977).

Of interest here are the radioactive  $^{45}\text{Ca}$  experiments of Clothier and Timourian (1972) demonstrating three peaks of  $\text{Ca}^{++}$  uptake (transport in) from sea water followed by its release (transport out) back into the sea water during S. purpuratus zygote division. Since the  $^{45}\text{Ca}$  seems to be freely exchangeable, it is thought that it remains free in the cytoplasm. The first two peaks occur at prophase and metaphase and may have a role in mitosis. Unfortunately, their results show that intracellular  $\text{Ca}^{++}$  probably increases during prophase until its midpoint and then declines to its normal level by the end of prophase. Rising from this level,  $\text{Ca}^{++}$  concentration again peaks at the end of metaphase and then declines to normal during anaphase. Thus, during most of prophase and much of metaphase, intracellular  $\text{Ca}^{++}$  is actually being increased while MTs are polymerized.

One way to explain this apparent contradiction is to remember that the  $\text{Ca}^{++}$ -stimulated ATPase peaks during prophase and metaphase (Petzelt, 1972; Petzelt and Von Ledebur-Villegger, 1973), probably protecting the mitotic apparatus area by reducing its local  $\text{Ca}^{++}$  concentration. Evidence for this can be found in that during late prophase,  $^{45}\text{Ca}$  was removed from the cell. This suggests that the  $\text{Ca}^{++}$  pumps are indeed working. Thus, prophase ends and metaphase actually begins with a low level of free intracellular  $\text{Ca}^{++}$  permitting the great increase in MTs polymerizing as the mitotic apparatus forms.

The results of Clothier and Timourian also show that the prophase peak occurs just before nuclear disappearance and that the metaphase-anaphase transition occurs at the metaphase peak. This suggests that  $\text{Ca}^{++}$  concentration may have a role in signalling or triggering these events. For example, an increase of  $\text{Ca}^{++}$  at the metaphase plate may cause a rapid disassembly of certain MTs there and lead to chromosome separation. Such a mechanism fits easily into the dynamic equilibrium theory of chromosome motion (Inoué and Sato, 1967). Other, non-mitotic, roles for  $\text{Ca}^{++}$  fluxes have been proposed (Clothier and Timourian, 1972).

Smooth vesicular ER, like its tubular counterpart may also act as a  $\text{Ca}^{++}$  regulator. This is supported by the relationship between vesicular ER and mitochondria, an organelle known to act as a  $\text{Ca}^{++}$  regulator (Rasmussen and Goodman, 1975), and by the vesicular nature of the  $\text{Ca}^{++}$  sequestering organelle recently isolated from mammalian brain by Blitz et al. (1977). These vesicles were reported to behave like sarcoplasmic reticulum and to be biochemically very similar. For instance,

they contain a Ca-ATPase that is immunologically identical to that of sarcoplasmic reticulum. The vesicles were described as small, usually coated, and capable of fusing to form larger uncoated vesicles. Coated vesicles are often a product of Golgi apparatus and recently immunofluorescence was used to show that calsequestrin, the Ca-sequestering protein of sarcoplasmic reticulum, first accumulates in the Golgi region in differentiating rat skeletal muscle cultures (Jorgensen et al., 1977). This could explain why Golgi apparatus is observed near the region reserved for the mitotic apparatus from the streak stage at least through anaphase as reported here. Finally, in a recent review, Sanger (1977) found many reports of vesicles within and around mitotic and meiotic spindles in both plant and animal cells.\*

That Ca-sequestering vesicles may affect MTs is suggested by experiments using crude chick embryo fractions containing such vesicles. These studies demonstrate that such fractions cannot support MT assembly if the vesicles are made to release their  $\text{Ca}^{++}$  by treatment with caffeine, Triton X-100, or phospholipase. Without these agents or without the vesicles, the fractions easily support MT polymerization (Bryan, 1975). Thus, the idea that ER may act as a  $\text{Ca}^{++}$  pump to control MT growth seems reasonably well supported.

ER, however, may not act alone. As already mentioned, mitochondria alone can act as  $\text{Ca}^{++}$  regulators (Rasmussen and Goodman, 1975). It is possible that their dense granules may simply be a storage form of calcium. Also, all pumps need energy and the proximity of the mitochondria to the ER membranes suggests that the energy producer is near the consumer.

\* Footnote: Direct evidence has been found for ATP-dependent  $^{45}\text{Ca}$  uptake by vesicles in mitotic apparatuses from sea urchin zygotes mechanically lysed in polymerizing medium. Triton X-100 disrupts the vesicles releasing the  $^{45}\text{Ca}$ . (R.B. Silver, W.Z. Cande, J.K. Holtz, and R.D. Cole, J. Cell Biol. 79: 299a).

## 2. C-Microtubules

This study clearly demonstrates that C-MTs constitute a major percentage of MTs found in the interzone of sea urchin zygotes in situ and confirms their existence in spindles isolated in hexylene glycol (Cohen and Gottlieb, 1971). Furthermore, polarization microscopy on L. variegatus showing lack of birefringence in the anaphase interzone is interpretable as an effect of C-MTs in vivo. Such C-MTs are probably caused by an opening up of the MT cylinder (Bryan, 1976) and have been found in diverse systems. Some of these are natural, e.g., B-subfibers of cilia and flagella, normal binary fission of the ciliate Nassula (Tucker, 1967), and cell division of Haemanthus endosperm (Lambert and Bajer, 1972; Jensen and Bajer, 1973). Others involve experimental treatment of cells and include blood platelets recovering from cold (Behnke, 1967), Heliozoan axopods retracted by nickelous ion (Roth and Shigenaka, 1970), and cold-shocked mammalian spindles (Brinkley and Cartwright, 1975). They were overlooked in micrographs of HeLa spindles recovering from pressure-induced depolymerization (Salmon et al., 1976). C-MTs have also been observed in vitro, especially at the beginning of tubulin assembly (Erickson, 1974; Bryan, 1976). All this suggests that C-MTs are formed when there is either sudden growth or rapid disassembly of MTs. Apparently, it makes no difference whether this is a result of a natural dynamic situation as in sea urchin spindles or the result of experimental manipulation as in cold-shocked cells. The finding of C-MTs under conditions of sudden and rapid assembly in vitro (Erickson, 1974) supports this hypothesis.

The use of tannic acid during fixation results in the staining of the spaces between MT subunits so that they appear almost

as if they were negatively stained (Fig. 54). C-MTs of isolated mitotic apparatuses so fixed reveal fewer than the usual 13 protofilaments suggesting that they are sites of subunit addition or removal. (Burton and Himes (1978) found more than 13 under certain conditions of in vitro polymerization.) The finding reported here of reduced numbers of C-MTs in A. punctulata spindles isolated in modified polymerization medium suggests some filling in of the C-MTs transforming them into normal ones. Consistent with this hypothesis was the recent report that regenerating Chlamydomonas flagella have such a C-MT at the distal end of the A-subfiber (Dentler and Rosenbaum, 1977). Studies using radioactively labelled tubulin have shown this end is the site of addition of new subunits during growth (Witman, 1975). Thus, it appears that C-MTs represent an active intermediate stage in the MT polymerization/depolymerization reaction.

The presence of C-MTs in the interzone region at anaphase indicates, therefore, that the interzone is an active region of spindle assembly/disassembly and MT polymerization/depolymerization in the interzone occurs via a mechanism similar to that studied in vitro for neurotubulin (Erickson, 1974). That this region is indeed different from other spindle regions is supported by the reduced amount of ER present there (see Results section). Similar reduction in other cell types have been overlooked, as in the HeLa cell interzone (Robbins and Jentzsch, 1969).

If ER acts as a  $Ca^{++}$  pump, which seem likely, then an explanation for C-MTs in this region is readily apparent.  $Ca^{++}$  diffusing into the interzone destabilizes MTs so that they depolymerize and form C-MTs. Reduced ER in anaphase interzone may also explain Brinkley and Cartwright's results (1975) demonstra-

ting differences in stability of (presumably) the same interzonal MTs between early anaphase and telophase (midbody) in cultured mammalian cells. Early anaphase interzonal MTs were found to be cold-labile while those of the telophase midbody were not. This also suggests that a region active in assembly/disassembly is more sensitive to cold and perhaps other physical and chemical agents than regions not so active.

With regard to the sea urchin spindle, C-MTs at the metaphase plate are probably the result of rapid interpolar MT assembly while those of anaphase interzone are more likely the result of their rapid depolymerization. C-MTs in the chromosome-to-pole region, although present in reduced numbers, require further explanation. One possibility is that cycling of tubulin through MTs may occur as suggested by Rebhun et al. (1975) based upon the effects of certain pairs of agents on the MT assembly/disassembly equilibrium in vivo. This theory states that tubulin subunits are constantly being added to MTs as others are removed, forming a continuous cycle of tubulin on and off the MT while maintaining a steady-state. The active sites of such MTs would presumably show up as C-MTs. Recently, Margolis and Wilson (1978), using  $^3\text{H}$ -GTP as a tubulin marker in a steady-state assembly system, have found evidence of such cycling in vitro.

The fact that no C-MT with 13 protofilaments could be found suggests that the addition of the thirteenth subunit (or protofilament) causes immediate closure of the MT cylinder. Since B-subfibers of sea urchin flagella are naturally composed of 11 subunits (Tilney et al., 1973), they apparently remain unclosed. Probably there is something unique about such tubulin that maintains specific binding affinity for par-

ticular subunits of A-subfibers (Tilney et al., 1973). Indeed, biochemical evidence already exists showing sea urchin ciliary and flagellar tubulin to be different from mitotic tubulin of the same species (Bibring et al., 1976) as mentioned in the introduction.

### 3. Streak Stage Endoplasmic Reticulum

The most obvious characteristic of the streak stage is the streak formed by sheets of (mostly) rough saccular ER (Fig. 15). The streak excludes most granules from a zone stretching across the nucleus from one side of the cell to the other. Since the unfertilized egg does not have saccular ER, it must be newly assembled. Although the origin of these membranes is obscure, two possibilities are supported by ultrastructural evidence reported here. The most likely is that a large part of the vesicular ER, especially the larger vesicles, is transformed by the cell into the saccular ER, since the appearance of the latter is concomitant with a big decrease in the former. The other possibility is supported by the distribution of saccular ER around the nucleus and a small amount of nuclear envelope vesiculation, suggesting a nuclear origin for at least some of the ER produced. Arguing against this, however, is the fact that the nucleus actually grows during streak stage.

Other possibilities exist. For example, since lipid synthesis increases five-fold (Epel et al., 1969) after fertilization, de novo synthesis may be possible. It is important to remember, though, that this is a late change and probably could not account for all the saccular ER. Another possibility is that mitochondria are responsible for saccular ER elabora-

tion. They appear to be vesiculating (Fig. 18, inset) and are in contact with lipid droplets which could act as a reservoir of raw material. Arguing against this, however, is the RQ\* of the fertilized egg which is 0.71 (Root, 1930) indicative of a lipid energy source (Lehninger, 1975) and explaining the obvious mitochondrial propensity for lipid droplet association. Furthermore, this association continues at least through anaphase, well beyond the time of saccular ER elaboration during the streak stage.

If the origin of saccular ER is obscure, so too is its function. One obvious role might be as a  $\text{Ca}^{++}$  regulator analogous to muscle sarcoplasmic reticulum. As such, it could decrease local  $\text{Ca}^{++}$  concentrations to allow mitotic apparatus MTs to grow. In fact a few MTs are present in the streak, especially around annulate lamellae and heavy bodies. Unfortunately, there is no evidence that the  $\text{Ca}^{++}$ -activated ATPase is active at streak stage (Petzelt and Von Ledebur-Villeger, 1973). The same is true for the  $^{45}\text{Ca}$  flux (Clothier and Timourian, 1972) which shows no peaks at this time. Thus, a  $\text{Ca}^{++}$  regulating role seems to be precluded by lack of any evidence in its favor.

Another and more likely role would be as a membrane pool for the future tubular ER, daughter nuclei, or even plasma membrane during cleavage. ER is responsible for repair of damaged ameba nucleus (Fleckinger, 1974; 1976) and Longo (1972) reported that nuclear envelope breaks down into saccular elements in A. punctulata. Animal as well as plant nuclear envelope resembles ER biochemically (Philipp et al., 1976) so they may be interconvertible with ease. Also, Golgi apparatus, thought to be in-

\*Footnote: RQ, the respiratory quotient, is defined as the ratio of  $\text{CO}_2$  produced to  $\text{O}_2$  consumed and is different for each substrate respired.

volved in membrane transformations (Whaley et al., 1975), is present in the streak easily available for such membrane alterations. Thus, there is some evidence that one form of membrane may be transformed into others.

An alternative, or perhaps additional, possibility is that ER acts as a physical barrier, keeping the area free of many large granules and organelles, and permitting assembly of the mitotic apparatus. Certainly, the orientation of the streak is such that it presages the spindle plane and axis suggesting a causal relationship.

It is possible to prolong streak stage by treatment of eggs with cycloheximide which inhibits protein synthesis (Suzuki and Yoshitake, 1973). Another way is to subject sperm to X-rays before fertilization, in which case caffeine and several other methyl xanthines (but not all) reverse prolongation only when added at the start of the streak (Nakamura, 1974). Since methyl xanthines are known to increase cAMP levels, it was felt that this may be responsible for their effects. Although both exogenous and endogenous cAMP do not affect normal cell division in sea urchin and Spisula eggs (Rebhun et al., 1975), it may play a role in reversing abnormal prolongation. A. punctulata DNA is synthesized during streak stage (Longo and Plunkett, 1973) and it is possible that the X-ray damage to sperm DNA is then repaired, delaying synthesis and prolonging the streak stage. It is unknown if cAMP is capable of circumventing or speeding such repair. Cycloheximide was also found to delay DNA synthesis (Suzuki and Yoshitake, 1973), so this may be a common mechanism.

Puromycin, another inhibitor of protein synthesis, has

a different effect on sea urchin eggs. It arrests cells at streak stage (Bibring and Cousineau, 1964) rather than just prolonging streak stage. Yet, it has no effect on DNA synthesis (Wilt et al., 1967). Since puromycin prevents the increased activity of the  $\text{Ca}^{++}$ -stimulated ATPase, Bryan (1975) suggested that the enzyme is responsible for the developmental arrest. Why the two inhibitors of protein synthesis differ in their effects remains a question that could lead to more information about the streak stage.

#### 4. Annulate Lamellae and Nuclear Pores

Annulate lamellae have been extensively reviewed (Kessel, 1968; Wischnitzer, 1970) but still remain an enigma. The best evidence suggests that they are produced by the nuclear envelope, the pores of which closely resemble those of annulate lamellae. Annulate lamellae are usually found in synthetically active and mitotic cells, e.g., germ and embryonic cells, cancer and tumor cells, and in some adult somatic cells including cells from epididymus epithelium, endometrium, axillary gland and adrenal cortex. Because they are basophilic, they are thought to contain ribonucleoprotein or nucleic acid. Continuities often exist between annulate lamellae and rough ER, vesicular ER, mitochondria, Golgi apparatus, and even yolk.

The present study finds a relationship between annulate lamellae and mitotic MTs that suggests a role as a tubulin-storing organelle. It is based upon ultrastructural evidence showing annulate lamellae to be in intimate contact with MTs and even perhaps C-MTs. Also, annulate lamellae are sometimes observed near centrioles (Kessel, 1968) and both organelles are associated with an amorphous "fuzzy" material that may

be tubulin. Their location in the streak plane, their disappearance and replacement by mitotic apparatus assembly and growth suggests such a relationship. The literature describes many instances of treatment that results in both proliferation of annulate lamellae and increased mitoses. Examples include work with amino acid analogs, chick embryo myocardium incubated at reduced temperature, and endometrium treated with high concentrations of estrogen-progesterone (Kessel, 1968).

More direct evidence linking annulate lamellae to tubulin was provided by DeBrabander and Borgers (1975) as mentioned in the Introduction. They reported that this organelle appears in cultured cells when treated with drugs (colchicine, vinblastine, vincristine, podophyllotoxin, and rotenone) that disassemble MTs by different pathways. Since Dales et al. (1973) had reported labelling nuclear pores and annulate lamellae with ferretin-labelled tubulin antibody, DeBrabander and Borgers suggested that annulate lamellae and nuclear pores were sites of either tubulin synthesis or MT polymerization. Prior to this, functions proposed included transport of nuclear information, control of ER form or function, and storage of specific raw materials. The present study supports this latter view and suggests tubulin is the raw material.

Similar evidence exists for nuclear pores. Their location, disappearance, and replacement by spindle MTs is supportive. The literature shows that proliferating cells and tumor cells have a greater number of pores than do normal cells (Svejda et al., 1975). For example, lymphocytes stimulated by treatment with phytohemagglutinin (PHA) have twice as many as controls (Maul et al., 1971), hypertrophied myocardium has many more than normal myocardium (Bloom, 1975),

and in a study reminiscent of chick embryo myocardial annulate lamellae, plants grown at lowered temperatures had more nuclear pores than those grown at normal temperatures to the same stage (Lott and Vollmer, 1975). Such temperature experiments can be interpreted as an attempt to restore assembly equilibrium by counteracting temperature reduction with concentration increase in the equilibrium equation. A fuzzy material is also found in the nuclear pore complex (Scheer and Franke, 1969) and purified rat liver nuclei with no MTs have high colchicine binding activity (Douvas et al., 1975), usually associated with tubulin, and supporting the tubulin-antibody labelling results of Dales et al. (1973). All of these observations are consistent with a tubulin-storing role for nuclear pores.

#### 5. Heavy Bodies and a Unifying Hypothesis for Tubulin-Containing-Structures

Heavy bodies consist of a dense mass of granular and fuzzy material bounded incompletely by annulate lamellae. Like annulate lamellae, they align in the streak and disappear when the nucleus does. This also suggests a role in the formation of the mitotic apparatus. An attractive hypothesis is that the granules found in the dense mass of heavy bodies is the same material as the central granules found in the pores of annulate lamellae and nuclear envelope (Fig. 17, inset) and that these are a particulate form of tubulin. Of course, the fuzzy material may be the tubulin or they both may be tubulin, perhaps in equilibrium with each other.

Weisenberg (1972b) identified such a non-MT form of tubulin in Spisula eggs by colchicine binding. He found that

these tubulin-containing-structures are spheres of 10 to 20  $\mu\text{m}$  in diameter with an attached membranous structure and containing 200  $\text{\AA}$  granules as well as a few short MTs. They disappear at the time the nucleus does and decrease in number whenever MTs are assembled, suggesting that they are either a storage form or an intermediate form of tubulin for MT assembly. Overlooked by Weisenberg (1972; Weisenberg and Rosenfeld, 1975) is the fact that they are quite similar to sea urchin heavy bodies. Similarly, mammalian brain and liver may have particulate forms of tubulin and in A. punctulata unfertilized eggs as much as 20% of colchicine binding activity is found in the particulate fraction (Raff, 1975).

The possible importance of heavy bodies to cell division in Echinoderm eggs warranted a survey of the literature on other phyla for similar or related organelles. While eggs or oocytes of humans (Hertig, 1963), chickens (Bellairs, 1967), and mollusks (Rebhun, 1961) have interesting structures involving annulate lamellae, the dragonfly oocyte has the one most similar to heavy bodies. Dragonfly oocytes contain a cytoplasmic organelle called yolk nuclei (or Balbiani bodies) which are not nuclei nor do they have anything to do with yolk. Kessel and Beams (1969) studied them in detail and their description suggests that they are analogous to sea urchin heavy bodies or surf clam tubulin-containing-structures. Yolk nuclei consist of granular dense masses with amorphous material in which numerous annulate lamellae appear to be produced. Like heavy bodies, these structures contain RNA, are associated with annulate lamellae, are present in oocytes, and have a granular-amorphous structure. Of even more importance, however, is

their association with MTs which often course through their dense masses although everything else is excluded from these masses. The major differences, then, are simply how the structures are organized. In heavy bodies the annulate lamellae surround the dense mass and the MTs are just outside while in yolk bodies the annulate lamellae and MTs are inside the dense mass. In both cases the dense masses have been described as containing granules and filaments and appearing amorphous.

Such interesting structures are not limited to eggs and oocytes, however. Another similar structure was found in a study of ciliogenesis in fetal rat lung by Sorokin (1968). During ciliogenesis one of the first steps is the formation of "amorphous fibro-granular aggregates" out of which the basal bodies, which are composed of MTs, seem to form. These aggregates are associated with annulate lamellae which often penetrate the aggregates and thus resemble yolk nuclei. In fact, Sorokin's micrographs show that the material in the pores of the annulate lamellae resemble the aggregates although this was overlooked. Golgi apparatus also appears to contribute to these aggregates which, as far as is known, is not the case with the other structures. Whether these fibro-granular aggregates contain tubulin or not is unknown but its association with basal body and cilia formation is suggestive. Also, biochemical techniques (Seaman, 1960; 1962; Argetsinger, 1965; Hoffman, 1965), tritiated thymidine incorporation, and acridine orange staining (Randall and Disbrey, 1965) have implicated the presence of RNA in basal bodies. If the fibro-granular mass also contains RNA, its analogy to heavy bodies and yolk nuclei is strengthened.

From all of the above it is possible to hypothesize that

there is a separate pool of tubulin in particulate form resembling granules and amorphous "fuzz". This form is found in pores of nuclear envelope and annulate lamellae, as well as in heavy bodies, tubulin-containing-structures, yolk nuclei, and fibro-granular aggregates. All forms are probably interconvertible. Particulate tubulin is probably released to form mitotic apparatus (or ciliary) MTs when structures storing such tubulin disappear and the tubulin becomes soluble (or at least available). Extranuclear forms, e.g., annulate lamellae and heavy bodies, are probably required when the mitotic apparatus is extremely large as in sea urchin zygotes; or when many are needed quickly as is the case with short cell cycles of early development and insect egg mitosis; or to separate large but different pools of tubulin as is the case with sea urchin mitotic and ciliary tubulins which differ biochemically (Bibring et al., 1976) yet have large pools of equal size (Raff et al., 1975). It might also explain why S. purpuratus has 1500 heavy bodies per egg (Harris, 1967) while A. punctulata has so few (tens at most). The former egg with a diameter of 100  $\mu\text{m}$  has twice the volume ( $524,000 \mu\text{m}^3$ ) of the latter egg of 75  $\mu\text{m}$  diameter ( $230,000 \mu\text{m}^3$ ). Thus, more tubulin-containing heavy bodies would be required to raise the tubulin concentration in the larger cell to reach the critical level.

Particulate tubulin may be important in the control of mitotic apparatus assembly. It could reduce the concentration of available tubulin below the critical point required for polymerization as has been found for assembly in vitro, thus assuring that the mitotic apparatus won't form until the cell is ready for mitosis (Bryan, 1975).

Sluder (1976) has already shown that the amount of tubulin available for sea urchin spindle formation can be controlled by "titration" with colcemid, a colchicine derivative. Of special interest here is that it only works if added at early prophase or before, the time when annulate lamellae, heavy bodies, and nuclear envelope are still present, and not afterward. Since he used only a 1 to 6 min "pulse" of colcemid and then washed away whatever free colcemid remained, only bound colcemid is present to work. It would be interesting to know if colcemid binds to these structures or their tubulin stores.

Additional evidence that tubulin exists in an unavailable state in annulate lamellae and heavy bodies and nuclear envelope comes from Stephen's (1972) temperature jump experiments on S. droebachiensis, a cold-water sea urchin. These demonstrated that the size of the pool available for mitotic apparatus assembly depends specifically upon the temperature just before nuclear breakdown. According to the general hypothesis presented here, this is the time when annulate lamellae and heavy bodies would release their tubulin into the pool. Electron microscopy on S. droebachiensis at the various temperatures could be important and informative.

Another interesting feature of these potential tubulin-containing structures is that RNA has been implicated in all but that of Spisula, which was not assayed (Weisenberg, 1972b; Weisenberg and Rosenfeld, 1975). It is believed that RNA may play a role in MT assembly or function since it has been found in the interzone of the isolated mitotic apparatus (Zimmerman, 1963) and at the spindle poles where its destruction in vivo at prophase blocks mitotic apparatus assembly (Peterson and

Berns, 1977). RNA and other polyanions prevent MT polymerization in vitro, presumably by removing at least one of the MT-associated proteins, thought to be  $\gamma$ -factor, inhibiting nucleation (Bryan, 1975). It thus seems logical that RNA may be present to prevent polymerization of the highly-concentrated tubulin within these structures.

Particulate tubulin may have other functions as well. It could conserve this important and re-used protein by preventing its destruction. Evidence from cell culture studies have shown such loss of tubulin to occur during interphase (Klevecz and Forrest, 1975) but may not be a problem in cells of low tubulin requirements. Tubulin can be brought to where it is needed and concentrated there without assembly as suggested by annulate lamellae and heavy bodies in the streak and aster before MT polymerization. Finally, tubulin may be processed in these structures. Various authors have suggested that the tubulin molecule is altered to control its in vivo activity. Proposals include phosphorylation, reduction or oxidation of sulfhydryl groups, nucleotide changes or exchanges, tyrosylation, carbohydrate addition, and MT-associated protein attachment (Snyder and McIntosh, 1976; Stephens and Edds, 1976; Rebhun, Nath, and Remillard, 1976).

## 6. The Nucleus

During prophase the nucleus is surrounded by smooth tubular and vesicular ER, as well as by mitochondria. These organelles are probably associated with  $Ca^{++}$  regulation (Rasmussen and Goodman, 1975) and are at the expected location for such function at the time when mitotic apparatus growth begins (Wilson, 1895b). Since membrane integrity, at least in terms of permeability, requires calcium (Davson, 1964), they

may also be responsible for triggering nuclear envelope breakdown.

Prophase is also the time when disorganized streak MTs, which seem to course through the streak in all directions, are replaced by organized ones around the nucleus. Such reorganization at prophase was recently confirmed by Bajer et al. (1977) in both Haemaphysalis endosperm and (Taricha) lung epithelium, and may be common to mitosis in general. Its timing at prophase correlates with loss of nuclear pores, annulate lamellae, and heavy bodies suggesting that in sea urchins these structures may have something to do with MT nucleation or reorganization or tubulin storage as discussed above. Work with marine egg assembly systems in vitro has shown that nucleation is necessary for polymerization (Rebhun et al., 1975) and that centrioles (one type of MT-organizing center) must be "activated" during fertilization in order to produce organized asters as opposed to just disorganized MTs when allowed to seed MT polymerization in vitro (Weisenberg, 1972c).

The presence of long cytoplasmic "fingers" which contain MTs and penetrate the nucleoplasm at prophase is a major discovery of this investigation. They are formed by invaginations of nuclear envelope, probably induced by their MTs since they are only as wide as the collection of MTs accompanying them. Like ciliary or flagellar MTs, they terminate shortly before the apex of the finger. Although apparently never before reported, such invaginations may be common to other phyla but perhaps exist for so short a time during nuclear envelope breakdown that it is usually impossible to fix them at just that instant. In fact, only one cell among the thousands

scanned for staging was found to be at the critical point of aster growth in the presence of an intact nucleus. Thus, just finding such a cell is a major undertaking even by the method used here and may explain why such unique ultrastructure was not previously reported.

The function of such fingers can only be guessed at presently. Since they contain MTs and appear to grow inward for several micrometers toward chromosomes (Fig. 35), the fingers may be a device to bring MTs to chromosomes. The possibility that these MTs differ from other mitotic MTs should not be discounted. After all, the others grow in the same direction but only run along the nuclear surface while these seem capable of inducing invagination.

The simplest possibility is that the fingers function to bring continuous (interpolar) MTs into the nucleus before nuclear breakdown, perhaps in preparation for interaction with chromosomal MTs when the latter appear. Such an interaction is expected in sliding MT theories of chromosome movement (McIntosh et al., 1969). They may even play a role in the process of nuclear dismantling if the fingers become vesicles detached from the nuclear envelope in agreement with Longo's (1972) observation that the nucleus breaks down by forming vesicles. An alternate method of nuclear envelope breakdown is suggested by the presence of these fingers and leads to an astonishing result. If enough fingers are formed and continue to grow through the nucleus, the result would in many ways resemble a metaphase spindle: MTs running parallel to and sandwiched among membranes. Such membranes might even be considered tubular, the dominant form of spindle ER at metaphase.

In any event, direct structural interaction between MTs and nuclear envelope is not unique. A well-known previous example of this is the nuclear spindle plaque encountered in yeast mitosis which forms an intranuclear spindle (Peterson et al., 1972). Also, relationships between nuclear envelope and chromosomes during cell division have been well documented as have the relationship between tubulin and membrane (Pickett-Heaps, 1969; Hepler and Palevitz, 1974; Stephens and Edds, 1976).

While the assumption that the MTs in the nuclear invaginations are continuous (interpolar) is the one most likely to be correct, the other alternative, that they are non-continuous or "chromosomal" cannot be ruled out. In this case, they would grow to the kinetochore rather than from the kinetochore. They would be unique because they would be of opposite polarity and offer a new twist to sliding filament hypotheses of chromosome movement. They might even be responsible for the loss of material noted at the kinetochore during anaphase based upon measurements of birefringence along single fibers (Forer, 1976). Alternatively, they may be MTs specialized to contain actin filaments. Forer (1974) has already suggested this possibility among others in explaining why actin filaments have not generally been seen in the mitotic apparatus, as was the case in the present work. It has been shown that when purified tubulin and actin are polymerized together in vitro, only MTs are observed although actin is definitely present (Izant and McIntosh, 1977). Still another possibility is that they may act as guides to help move chromosomes to their specific places on the metaphase plate and then, during anaphase, along their specific paths to the poles.

Of course, it is possible that these MT-containing fingers are involved only in prophase activity. The simultaneous appearance of these MTs with prophase condensation suggests that the former may be involved in the latter process. Indeed, evidence has been recently gathered demonstrating that MTs may help organize spermatid chromosomes (Myles and Hepler, 1977). During spermiogenesis, chromatin normally condenses at the end of the nucleus associated with a ribbon of MTs in the species (Marsilea) studied. When drugs (colchicine, vinblastine, and podophyllotoxin) are used to prevent this ribbon from forming, the nucleus becomes polymorphous and the chromatin becomes partially condensed at several points along the nuclear envelope. It is interesting to note that these condensing points were described as usually associated with "dense material normally found associated with basal bodies or forming MTs."

The role of the vacuole in the nucleus is difficult to assess but may be related to water released by MT assembly (Salmon, 1975) or chromosome condensation or both. It might also act as a  $\text{Ca}^{++}$  regulator, i.e., as an intranuclear vesicular ER. In fact, what appears to be tubular ER segments were observed inside the vacuole (Fig. 36, inset). It is also interesting to note that intranuclear membranes were observed near the vacuole (Fig. 36).

## B. Summary and Conclusions

During this ultrastructural study, it was found that the fine structure of the sea urchin zygote changes as mitosis proceeds (summarized in Table 7, p. 120). Many of these changes are thought to play a direct role in either the preparation for mitosis or mitosis itself. The organelles involved include the nucleus, ER, annulate lamellae, heavy bodies, and MTs.

Many of these organelles are involved in the streak stage during which rough saccular ER forms a thick band-- the streak -- around the nucleus, delimiting the future area and axis of the mitotic apparatus. Besides ER (and a few MTs), the streak contains annulate lamellae and heavy bodies but excludes all other organelles. Normal MTs are always observed in or near heavy bodies and annulate lamellae, but only the latter organelle seems to contain C-MTs among its lamellae. Both organelles disappear by the time of nuclear envelope breakdown at prophase.

During prophase, the ER of the streak changes again, becoming smooth with tubular elements near the nucleus. This tubular ER is observed at the same time as a peak in activity of the  $\text{Ca}^{++}$ -ATPase. The prophase nucleus also undergoes many changes. Its generally regular spherical shape is transformed by both long invaginations and evaginations, the former often containing MTs. These MTs never penetrate the nuclear envelope, terminating, sometimes as a C-MT. (Fig. 35c) at the end of the invagination. Areas of prophase nuclear envelope appear to be breaking down allowing some mixing of nucleoplasm and cytoplasm. Furthermore, what seem to be unattached pores can be observed near the nucleus, perhaps being released from the

nuclear envelope.

Metaphase spindle ER consists of smooth tubular ER intermally with smooth saccular ER surrounding it. Although most MTs are normal, many C-MTs having less than the normal 13 protofilaments are found at the metaphase plate where the chromosomes are aligned. With the onset of anaphase, the sets of chromosomes separate forming the interzone. The ER of the interzone is much reduced compared to the rest of the spindle. Although the chromosome-to-pole region has some tubular ER, most anaphase spindle ER is of the smooth saccular type. Of the interpolar MTs passing through the interzone, most are C-MTs, their percentage increasing with time.

The observations presented here support some new hypotheses about mitosis, especially about mitotic apparatus assembly. They suggest that the streak stage is more important than previously thought and that its non-excluded organelles, annulate lamellae and heavy bodies, play a role in mitotic apparatus assembly. Thus, the following scheme is proposed: Tubulin is either processed or stored in particulate form in the pores of annulate lamellae and nuclear envelope as well as in heavy bodies. It is released from these structures when they disappear. Environmental conditions at the time of release, e.g., temperature and the presence of drugs, determine the pool size. The soluble pool of tubulin is assembled into MTs of the mitotic apparatus by the removal of  $\text{Ca}^{++}$  ion. This is accomplished by a  $\text{Ca}^{++}$ -ATPase located in the smooth tubular ER of prophase and metaphase acting in a manner analogous to muscle sarcoplasmic reticulum. The prophase nuclear invaginations containing MTs are an important intermediate stage in

spindle formation. It is further proposed that C-MTs are real and probably function as a site of assembly/disassembly during mitosis. Such C-MTs, as well as the reduction of ER in the interzone, may be important in mitotic apparatus function.

It is obvious that to investigate these hypotheses requires more biochemical work. The biochemical nature of the tubular ER, annulate lamellae, heavy bodies, and nuclear envelope must be determined before their exact relationship to MTs can be firmly established. MT polymerization in vivo has hardly been studied so it is impossible to know if the data from in vitro assembly can be directly applied.

In the beginning, it was felt that the increased knowledge of mitotic biochemistry called for an ultrastructural study. Now it appears that there are many more biochemical questions to answer. Obviously, both types of study are required to synergistically find a solution to the enigma of cell division.

## BIBLIOGRAPHY

- Afzelius, B.A. (1957) Electron microscopy on the basophilic structures of the sea urchin egg, *Z. Zellforsch.* 45: 660-675.
- Anderson, E. (1968) Oocyte differentiation in the sea urchin, *Arbacia punctulata*, with particular reference to the origin of cortical granules and their properties in the cortical reaction, *J. Cell Biol.* 37: 514-539.
- Anderson, E. (1970) A cytological study of the centrifuged whole, half, and quarter eggs of the sea urchin *Arbacia punctulata*, *J. Cell Biol.* 47: 711-733.
- Argetsinger, J. (1965) The isolation of ciliary basal bodies (kinetosomes) from *Tetrahymena pyriformis*, *J. Cell Biol.* 24: 154-156.
- Bajer, A. (1973) Interaction of microtubules and the mechanism of chromosome movement (zipper hypothesis). I. General principle, *Cytobios* 8: 139-160.
- Bajer, A. and Molé-Bajer, J. (1972) In *Spindle Dynamics and Chromosome Movements*, G.H. Bourne and J.F. Danielli, eds., Academic Press, New York, 1-271.
- Bajer, A., Sato, H., and Ohnuki, Y. (1977) Regularity and randomness of spindle structure and function, *J. Cell Biol.* 75: 270a.
- Bal, A. Jubinville, F., Cousineau, G.H., and Inoué, S. (1968) Origin and fate of annulate lamellae in *Arbacia punctulata* eggs, *J. Ultrastruct. Res.* 25: 15-28.
- Behnke, O. (1967) Incomplete microtubules observed in mammalian blood platelets during microtubule polymerization, *J. Cell Biol.* 34: 697-701.
- Bellairs, R. (1967) Aspects of the development of yolk spheres in the hen's oöcyte, studied by electron microscopy, *J. Embryol. Exp. Morphol.* 17: 267-281.
- Bibring, T., Baxandall, J., Denslow, S., and Walker, B. (1976) Heterogeneity of the alpha subunit of tubulin and the variability of tubulin within a single organism, *J. Cell Biol.* 69: 301-312.
- Bibring, T. and Cousineau, G.H. (1964) Percentage incorporation of leucine labelled with carbon-14 into isolated mitotic apparatus during early division of sea urchin eggs, *Nature* 204: 805-807.
- Blitz, A.L., Fine, R.E. and Toselli, P.A. (1977) Evidence that coated vesicles isolated from brain are calcium-sequestering organelles resembling sarcoplasmic reticulum, *J. Cell Biol.* 75: 135-147.

- Bloom, S. (1975) Nuclear pores in nuclei of heart muscle cells, *J. Mol. Cell Cardiol.* 7: 305-306.
- Brinkley, B.R. and Cartwright, J.J. (1975) Cold-labile and cold-stable microtubules in the mitotic spindle of mammalian cells, *Ann. N.Y. Acad. Sci.* 253: 428-439.
- Bryan, J. (1975) Some factors involved in the control of microtubule assembly in sea urchins, *Am. Zool.* 15: 649-660.
- Bryan, J. (1976) A quantitative analysis of microtubule elongation, *J. Cell Biol.* 21: 749-767.
- Burton, P.R. and Himes, R.H. (1978) Electron micrographic studies of pH effects on assembly of tubulin free of associated protein. Delineation of substructure by tannic acid staining, *J. Cell Biol.* 22: 120-133.
- Cande, W.Z., Lazarides, E., and McIntosh, J.R. (1975) Visualization of actin in functional lysed mitotic cell preparations, *J. Cell Biol.* 67: 54a.
- Cande, W.Z., Lazarides, E., and McIntosh, J.R. (1977) A comparison of the distribution of actin and tubulin in the mammalian mitotic spindle as seen by indirect immunofluorescence, *J. Cell Biol.* 22: 552-567.
- Cande, W.Z., Snyder, J., Smith, D., Summers, K., and McIntosh, J.R. (1974) A functional mitotic spindle prepared from mammalian cells in culture, *Proc. Natl. Acad. Sci.* 71: 1559-1563.
- Carter, S.B. (1967) Effects of cytochalasin on mammalian cells, *Nature* 213: 261-264.
- Clothier, G. and Timourian, H. (1972) Calcium uptake and release by dividing sea urchin eggs, *Exp. Cell Res.* 75: 105-110.
- Cohen, W.D. (1968) Polyelectrolyte properties of the isolated mitotic apparatus, *Exp. Cell Res.* 51: 221-236.
- Cohen, W.D. and Gottlieb, T. (1971) C-microtubules in isolated mitotic spindles, *J. Cell Sci.* 2: 603-619.
- Cohen, W.D. and Rebhun, L.I. (1970) An estimate of the amount of microtubule protein in the isolated mitotic apparatus, *J. Cell Sci.* 6: 159-176.
- Dales, S., Hsu, K.C., and Nagayama, A. (1973) The fine structure and immunological labelling of the achromatic mitotic apparatus after disruption of cell membranes, *J. Cell Biol.* 59: 643-660.
- Davson, H. (1964) *In* A Textbook of General Physiology, Third Edition, Little Brown and Co., Boston, p. 321.
- Dawes, C.J. (1971) *In* Biological Techniques in Electron Microscopy, Barnes and Noble, New York.

- DeBrabander, M. and Borghers, M. (1975) The formation of annulated lamellae induced by the disintegration of microtubules, *J. Cell Sci.* 19: 331-340.
- Dentler, W.L. and Rosenbaum, J.L. (1977) Flagellar elongation and shortening in *Chlamydomonas*. III. Structures attached to the tips of flagellar microtubules and their relationship to the directionality of flagellar microtubule assembly, *J. Cell Biol.* 74: 747-759.
- Douvas, A.S., Harrington, C.A., and Bonner, J. (1975) Major nonhistone proteins of rat liver chromatin: Preliminary identification of myosin, actin, tubulin, and tropomyosin, *Proc. Natl. Acad. Sci.* 72: 3902-3906.
- Ebashi, S. and Endo, M. (1968) Calcium ion and muscle contraction, *Prog. Biophys. Mol. Biol.* 18: 125-183.
- Epel, D. (1975) The program of and mechanisms of fertilization in the Echinoderm egg, *Amer. Zool.* 15: 507-522.
- Epel, D. (1977) The program of fertilization, *Scientific American* 237: 128-138.
- Epel, D., Pressman, B.C., Elsaesser, S., and Weaver, A.M. (1969) The program of structural and metabolic changes following fertilization of sea urchin eggs, *In The Cell Cycle: Gene-Enzyme Interactions*, Academic Press, New York, 279-298.
- Erickson, H.P. (1974) Microtubule surface lattice and subunit structure and observations on reassembly, *J. Cell Biol.* 60: 153-167.
- Flickinger, C.J. (1974) The role of endoplasmic reticulum in the repair of amoeba nuclear envelopes damaged micro-surgically, *J. Cell Sci.* 14: 421-437.
- Flickinger, C.J. (1976) Metabolic requirements for interactions between nuclear and cytoplasmic membranes in the repair of damaged amoeba nuclei, *J. Cell Sci.* 21: 291-302.
- Forer, A. (1969) Chromosome movements during cell division, *In Handbook of Molecular Cytology*, A. Lima-de-Faria, ed., North Holland Publishing Co., Amsterdam, Holland and London, England, 553-601
- Forer, A. (1974) Possible roles of microtubules and actin-like filaments during cell-division, *In Cell Cycle Controls*, G.M. Padilla, I.L. Cameron, and A. Zimmerman, eds., Academic Press, New York, 319-336.
- Forer, A. (1976) Actin filaments and birefringent spindle fibers during chromosome movements *In Cell Motility*, R. Goldman, T. Pollard, and J. Rosenbaum, eds., Cold Spring Harbor Laboratory, 1273-1293.
- Forer, A. and Behnke, O. (1972) An actin-like component in spermatocytes of a crane fly (*Nephrotoma saturalis* Loew). I. The spindle, *Chromosoma* 39: 145-173.

- Forer, A. and Goldman, R.D. (1972) The concentration of dry matter in mitotic apparatus in vivo and after isolation from sea-urchin zygotes, *J. Cell Sci.* 10: 387-418.
- Fujiwara, K. and Pollard, T. (1975) Staining of cells with fluorescent antibody against myosin, *J. Cell Biol* 67: 125a.
- Fuller, G.M., Brinkley, B.R., and Boughter, J.M. (1975) Immunofluorescence of mitotic spindles using mono-specific bovine brain antitubulin, *Science* 187: 948-950.
- Fuller, G.M., Artus, C.S., and Ellison, J.J. (1976) Calcium as a regulator of cytoplasmic microtubule assembly and disassembly, *J. Cell Biol.* 70: 68a.
- Goldman, R.D. and Rebhun, L.I. (1969) The structure and some properties of the isolated mitotic apparatus, *J. Cell Sci.* 4: 179-209.
- Goode, D. and Roth, L.E. (1969) The mitotic apparatus of a giant ameba: solubility properties and induction of elongation, *Exp. Cell Res.* 58: 343-352.
- Grimstone, A.V. and Klug, A. (1966) Observations on the sub-structure of flagellar fibres, *J. Cell Sci.* 1: 351-362.
- Harris, P. (1965) Some observations concerning metakinesis in sea urchin eggs, *J. Cell Biol.* 25(1, pt. 2): 73-77.
- Harris, P. (1967) Structural changes following fertilization in the sea urchin egg. Formation and dissolution of heavy bodies, *Exp. Cell Res.* 48: 569-581.
- Harris, P. (1969) Relation of fine structure to biochemical changes in developing sea urchin eggs and zygotes, In *The Cell Cycle: Gene-Enzyme Interactions*, G.M. Padilla, G.L. Whitson, and I.L. Cameron, eds., Academic Press, New York, 315-340.
- Harvey, E.B. (1956) *The American Arbacia and Other Sea Urchins*, Princeton University Press, Princeton, New Jersey.
- Harvey, E.B. and Anderson, T.F. (1943) The spermatozoon and fertilization membrane of Arbacia punctulata as shown by the electron microscope, *Biol. Bull* 85: 151-156.
- Hertig, A.T. (1968) The primary human oocyte: Some observations on the fine structure of Balbiani's vitelline body and the origin of annulate lamellae, *Amër. J. Anat.* 122: 107-137.
- Hepler, P.K. and Palevitz, B.A. (1974) Microtubules and microfilaments, *Ann. Rev. Plant Physiol.* 25: 309-362.
- Hoffman, E.J. (1965) The nucleic acids of basal bodies isolated from Tetrahymena pyriformis, *J. Cell Biol.* 25: 219-228.

- Inoué, S. (1964) Organization and function of the mitotic spindle, *In* Primitive Motile Systems in Cell Biology, R.D. Allen and N. Kamiya, eds., Academic Press, New York, 549-594.
- Inoué, S. and Sato, H. (1967) Cell motility by labile association of molecules, *J. Gen. Physiol.* 50: 259-292.
- Inoué, S. and Stephens, R.E., eds. (1975) Molecules and Cell Movement, Raven Press, New York.
- Izant, J.G. and McIntosh, J.R. (1977) In vitro association of cytoplasmic actin with microtubules, *J. Cell Biol.* 75: 263a.
- Jensen, C. and Bajer, A. (1973) Spindle dynamics and arrangement of microtubules, *Chromosoma* 44: 73-89.
- Jorgensen, A.O., Kalnins, V.I., Zubrzycka, E., and MacLennan, D.H. (1977) Assembly of the sarcoplasmic reticulum: localization by immunofluorescence of sarcoplasmic reticulum proteins in differentiating rat skeletal muscle cell cultures, *J. Cell Biol.* 74: 287-298.
- Kane, R.E. (1962a) The mitotic apparatus: isolation by controlled pH, *J. Cell Biol.* 12: 47-55.
- Kane, R.E. (1962b) The mitotic apparatus: fine structure of the isolated unit, *J. Cell Biol.* 15: 279-287.
- Kane, R.E. (1965) The mitotic apparatus: physical-chemical factors controlling stability, *J. Cell Biol.* 25 (1, pt. 2): 137-144.
- Kessel, R.G. (1968) Annulate lamellae, *J. Ultrastruct. Res. Suppl.* 10: 5-82.
- Kessel, R.G. and Beams, H.W. (1969) Annulate lamellae and "yolk nuclei" in oocytes of the dragonfly, *Libellula pulchella*, *J. Cell Biol.* 42: 185-201.
- Kiehart, D.P. and Inoué, S. (1976) Local depolymerization of spindle microtubules by microinjection of calcium ions, *J. Cell Biol.* 70: 230a.
- Kiehart, D.P., Inoué, S., and Mabuchi, I. (1977) Evidence that force production in chromosome movement does not involve myosin, *J. Cell Biol.* 75: 258a.
- Kinoshita, S. and Yazaki, I. (1967) The behavior and localization of intracellular relaxing system during cleavage in the sea urchin egg, *Exp. Cell Res.* 47: 449-458.
- Klevecz, R.R. and Forrest, G.L. (1975) Regulation of tubulin expression through the cell cycle, *Ann. N.Y. Acad. Sci.* 253: 292-303.
- Lambert, A. and Bajer, A.S. (1972) Dynamics of spindle fibers and microtubules during anaphase and phragmoplast formation, *Chromosoma* 39: 101-145.

- Ledbetter, M.C. and Porter, K.R. (1963) A microtubule in plant cell fine structure, *J. Cell Biol.* 19: 239-250.
- Lehninger, A.L. (1975) *In Biochemistry*, second edition, Worth Publishers, New York, 824-825.
- Levine, L., ed. (1963) *The Cell in Mitosis*, Academic Press, New York.
- Lockwood, A.H. (1977) Immunofluorescent and immunochemical studies on the function and distribution of tubulin assembly protein, *J. Cell Biol.* 75: 294a.
- Longo, F.J. (1972) An ultrastructural analysis of mitosis and cytokinesis in the zygote of the sea urchin Arbacia punctulata, *J. Morphol.* 138: 207-238.
- Longo, F.J. and Anderson, E. (1968) The fine structure of pronuclear development and fusion in the sea urchin Arbacia punctulata, *J. Cell Biol.* 39: 339-368.
- Longo, F.J. and Plunkett, W. (1973) The onset of DNA synthesis and its relation to morphogenetic events of the pronuclei in activated eggs of the sea urchin Arbacia punctulata, *Dev. Biol.* 30: 56-67.
- Lott, J.N.A. and Vollmer, C.M. (1975) Changes in cotyledons of Cucurbita maxima during germination. V. The nuclear envelope, *J. Ultrastruct. Res.* 52: 156-166.
- Marcum, J.M., Dedman, J.R., Brinkley, B.R., and Means, A.R. (1978) Control of microtubule assembly-disassembly by calcium-dependent regulator protein, *Proc. Natl. Acad. Sci.* 75: 3771-3775.
- Margolis, R.L. and Wilson, L. (1978) Opposite end assembly and disassembly of microtubules at steady state in vitro, *Cell* 13: 1-8.
- Maul, G.G., Price, J.W., and Lieberman, M.W. (1971) Formation and distribution of nuclear pore complexes in interphase, *J. Cell Biol.* 51: 405-418.
- Mazia, D. (1961) Mitosis and the physiology of cell division. In The Cell, J. Brachet and A.E. Mirsky, eds., Vol. 3, Meiosis and Mitosis, Academic Press, New York, 77-412.
- Mazia, D., Chaffee, R.R., and Iverson, R.M. (1961) Adenosine triphosphatase in the mitotic apparatus, *Proc. Natl. Acad. Sci.* 47: 788-790.
- Mazia, D. and Dan, K. (1952) The isolation and biochemical characterization of the mitotic apparatus of dividing cells, *Proc. Natl. Acad. Sci.* 38: 826-838.
- Mazia, D., Mitchison, J.M., Medina, H., and Harris, P. (1961) The direct isolation of the mitotic apparatus, *J. Biophys. Biochem. Cytol.* 10: 467-474.

- Mazia, D., Petzelt, C., Williams, R.O., and Meza, I. (1972) A Ca-activated ATPase in the mitotic apparatus of the sea urchin egg (isolated by a new method), *Exp. Cell Res.* 70: 325-332.
- MBL Formulae and Methods V, G.M. Cavanaugh, ed., (1956) Marine Biological Laboratory, Woods Hole, Mass.
- McIntosh, J.R., Hepler, P.K., and Van Wie, D.G. (1969) Model for mitosis, *Nature* 224: 659-663.
- Mizuhira, V. and Futaesaku, Y. (1971) On the new approach of tannic acid and digitonine to the biological fixatives, *In 29th Annual Proceedings of the Electron Microscope Society of America, Boston, Mass., Claitor's Publishing Division, Baton Rouge, 494-495.*
- Myles, D.G. and Hepler, P.K. (1977) The effects of microtubule inhibitors on nuclear shaping and chromatin condensation, *J. Cell Biol.* 75: 174a.
- Nakamura, I. (1974) "Indent" formation and mitotic delay of sea urchin eggs fertilized with X-irradiated sperms, *J. Radiat. Res.* 15: 111-113.
- Nicklas, R.B. (1971) Mitosis. *In Advances in Cell Biology, Vol. 2, D.M. Prescott, L. Goldstein, and E. H. McConkey, eds., Appleton-Century-Crofts, New York, 225-279.*
- Peterson, J.B., Gray, R.H., and Ris, H. (1972) Meiotic spindle plaques in *Saccharomyces cerevisiae*, *J. Cell Biol.* 53: 837-841.
- Peterson, S.P. and Berns, M.W. (1977) Evidence for the role of centriolar RNA in spindle formation of dividing cells, *J. Cell Biol.* 75: 282a.
- Petzelt, C. (1972a) Ca<sup>2+</sup>-activated ATPase during the cell cycle of the sea urchin *Strongylocentrotus purpuratus*, *Exp. Cell Res.* 70: 333-339.
- Petzelt, C. (1972b) Further evidence that a Ca<sup>2+</sup>-activated ATPase is connected with the cell cycle, *Exp. Cell Res.* 74: 156-162.
- Petzelt, C. and Von Ledebur-Villegier, M. (1973) Ca<sup>2+</sup>-stimulated ATPase during the early development of parthenogenetically activated eggs of the sea urchin *Paracentrotus lividus*, *Exp. Cell Res.* 81: 87-94.
- Philipp, E-L, Franke, W.W., Keenan, T.W., Stadler, J. and Jarasch, E-D. (1976) Characterization of nuclear membranes and endoplasmic reticulum isolated from plant tissue, *J. Cell Biol.* 68: 11-29.
- Pickett-Heaps, J.D. (1969) The evolution of the mitotic apparatus: an attempt at comparative ultrastructural cytology in dividing plant cells, *Cytobios* 1: 257-280.

- Pickett-Heaps, J.D., McDonald, K.L., and Tippit, D.H. (1975) Spindle structure and function in diatoms, *J. Cell Biol.* 67: 336a.
- Podolsky, R.J. (1968) Membrane systems in muscle cells. In *Aspects of Cell Motility, Symposia of the Society for Experimental Biology, Vol. 23*, Academic Press, New York, 87-99.
- Raff, R.A. (1975) Regulation of microtubule synthesis and utilization during early embryonic development of the sea urchin, *Am. Zool.* 15: 661-678.
- Raff, R.A., Brandis, J.W., Green, L.H., Kaumeyer, J.F. and Raff, E.C. (1975) Microtubule protein in early development, *Ann. N.Y. Acad. Sci.* 253: 304-317.
- Randall, J.T. and Disbrey, C. (1965) Evidence for the presence of DNA at basal body sites in *Tetrahymena pyriformis*, *Proc. R. Soc. B* 162: 473-491.
- Rasmussen, H. and Goodman, D.B.P. (1975) Calcium and cAMP as interrelated intracellular messengers, *Ann. N.Y. Acad. Sci.* 253: 789-796.
- Rebhun, L.I. (1961) Some electron microscope observations on membranous basophilic elements of invertebrate eggs, *J. Ultrastruct. Res.* 5: 208-225.
- Rebhun, L.I. (1976) Personal communication.
- Rebhun, L.I., Jemiolo, D., Ivy, N., Mellon, M., and Nath, S. (1975) Regulation of the *in vivo* mitotic apparatus by glycols and metabolic inhibitors, *Ann. N.Y. Acad. Sci.* 253: 363-377.
- Rebhun, L.I., Nath, J., and Remillard, S.P. (1976) Sulfhydryls and regulation of cell division. In *Cell Motility*, R. Goldman, T. Pollard, and J. Rosenbaum, eds., Cold Spring Harbor Laboratory, 1343-1366.
- Rebhun, L.I., Rosenbaum, J., Lefebvre, P., and Smith, G. (1974) Reversible restoration of the birefringence of cold-treated, isolated mitotic apparatus of surf clam eggs with chick brain tubulin, *Nature* 249: 113-115.
- Rebhun, L.I. and Sander, G. (1967) Ultrastructure and birefringence of the isolated mitotic apparatus of marine eggs, *J. Cell Biol.* 34: 859-883.
- Reynolds, E.S. (1963) The use of lead citrate at high pH as an electron-opaque stain in electron microscopy, *J. Cell Biol.* 17: 208-212.
- Robbins, E. and Jentzsch, G. (1969) Ultrastructural changes in the mitotic apparatus at the metaphase-to-anaphase transition, *J. Cell Biol.* 40: 678-691.

- Root, W.S. (1930) The influence of carbon dioxide upon the oxygen consumption of *Paramecium* and the egg of *Arbacia*. Biol. Bull. 59: 48-62.
- Roth, L.E. and Shigenaka, Y. (1970) Microtubules in the Heliozoan axopodium. II. Rapid degradation by cupric and nickelous ions, J. Ultrastruct. Res. 31: 356-374.
- Sabatini, D.D., Bensch, K.G., and Barnett, R.J. (1962) New means of fixation for electron microscopy and histochemistry, Anat. Record 142: 274.
- Sabatini, D.D., Bensch, K.G., and Barnett, R.J. (1963) Cytochemistry and electron microscopy. The preservation of cellular ultrastructure and enzymatic activity by aldehyde fixation, J. Cell Biol. 12: 19-58.
- Sabatini, D.D., Miller, F., and Barnett, R.J. (1964) Aldehyde fixation (method) for morphological and enzyme histochemical studies with the electron microscope, J. Histochem and Cytochem. 12: 57-71.
- Sachs, M.I. and Anderson, E. (1970) A cytological study of artificial parthenogenesis in the sea urchin *Arbacia punctulata*, J. Cell Biol. 47: 140-158.
- Salmon, E.D. (1975) Spindle microtubules: thermodynamics of in vivo assembly and role in chromosome movement, Ann. N.Y. Acad. Sci. 253: 383-406.
- Salmon, E.D., Goode, D., Mangel, T.K., and Bonar, D.B. (1976) Pressure-induced depolymerization of spindle microtubules. III. Differential stability in HeLa cells, J. Cell Biol. 69: 443-454.
- Salmon, E.D. and Jenkins, R. (1977) Isolated mitotic spindles are depolymerized by  $\mu\text{M}$  calcium and show evidence of dynein, J. Cell Biol. 75: 295a.
- Sanchez, S. and Porra, L. (1972) Synthèse de données ultrastructurales et cytochimiques sur l'oeuf d'Echinoderme en segmentation (*Paracentrotus lividus*), Arch. Biol. 82: 471-527.
- Sanger, J.W. (1975) Presence of actin during chromosomal movement, Proc. Natl. Acad. Sci. 72: 2451-2455.
- Sanger, J.W. (1977) Non-tubulin molecules in the spindle. In Mitosis: Facts and Questions, M. Little, N. Paweletz, C. Petzelt, H. Postingl, D. Schroeter, and H.-P. Zimmerman, eds., Springer Verlag, New York.
- Schatten, H. and Schatten, G. (1977) The mitotic apparatus: high resolution scanning electron microscopy of the surface, J. Cell Biol. 75: 284a.
- Scheer, U and Franke, W. (1969) Negative staining and adenosine triphosphatase activity of annulate lamellae of newt oocytes, J. Cell Biol. 42: 519-533.

- Schliwa, M. (1976) The role of divalent cations in the regulation of microtubule assembly. In vivo studies on microtubules of the heliozoan axopodium using the ionophore A23187, *J. Cell Biol.* 70: 527-540.
- Schmidt, W.A. (1973a) Nucleotide phosphatase in Strongylocentrotus purpuratus eggs. I. Localization, *J. Exp. Zool.* 185: 1-16.
- Schmidt, W.A. (1973b) Nucleotide phosphatase activity in Strongylocentrotus purpuratus eggs. III. Multiple enzymatic activities in mature and immature eggs, *J. Exp. Zool.* 185: 27-43.
- Schrader, F. (1953) *Mitosis: the Movements of Chromosomes in Cell Division*, Second Edition, Columbia University Press, New York.
- Seaman, G.R. (1960) Large-scale isolation of kinetochores from the ciliated protozoan Tetrahymena pyriformis, *Exp. Cell Res.* 21: 292-302.
- Seaman, G.R. (1962) Protein synthesis by kinetosomes isolated from the protozoan Tetrahymena pyriformis, *Biochim. Biophys. Acta* 55: 889-899.
- Sherline, P. and Schiavone, K. (1977) Immunofluorescence localization of proteins of high molecular weight along intracellular microtubules, *Science* 198: 1038-1040.
- Sisken, J.E. and VedBrat, S.S. (1977) On the effects of variations in intracellular and extracellular calcium ions on mitosis and cytokinesis of HeLa cells, *J. Cell Biol.* 75: 263a.
- Sluder, G. (1976) Experimental manipulation of the amount of tubulin available for assembly into the spindle of dividing sea urchin eggs, *J. Cell Biol.* 70: 75-85.
- Soifer, D. ed. (1975) *The Biology of Cytoplasmic Microtubules*, Annals of the New York Academy of Sciences, Vol. 253, The New York Academy of Sciences, New York.
- Sorokin, S.P. (1968) Reconstructions of centriole formation and ciliogenesis in mammalian lungs, *J. Cell Sci.* 3: 207-230.
- Snyder, J.A. and McIntosh, J.R. (1976) Biochemistry and physiology of microtubules, *Ann. Rev. Biochem.* 45: 699-720.
- Stephens, R.E. (1972) Studies on the development of the sea urchin Strongylocentrotus droebachiensis. II. Regulation of mitotic spindle equilibrium by environmental temperature, *Biol. Bull.* 142: 145-159.
- Stephens, R.E. and Edds, K.T. (1976) Microtubules: structure, chemistry, and function, *Physiol. Revs.* 56: 709-777.

- Suzuki, N. and Yoshitake, M. (1973) Dependence of periodic DNA synthesis on protein synthesis: delay of DNA synthesis in the early cleavage stage of sea urchin embryos treated with cycloheximide and colchicine, *Dev. Growth Differ.* 15: 113-125.
- Svejda, J., Vrba, M., and Blumajer, J. (1975) A freeze-etch study of occurrence of nuclear pores in normal and tumor cells, *Neoplasma (Bratislava)* 22: 385-390.
- Tilney, L.G., Bryan, J., Bush, D.J., Fujiwara, K., Mooseker, M.S., Murphy, D.B., and Snyder, D.H. (1973) Microtubules: evidence for 13 protofilaments, *J. Cell Biol.* 59 (2, pt. 1): 267-275.
- Tilney, L.G. and Gibbins, J.R. (1969) Microtubules in the formation and development of the primary mesenchyme in *Arbacia punctulata*. II. An experimental analysis of their role in development and maintenance of cell shape, *J. Cell Biol.* 41: 227-250.
- Tilney, L.G. and Marsland, D. (1969) A fine structural analysis of cleavage induction and furrowing in the eggs of *Arbacia punctulata*, *J. Cell Biol.* 42: 170-184.
- Tippit, D.H., McDonald, K.L., and Pickett-Heaps, J.D. (1975) Cell division in the centric diatom *Melosira varians*, *Cytobiologie* 12: 52-73.
- Tucker, J.B. (1967) Changes in nuclear structure during binary fission in the ciliate *Nassula*, *J. Cell Sci.* 2: 481-498.
- Turner, J.L. and McIntosh, J.R. (1977) Isolation of the mitotic apparatus. In *Methods in Cell Biology*, Vol. XVI, G. Stein, J. Stein, and L.J. Kleinsmith, eds., Academic Press, New York, 373-379.
- Verhey, G.A. and Moyer, F.H. (1967) Fine structural changes during sea urchin oogenesis, *J. Exp. Zool.* 164: 195-226.
- Virchow, R. (1858) Cellular-pathologie, *Arch. Path. Anat. Phys.* VIII: 1. Also quoted in Wilson, E.B. (1928) *The Cell*, 114.
- Weisenberg, R.C. (1972a) Microtubule formation in vitro in solutions containing low calcium concentrations, *Science* 177: 1104-1105.
- Weisenberg, R.C. (1972b) Changes in the organization of tubulin during meiosis in the eggs of the surf clam, *Spisula solidissima*, *J. Cell Biol.* 54: 266-278.
- Weisenberg, R. and Rosenfeld, A. (1975a) Role of intermediates in microtubule assembly in vivo and in vitro, *Ann. N.Y. Acad. Sci.* 253: 78-89.
- Weisenberg, R.C. and Rosenfeld, A. (1975b) In vitro polymerization of microtubules into asters and spindles in homogenates of surf clam eggs, *J. Cell Biol.* 64: 146-157.

- Welsh, M.J. and Dedman, J.R. (1977) Calcium dependent regulator protein associated with the mitotic apparatus of mammalian cells, *J. Cell Biol.* 25: 262a.
- Whaley, W.G., Dauwalder, M., and Leffingwell, T.P. (1975) Differentiation of the Golgi apparatus in the genetic control of development, *Cur. Top. Dev. Biol.* 10: 161-186.
- Wilson, E.B. (1895) Archoplasm, centrosome, and chromatin in the sea-urchin egg, *J. Morphol.* 11: 443-478.
- Wilson, E.B. (1928) *The Cell in Development and Heredity*, Third Edition, The MacMillan Co., New York, 114-225.
- Wilson E.B. and Mathews, A.P. (1895) Maturation, fertilization, and polarity in the echinoderm egg, *J. Morphol.* 10: 319-342.
- Wilt, F.H., Sakai, H., and Mazia, D. (1967) Old and new protein in the formation of the mitotic apparatus in cleaving sea urchin eggs, *J. Mol. Biol.* 27: 1-7.
- Wischnitzer, S. (1970) The annulate lamellae, *Int. Rev. Cytol.* 27: 65-100.
- Witman, G.B. (1975) The site of in vivo assembly of flagellar microtubules, *Ann. N.Y. Acad. Sci.* 253: 178-191.
- Zimmerman, A.M. (1960) Physico-chemical analysis of the isolated mitotic apparatus, *Exp. Cell Res.* 20: 529-547.
- Zimmerman, A.M. (1963) Chemical aspects of isolated mitotic apparatus. In *The Cell in Mitosis*, L. Levine, ed., Academic Press, New York, 159-184.
- Zimmerman, A., Zimmerman, S., and Forer, A. (1977) The mitotic apparatus: methods for isolation. In *Methods in Cell Biology*, Vol. XVI, G. Stein, J. Stein, and L.J. Klein-smith, eds., Academic Press, New York, 361-371.